RUSSIAN ACADEMY OF SCIENCE
FEDERAL AGENCY ON EDUCATION OF RUSSIAN FEDERATION
RUSSIAN NATIONAL COMMISSION FOR UNESCO
COMMITTEE ON SCIENCE AND HIGHER EDUCATION OF THE GOVERNMENT OF SAINT-PETERSBURG
COUNCIL OF RECTORS OF SAINT-PETERSBURG HIGHER EDUCATION ESTABLISHMENTS
SAINT-PETERSBURG STATE UNIVERSITY OF AEROSPACE INSTRUMENTATION (SUAI)
UNESCO CHAIR "DISTANCE EDUCATION IN ENGINEERING" OF SUAI

ФОРМИРОВАНИЕ СОВРЕМЕННОГО ИНФОРМАЦИОННОГО ОБЩЕСТВА – ПРОБЛЕМЫ, ПЕРСПЕКТИВЫ, ИННОВАЦИОННЫЕ ПОДХОДЫ

XIV Международный форум
2–6 июня 2013 года

MODERN INFORMATION SOCIETY FORMATION – PROBLEMS, PERSPECTIVES, INNOVATION APPROACHES

XIV International forum
2–6 June , 2013

PROCEEDINGS OF THE FORUM

РОССИЯ, САНКТ-ПЕТЕРБУРГ 2013 SAINT-PETERSBURG, RUSSIA

УДК 001.9
ББК 72.4
Ф79

Ф79 XIV International Forum « Modern information society formation- problems, perspectives, innovation approaches»: Proceedings of the Forum. St. Petersburg, 2–6 June / SUAI, SPb., 2013. 96 p.
ISBN 978-5-8088-0809-6

ISA District 12 (International Society of Automation) and SUAI (Saint-Petersburg State University of Aerospace Instrumentation) have organized the Ninth ISA European students paper competition (ESPC-2013). Papers of professors and the best students were included into this volume of the proceedings of the XIV International Forum «Modern information society formation- problems, perspectives, innovation approaches». Papers can be interesting for students, post-graduated students, professors and specialists.

ISBN 978-5-8088-0809-6

Setting the Standard for Automation™

On behalf of ISA, I extend congratulations to the ISA Russia Section, ISA District 12, and the St. Petersburg State University of Aerospace Instrumentation (SUAI) on successfully completing the ninth ISA European Student Paper Competition.

Students are the future for our Society. We are excited about these talented individuals who will help "set the standard for automation" and shape the processes that will enhance our lifestyle in the 21st century. No matter which career path they choose, we hope ISA will continue to play an important role in their continuing education and professional development.

The papers published in this volume, selected by the advisory committee, represent the best contributions from among an excellent group of papers. The students who committed their time to prepare a paper should be very proud to be selected for this publication.

Sincerely,

Terrence G. Ives
2013 ISA President

I would like to extend congratulations to the ISA Russia Section, ISA District 12, Indiana State University (ISU), and the St. Petersburg State University of Aerospace Instrumentation (SUAI) for successfully organizing the Ninth ISA European Student Paper Competition. This international forum has become one of the foremost conferences in the world.

As an education and member of ISA for almost 30 years, I continue to appreciate the sharing of technical information by students and faculty members. This global sharing will serve to help advance the technical knowledge base and help in the global collaboration of ideas. I always look forward to having the opportunity to share with students the amazing challenges and personal rewards that a life in automation can bring. ISA is honored to have the opportunity to nurture the next generation of automation professionals.

Indiana State University and the International Society of Automation look forward to our continued relationship between the Russia Section, District 12, and SUAI. Through distance learning classes on project management and ongoing international forums, we are developing new understandings in the technical, cultural, and personal arenas.

Congratulations to those who have developed papers for this volumn and to the advisort committee who have the difficult task of making paper selections.

Sincerely,

Gerald W. Cockrell

Gerald W. Cockrell
ISA Former President (2009)
Professor Emeritus (ISU)

Setting the Standard for Automation™

On behalf of ISA, I extend congratulations to the ISA Russia Section and the St. Petersburg State University of Aerospace Instrumentation (SUAI) on successfully completing the ninth ISA European Student Paper Competition.

We are all excited about these talented individuals who will be instrumental in shaping the processes that will enhance our lifestyle in the 21st century. No matter which career path the students choose, we hope ISA will continue to play an important role in their continuing education and professional development.

The papers published in this volume, selected by the advisory committee, represent the best contributions from among an excellent group of papers. The students who committed their time to prepare a paper should be very proud to be selected for this publication.

To the lecturers you are also playing an important part in shaping the future and you should feel very proud of the standard that is visible in this publication.

On behalf of ISA may I extend my best wishes to all students and attendees in the 2013 ISA European Student Paper Competition.

Sincerely,

Brian J. Curtis
ISA District 12 Vice-President

DIAGNOSTICS OF RAILWAY WHEEL COUPLES ON THE BASIS OF THE CONTACTLESS VIBROANALYSIS

Alexander Adadurov,
Director of the Institute, PhD
Alexander Bestugin,
Director of the Institute, PhD
Alexander Kryachko
Head of Department , Doctor of sciense

Saint-Petersburg State University of Aerospace Instrumentation, Russia
e-mail: vorudada@ya.ru

Abstract

One of the most effective and cost-efficient remote methods for assessment of the tread surface condition of mounted wheels is contactless vibroanalysis based on acoustic procession of the vibrations produced by the contact of the defects of a wheel pair with the rail. Although manufacturing and operational defects of mounted wheels differ in terms of impact on the vibration signal and have different diagnostic indicators, the right combination of indicators enables to detect defects and assess the tread surface condition of a wheel pair.

1. INTRODUTION

Vibration parameters are mostly characterized by the constructive features of the axle box, the wheel pair, and by the speed of the train. Factors affecting the parameters of the acoustic signal can be classified in three groups: the impact of the nonlinear rigidness of the track, the impact of manufacturing defects of the wheel pair and the consequences of operation (slid flats, chips, etc.). The latter two categories cover all possible wheel pair defects, the emergence of which can be interrelated. For instance, tread surface fatigue failure reveals itself in the form of pitting of the material and can be a result of an excessive load on the wheel pair [1].

The present paper is dedicated to the detection of wheel pair tread surface defects by means of acoustic processing of the signal produced by the contact of flawed wheel surface areas with the rail.

2. CONTACTLESS VIBROANALYSIS

In order to develop and test the detection algorithms for acoustic impulses produced by the contact of a wheel surface defect with the rail, the experts have been using microphones from the set of a device elaborated by the specialists of OAO NIIAS (the Research and Design Institute of Informatization, Automation and Communication), the so-called Acoustic Monitoring Post (AMP). The functional scheme of the AMP is presented in figure 1.

An AMP consists of:

- measuring microphones with preamplifiers protected by anti-vandal and heat-reflecting containers (measurement boxes), installed in the immediate vicinity of the track;

- station equipment located in the control room, namely the interface equipment, the acoustic data acquisition and processing system, a personal computer, the control system for climate adjustment and safety screen regulation of roadside equipment, and the connectivity system between the train passage monitoring system and the computer [2];

- software ensuring the functioning of the whole system, in particular, recording and processing the signals received from the microphones.

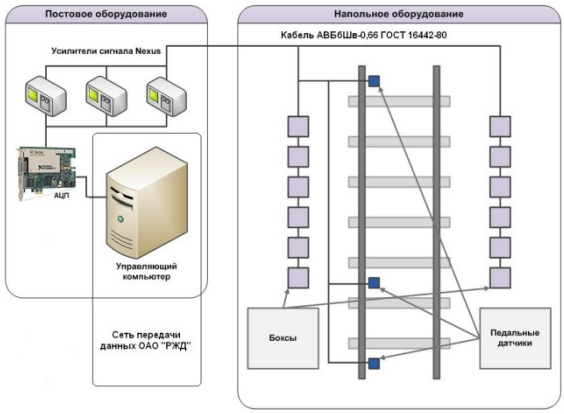

Figure 1.

Figure 2.

Measuring microphones and preamplifiers are installed in measurement boxes positioned in the line of the track in the measurement section, with six boxes on either side of the track. The distance between the adjacent boxes is 1.5 m, which guarantees the registration of two complete rotations of a standard wheel pair. Within the measurement boxes, microphones and preamplifiers are attached to special racks. Measurement boxes are installed along the track at such height that, when a train passes the measurement section of the AMP, the microphone's sensor would be level with the axle box of the wheel pair of the carriage (Fig. 2).

Measuring microphones and preamplifiers are connected by special microphone cables with conditioning amplifiers.

Acoustic noise is transformed by the measuring microphones into an electric signal which is received by the input terminal of the conditioning amplifier. In accordance with the pre-set program of the amplifier, the received signal is amplified within a given frequency bandwidth and transferred to the multi-channel analog-to-digital converter (hereafter – AD converter), plugged in the control computer for registration, further processing, and analysis. A high-quality AD converter enables to record all signals in a digital form with a sampling frequency of about 60 kHz.

When a train goes past the microphones, the acoustic signal envelope curve, registered by the control computer, has the aspect as shown in Fig. 3.

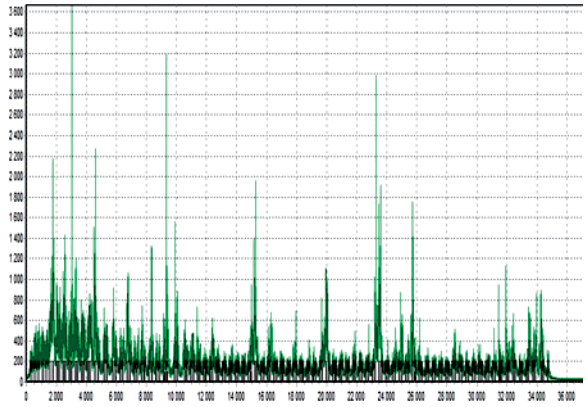

Figure 3.

On the diagram, the Y-axis indicates the time, and the X-axis, the amplitude of the envelope curve. The shape of the curve enables to determine with relative accuracy the moment when each axis passed the microphone (fig. 4); the vertical lines indicate the moments when wheel pair axes were located right opposite the microphone.

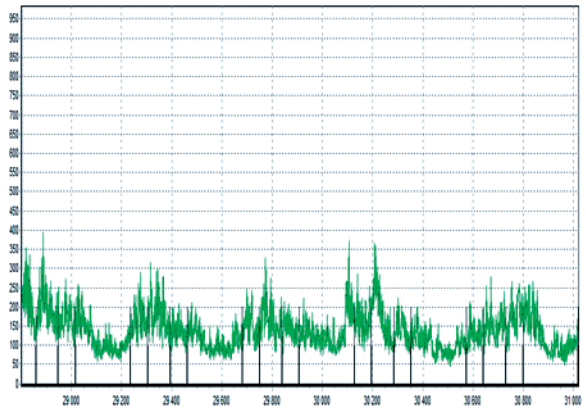

Figure 4.

The peaks of the curve refer to acoustic impulses (fig. 5) which can be caused by both shocks related to tread surface defects and external noise.

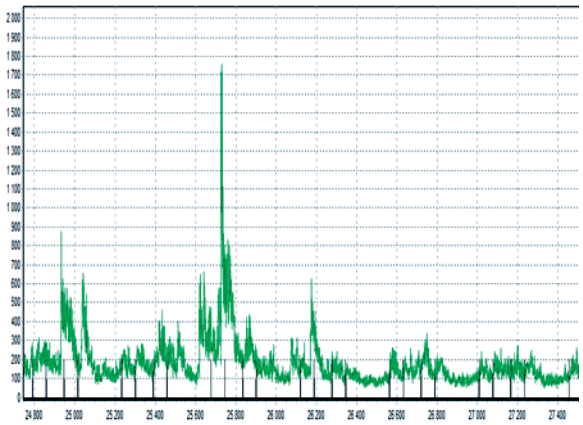

Figure 5.

A typical feature enabling to detect a tread surface defect is a repetition of the peak at intervals equal to the ratio of the wheel circumference (approximately 3 m) to the speed of the train. As an AMP includes six microphones on either side of the track, the distance between the first and the sixth microphones is 7.5 m. In the event of a tread surface defect, the system of microphones will detect at least three acoustic impulses. Thus, in the fig.6a and 6b, there are signals registered by three microphones. The distance between the microphones is 3 m. The signal from the first microphone in the direction of the train is highlighted in blue, from the next one, in green, and the last one, in purple.

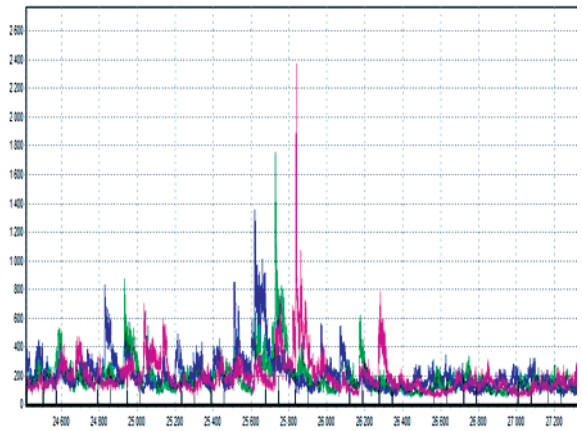

Figure 6a.

The signals in Fig. 6a refer to the passage of 26 axes of the train; furthermore, starting from the 26,400 mark, there are no envelope peaks, which indicated the absence of acoustic impulse sources, and, consequently, the absence of significant tread surface defects. Within the interval from 24,800 to 26,400, there are three groups of impulses with a steep rising edge, which leads to the conclusion that a total of three axes have tread surface defects. It is also clear that the most serious defect is reflected in the interval from 25,400 to 26,000.

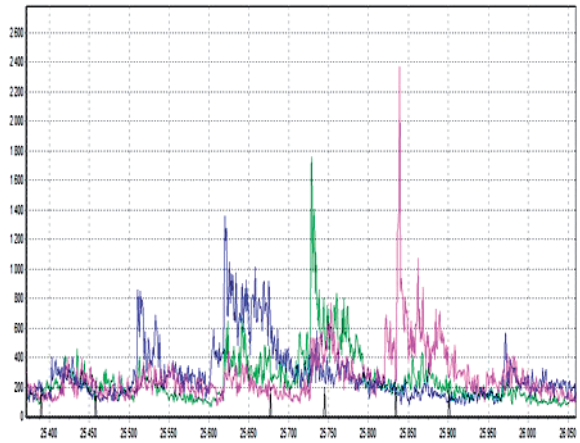

Figure 6b.

The analysis of the curve shapes at a larger scale (Fig. 6b) demonstrates that both the shape and the amplitude of the impulses are substantially different for different microphones. Such situation is typical; obviously, it is related to the fact that the contact point of the defect and the rail shifts from the axis of the microphone due to the discrepancy between the wheel circumference and the distance between the microphones.

Another typical feature is the registration of acoustic impulses causes by shocks on the opposite end of the wheel axis. Fig. 14a presents the envelope curves of microphones installed on opposite sides of the track. The signal of the flawed wheel is shown in fig. 7a, and fig. 7b shown the signal registered by the opposite microphone [3].

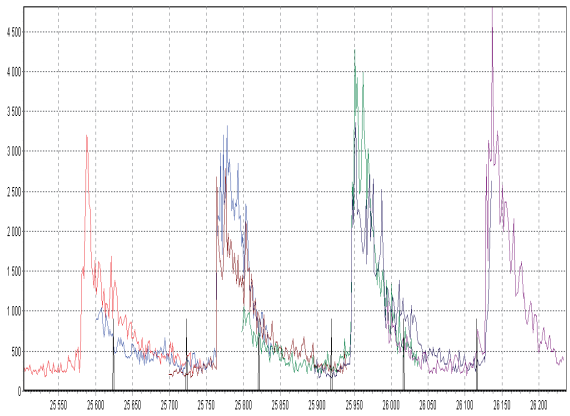

Figure 7a.

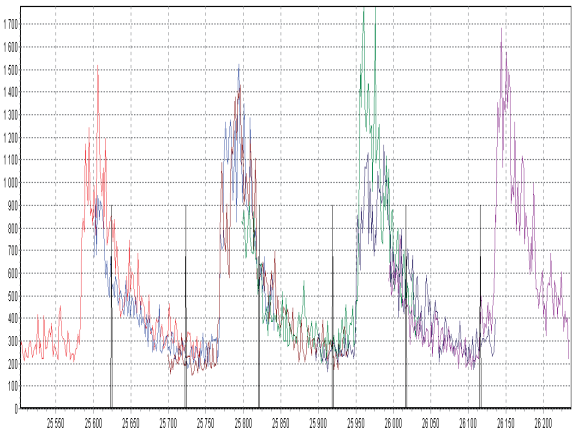

Figure 7b

It is evident that impulses in the first figure have an amplitude twice as large and a more distinct rising edge, which enables to make the unambiguous conclusion that the signal in the second figure is a consequence of the acoustic impulse from the opposite side.

At the same time, opposing microphones registering acoustic impulses with similar amplitudes can indicate a slid flat, which is mainly caused by the jamming of a wheel pair, resulting in the abrasion of both wheels. Moreover, given that the wheels and the rails are made from identical materials from both sides of the track, in the event of an equal load on the wheels, slid flats would appear on both wheels, and their size would be very similar. The example of such case is presented in fig.8a and 8b.

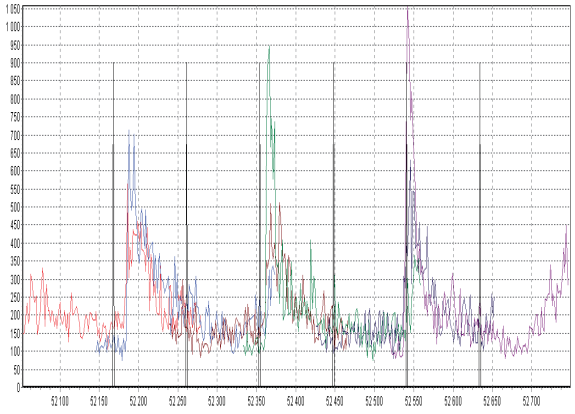

Figure 8a.

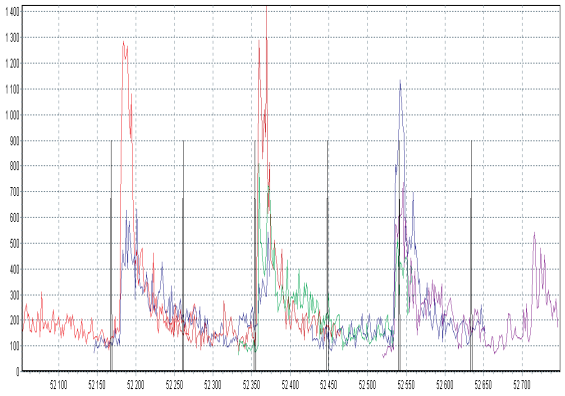

Figure 8b.

Another proof of the fact that the figures illustrate signals produced by two different defects is the discrepancy between the impulse amplitudes. Thus, on the first microphones (red), the amplitude of the first impulse is larger (fig. 8b), and on the second microphones, vice-versa. In the event of a one-sided defect (fig. 7), all impulses would have larger amplitude on the one side, than on the other.

The analysis of acoustic signal envelope curves obtained through the AMP microphones enables to determine the following informative indicators of tread surface defects of a wheel pair:

1) a minimum of three impulses must be registered;

2) the intervals between impulse peaks must correspond with the ratio of the wheel circumference to the motion speed of the wheel pair;

3) the rising edge of an impulse must be very steep;

4) in the event of a singular defect, a number of impulses might be registered on the opposite side,

however, their amplitude and the steepness of the rising edge must be less than on the side of the defect;

5) in the event of slid flats on both wheels, opposite microphones register impulses of approximately equal amplitude with a steeper rising edge.

The flowchart of the program detecting tread surface defects by means of acoustic signal processing is presented in Fig. 9. The flowchart features the following keys:

m – microphone sequential number (1 <= m <= 6);

i – peak sequential number (0 <= i <= Nm);

Ami – amplitude of the i-peak of the m-microphone.

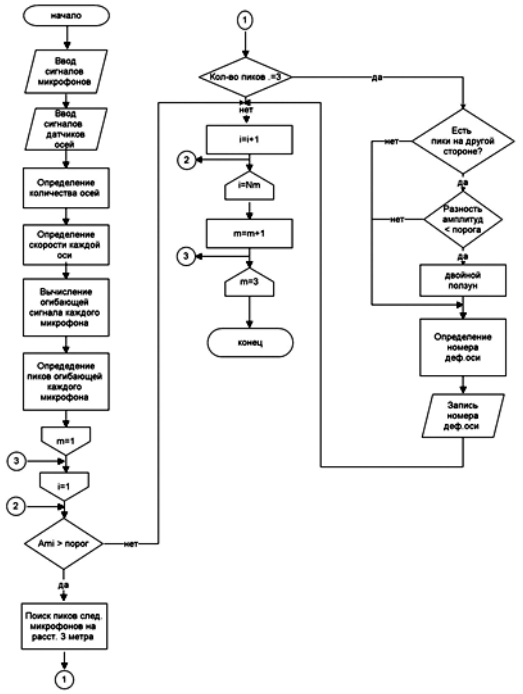

Figure 9.

III. CONCLUSION

The condition for defect detection has been the criterion of acoustic impulse repetition; therefore, within the interval of axis' passage before the microphone grill, the number of the detected peaks must exceed the number of complete wheel rotations by one, thus equaling 3. As a result, if there is an absence of impulses with an amplitude exceeding this limit on the first three microphones, the analysis cycle of the "starting" peaks is only carried out for the first three microphones.

REFERENCES

[1] Современные проблемы исследования быстропротекающих процессов и явлений катастрофического характера: к 75-летию В.П. Коробейникова // О.М. Белоцерковский, В.В. Марков, И.В. Семенов. – М.: Наука, 2007 . – 223 с.

[2] Крячко А.Ф., Крячко М.А., Волвенко С.В., Макаров С.Б. Мультисенсорная радиосистема передачи данных. Патент на полезную модель RU. H04B1. № 83886. Опубл. 30.09.2008.

[3] Крячко А.Ф. Методы повышения помехоустойчивости приема сообщений в радиотехнических системах телеуправления и контроля./ Пантенков А.П., Силаков Д.М. // Изв. вузов. Радиоэлектроника. 2007, т. 50, № 5-6, с. 47-54.

RANDOM NUMBER GENERATOR BASED ON BIOMETRIC APPROACH

Ekaterina Andreeva *(Ass.Professor)**,Sergey Bezzateev(**Professor),**Konstantin Zhidanov**(Ass.Professor)*

Department Technologies of Information Security, Saint-Petersburg State University of Aerospace Instrumentation,

Saint-Petersburg, Russia.
bsv@aanet.ru, eandreeva@guap.com

ABSRTACT

Security of medical information is the current problem in the modern society. Every year appear more and more telemedicine systems and m-health applications, for diagnosis of human condition and maintenance of life-support. Growing technological complexity of electronic medical devices leads not only to increased efficiency, but also increase risk of loss of personal information. The most important problems of information security in healthcare are access control to medical personal data and security data transmission. These problems especially important in systems of monitoring human condition, which is used sensors. Due to limited constraints of energy, memory and computation secure communication between sensors is not a trivial problem. The biometric technology using heart sounds and acoustic characteristics of the circulatory system allows constructing flexible information security systems, adapted to the specific characteristics of medical devices. This approach gives ability to used data which medical device gets during human condition monitoring. This feature allows not complicating medical device by information security system. Acoustic characteristics of the circulatory system allow developing a common key for the symmetric cryptosystems. Such acoustic characteristics of the circulatory as human heart sounds and inter-pulse interval are using in order to receive groups of similar random numbers to encrypt and decrypt the symmetric key.

In this article, analyze ability of using inter-pulse interval for generating random values to develop a common encryption key. Cryptographic resistance of random number generator is estimated using heart rate variability analysis.

INTRUDACTION

Development of informational technology makes possible to create Wireless Body Area Sensor Network, that is, a system of interconnected sensors located on the human body. This technology allows for continuous monitoring of the body by gathering information about parameters such as ECG, PCG, pulse, temperature, respiration, human position and others. Wireless Body Area Sensor Networks can be successfully applied in many areas, but have the greatest potential in healthcare. BASN allow remote monitoring of the patient for a long time without the limitations of its normal activity. [1] But with all the advantages of this technology, there is a question of information security systems and ensure an adequate level of protection of user data.

According to Russian law “About Personal Data” and international standard of processing medical information like HL7, medical human personal data have high level of privacy, so that it must be protected.

The main advantage of using Wireless Body Area Sensor Network is possibility of underwear sensors interconnected with the human body, to form initially secure communications network by receiving and processing of biometric data. Thus, the information circulating in the personal underwear sensor network is protected from unauthorized access by itself. As the biometric data used to form the pair of keys, the project has unique acoustic characteristics of the circulatory system.

But in order to develop a reliable system of information security based on biometric technology, necessary to check the efficiency of the chosen biometric characteristics. For this purpose, an analysis of heart rate variability and evaluated accident sequence obtained by calculating the difference inter-pulse intervals.

ARCHITECTURE OF WIRELESS BODY AREA SENSOR NETWORK

At present, the information technologies are extensively used extensively in medicine. It helps receiving and processing data required for the diagnosis of the patient, transfer and storage of medical information, and even surgery. But using of wireless and mobile technologies has allowed taking another look to the quality of medical services. Their combined use allows continuous remote monitoring of the patient and the timely receipt of all necessary data. In order to make the collection of medical information more convenient and unobtrusive from the patient point of view Wireless Body Area Sensor Networks replace the wearable medical devices. BASN is a system of interconnected sensors located on the body. In order to perform link patients and the data obtained from the sensors BASN must undergo four stages of processing:

- Collection and processing of data within BASN - medical patient data such as temperature, ECG, PCG, heart rate and other transmitted to the master node for pre-processing and further transmission.
- Data transfer to a personal device the patient - data from the head-end, are transferred to a private user's device (eg mobile phone)
- Transfer of data to the server - medical patient data are transmitted from your device to the server facility where being processed
- Inform your doctor - from server clinic patient data are transmitted directly to a personal device doctor

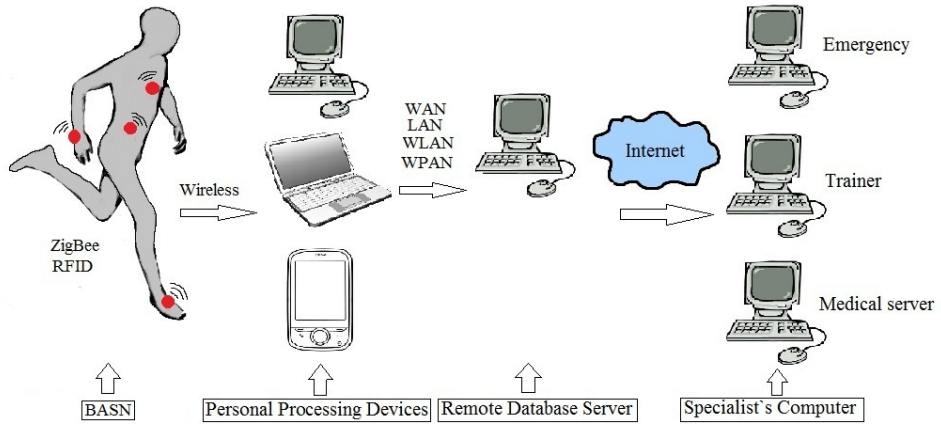

Figure 1. The system architecture providing data from BASN to specialist

The operation of such a system provides timely information on the professional health of the patient, but at the same time makes it vulnerable to medical personal data. For the second, third and fourth level of data in such a system, there are ways to protect information-designed, while the methods of information security at the level of data within BASN been adequately explored.

It is known that the network, working with sensors, has the following safety requirements:

- The data must remain confidential
- Data should be checked for authenticity
- It is necessary to maintain the integrity of data

Therefore, they should be protected with the help of methods of information security.

ACOUSTIC PROPERTIES OF HEART FOR SECURE COMMUNICATION IN BASN

In body networks sensors are located on, in or near the body of a person. Work of such network is handling the various indicators of the human body that are unique to each individual. Therefore, for information security in wireless body networks effective to use biometric technology, for both authentication and encryption of data [2,3,4].

The work of medical devices has some features which impose certain restrictions on the choice of biometric technology [5,6]:

These features include:

- Information security system should not depend on the user
- Information security system should not depend on the user's state

Also necessary to consider that sensors of wireless body area network can be placed around a person's body, not only in the field of obtaining standard biometric characteristics, such as a finger or retina.

Therefore, as the biometrics used in BASN individual signs the human bloodstream. A body area network remind the circulatory system structure, as in both cases there is a control node (in the case of the circulatory system - the heart), which provides the

relationship with all remote nodes. In the circulatory system in the course of the heart (the body life-support) is the body blood circulation, as well as underwear in the network is a constant exchange of information.

Work of the heart of every person is different [7], which means that an eclectic, acoustic, and other characteristics associated with the work of the heart can be seen as a sign of identity for a biometric system.

There are a number of works in which the approaches proposed by the construction of a cryptographic system, as well as authentication systems using electrocardiography characteristics of the heart [8,9,10].

As biometric data are used acoustic properties of the circulatory system, namely heart sounds and pulsation of blood. The advantage of this approach is low cost and availability of hardware resources that are necessary for the conduct of research. In paper [8] was proposed method of using group common random numbers generated from different biometrics traits from different parts of the body. These groups of same random numbers can be used to encrypt and decrypt messages in cryptosystem, that is perform functions of common key. Thus, as general biometric characteristics for two points on human body can be used inter-pulse intervals.

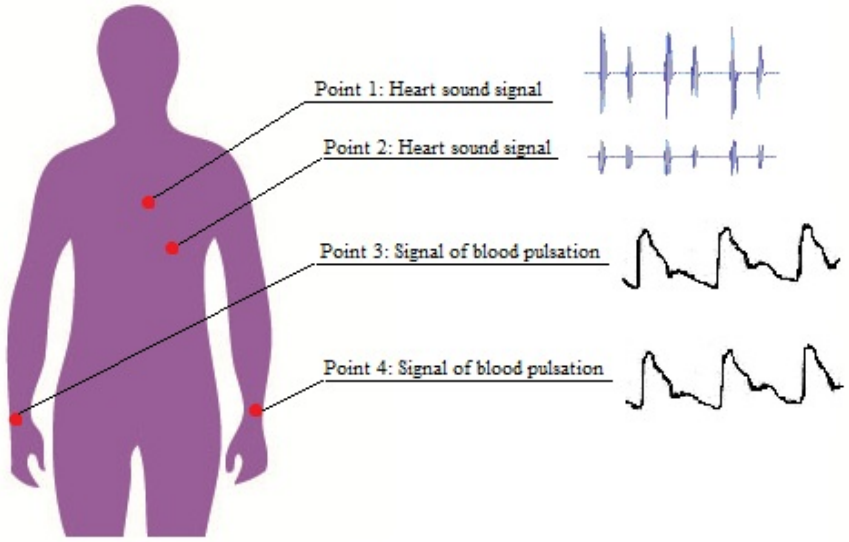

Figure 2. Scheme of sensor distribution on the human body

Interval values of heart sounds will correspond to intervals of blood pulsation in terms of synchronization. The origin of heart sounds, as the sounds of pulsation depends on one physical process - the work of systolic node, thus in the case of finding the correct synchronization settings can be calculated the total value of the intervals for this both characteristics.

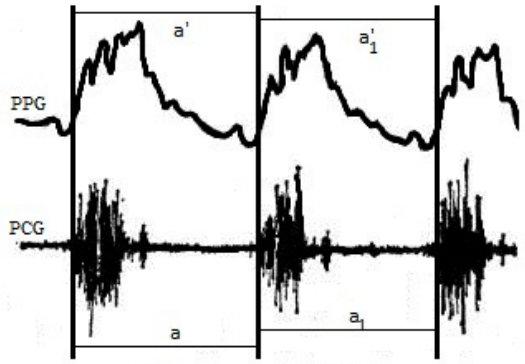

Figure 3. Synchronization photoplethysmogram and phonocardiogram

Figure 3 shows a diagram of synchronization hearts sounds, which are registered with the phonocardiogram (PCG) and the pulsation of blood in the vessels (detected using photoplethysmogram). Since these sounds are the result of the heart work and since there are interrelated, the distance between them (values of pulse intervals) will be the same. This can be illustrated by the following formula: $a = a'$, $a_1 = a_1'$, and so on for the whole set of inter-pulse intervals n.

The use of symmetric cryptography, with the common key, which is user's biometric data, provides resistance to attacks and efficacy In [7], as biometric data were used electrocardiography parameters of the heart, however, given the shortcomings of the existing systems proposed to use the acoustic properties of the heart.

Based on this knowledge, can be modeled a scheme of developing a common random numbers for the two points on human body. At first step, the received heart sound signals (PCG) and blood pulsation signals (PPG) are time synchronized and transferred to a

binary encoder. Then the calculated binary sequence is input to the algorithm of finding the Hamming distance. The output of the algorithm turns out the values by which we can determine the similarity of sequences. The final step is the evaluation of the acceptability of the results and a positive or negative decision makes.

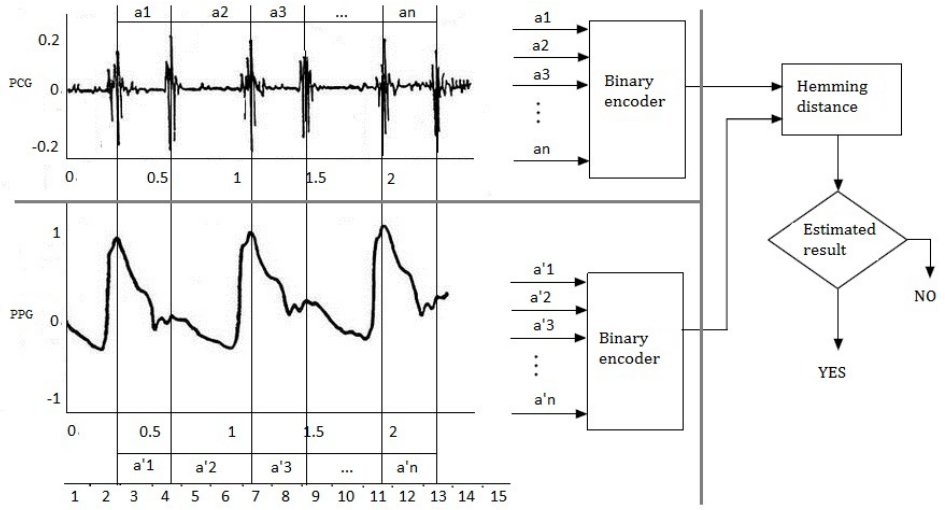

Figure 4. Generated of a common random group numbers for the 2 points

But there is a question of the suitability using inter-pulse intervals as a random numbers for input data of the algorithm generation a common key for a cryptosystem. To find answer to this question have been carried out research of characteristics of inter-pulse intervals.

HRV ANALYZE

To assess the effectiveness of using inter-pulses intervals as a source of random common key for symmetric cryptosystems have been analyzed the properties of heart rate variability. Analysis of heart rate variability will help answer the question: "Is there a correspondence between values of inter-pulse intervals and cryptographic random number generator." Values of inter-pulse intervals are obtained as a result of a physical process, i.e. as a result of human heart work. As it is known, random number generators, working on the basis of the physical process can generate truly random numbers. To confirm the hypotheses were used methods, which are commonly used in medical practice for heart rate variability analysis.

Currently, there are several methods to assess heart rate variability. Among them are three groups [11]:

- Time domain methods - based on statistical methods and aim to study the total variability
- Geometric methods
- Integral HRV (include autocorrelation analysis)

In the course of the research were obtained recording of heart rate long 5, 10 and 25 minutes. Using special software were calculated values of the sequence inter-pulse intervals, which have been evaluated with help of methods of heart rate variability analyze.

Time domains analyze:

Cardiointervalogram - variation series of RR intervals, depicted in the form of the segments of the direct, with a common starting point for each of them on the X-line. On the Y-line postponed the values of the duration of the cardiac cycle, at the X-line the numbers of the cycle. Figure 4 shows a cardiointervalogram, constructed by 200 values inter-pulse intervals. The values of the sequence is distributed in the interval from MIN = 0,68487 to MAX = 1,05836.

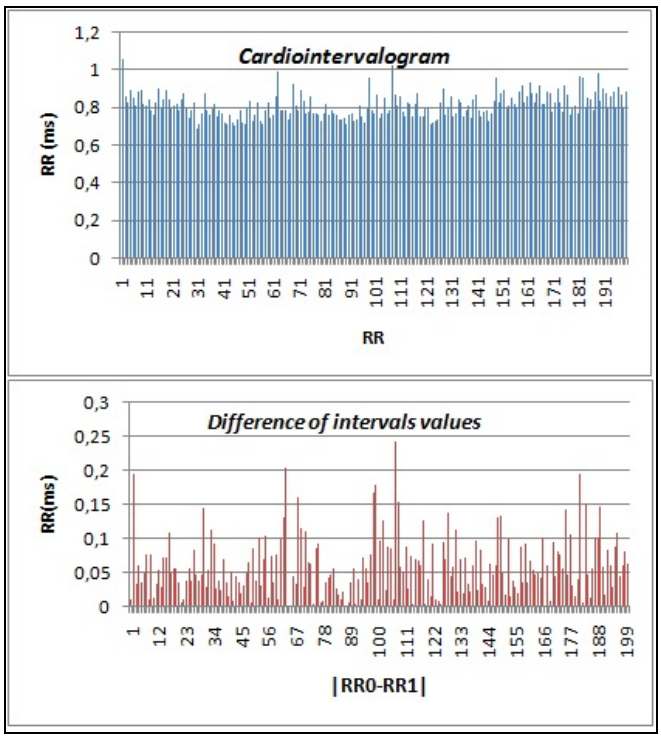

Figure 5. Cardiointervalogram

The lower diagram shows that the value of the inter-pulse intervals does not accept the constant value even on a small period of time. It can be seen, that in some places at second diagram values of intervals close to zero, but in fact there is no one value equal to zero. This means that the sequence does not occur even small periods of stability.

Geometric analyze:

The essence of the method is to obtain the distribution of the cardiointervals as random variables. The distribution of the duration of the cardiointervals displays a histogram.

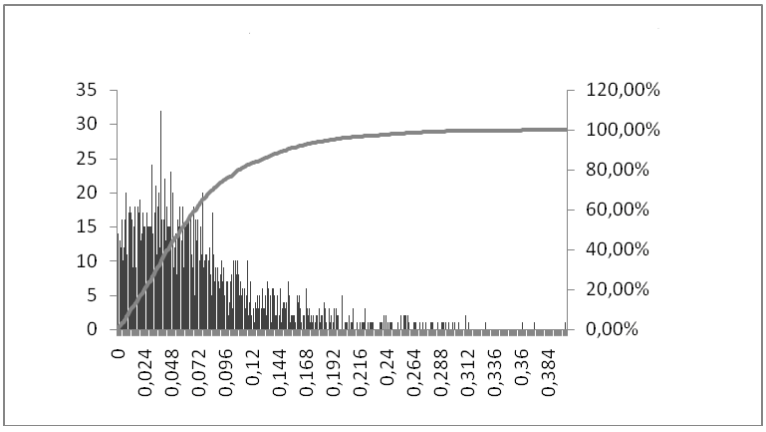

Figure 6. Bar chart of inter-pulse intervals

Analyze of integral indicators:

Autocorrelation analysis is used to assess the heart rate as a random process. The autocorrelation function is a diagram of the correlation coefficients obtained by sequential displacement of the analyzed time series on one number in relation to its own row. Is a qualitative analysis, according to which one can judge the influence of the autonomic system of the heart of the central management.

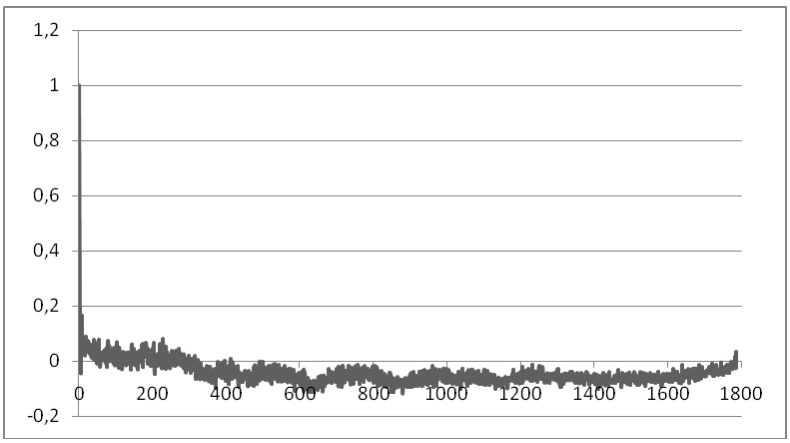

Figure 7. Autocorrelation function

As a result of carried out researches it is possible to make conclusions about the nature of the sequence inter-pulse intervals:

1. At all sequence of intervals is not observed periods of stability.
2. As the autocorrelation function has little value in the sequence, so that it has no intervals of repeated values.
3. The values of autocorrelation functions suitable for the formation of a cryptographically strongest generator of random numbers.

In future it is planned to investigate the sequence properties with the postulates of Golomb and Tests of Randomness to answer the question, is it possible to use the values of inter-pulse intervals in the cryptographic purposes.

CONCLUSION

This paper presents the method for use of Wireless Body Area Sensor Networks as applied to informational security systems. The method for division of the heart sonic signal into separate, independent informative portions is suggested. The reliability of the authentication system using the heart sonic signals may be increased with the help of this technology.

REFERENCE

1. Beritelli F, Spadaccini A. “Human Identity Verification Based on Heart Sounds: Recent Advances and Future Directions.” − University of Catania, Italy 2010, pp.1–18.
2. K. Jain, A. Ross, and S. Prabhakar. «An Introduction to Biometric Recognition», IEEE Transactions on Circuits and Systems for Video Technology, vol. 14, no. 1, pp. 4 – 20, January 2004.
3. Fen Miao, Lei Jiang, Ye Li and Yuan-Ting Zhang, «A Novel Biometrics Based Security Solution for Body Sensor Networks», IEEE Fellow Shenzhen Institutes of Advanced Technology Shenzhen, China, 2009.
4. Andreeva E. “Authentication system using heart sounds.” − Proceedings of the Tomsk State University of Control Systems and Radioelectronics, 1(25), part 2, 2012. pp. 153-157
5. Andreeva E. “System of continuous authentication using cardiology methods”. − Ryazan State Radio Engineering University, part 2, 2012. pp 176-179.
6. Carmen C. Y. Poon and Yuan-Ting Zhang. «A Novel Biometrics Method to Secure Wireless Body Area Sensor Networks for Telemedicine and M-Health» 2006.
7. Phua K, Dat T H, Chen J, Shue L. Human identification using heart sound. − Institute for Infocomm Research, Singapore 2008, pp 1-8
8. S. Cherukuri, K. K. Venkatasubramanian, and S. K. S. Gupta, “BioSec: A Biometric based Approach for Securing Communication in Wireless Networks of Biosensors Implanted in the Human Body,” Proc. IEEE Int’l. Conf. Parallel Processing Wksp., 6–9 Oct. 2003, pp. 432–39.
9. Fen Miao, Lei Jiang, Ye Li and Yuan-Ting Zhang, «A Novel Biometrics Based Security Solution for Body Sensor Networks», IEEE Fellow Shenzhen Institutes of Advanced Technology Shenzhen, China, 2009.
10. Biel, O. Pettersson, L. Philipson, and P. Wide. «ECG Analysis: A New Approach in Human Identification», IEEE Transactions on Instrumentation and Measurement, vol. 50, no. 3, pp. 808 – 812, June 2001.
11. Babunc I, «The ABC of heart rate variability analysis», 2002

DEVELOPMENT OF UWB SYSTEM WITH ADAPTIVE PATTERN

Bakin Eugene

jenyb@mail.ru

Gurnov Konstantine

Saint-Petersburg State University of Aerospace Instrumentation,
Saint-Petersburg, Russia
kocta4212@mail.ru

I Task Deskription

The use of ultra-wideband (UWB) signals in radio communication systems has several advantages [1,2]: the ability to reuse the selected part of the radio range, a large potential capacity, low sensitivity to multipath, which is especially important in urban areas and in the propagation of signals within the premises; high potential specific gravity data. The main application

UWB signals (UWB) signals is a wireless connection between the chips (wireless chip area network - WCAN), which due to the low cost of equipment and low power consumption are a promising technology [1].

One of the most important elements of the UWB system is the antenna system. The most widely phased arrays PAR, you always get a good directional properties and be able to effectively manage the pattern antenna system. In such systems as radiators PAR typically used microstrip antenna (MPA). Due to their small dimensions and weight and cost parameters [1,2].

The aim is to obtain a phased array antenna with the possibility of formation of a given DNA-based microstrip antennas (MPA). Array must operate over a wide frequency range of 3-8 GHz (relative bandwidth of the frequency > 50%) and have a standing wave ratio (VSWR) is not more than 2 in this range. NAM ($F(\Theta)$) array must be of the form shown in Figure 1.

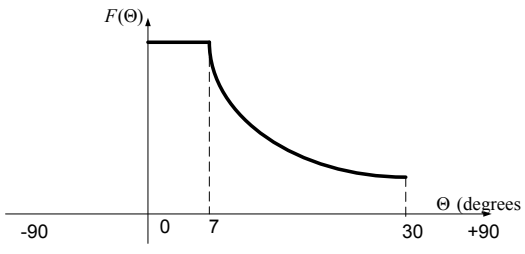

Figure 1 – Antenna pattern

II Microstrip antenna

Classical MPA has one serious drawback - because the resonant character planar lattice and MPA are narrowband, the relative bandwidth of the frequency of such an antenna is a fraction and a few percents. If you want a wider operating frequency band (20% and above), to replace the classical lateral radiators come wideband and ultra-wideband printed antenna longitudinal radiation, as well as design options combined longitudinal and lateral radiators These include spiral microstrip antennas, printed dipoles , patch antennas, and others [1,4].

Based on the above requirements on the basis of broad-band dipole transmitter take the following structure shown in Figure 2 Flat sheet foil fiberglass (FR-4), of a thickness of 1.5 mm and a thickness of 35 microns of copper. . On one side of the board is microstrip balun transformer, and the other two shoulder vibrator. Operating Frequency 1.8 GHz operating frequency band of 300 MHz (VSWR <2) [5].

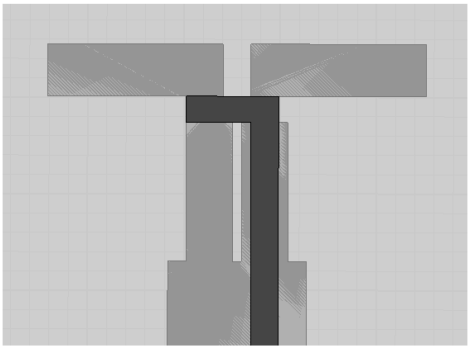

Figure 2 – Geometry of microstrip antenna

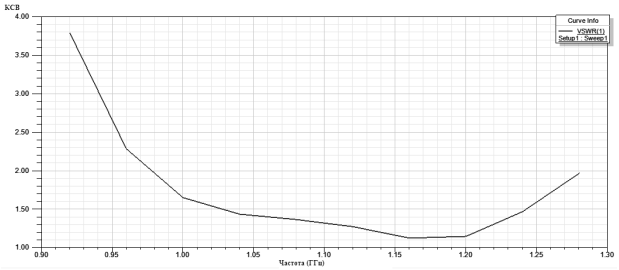

Figure 3 – VSWR microstrip antenna

To obtain the required parameters of the band, there have been modeling, optimization, and electromagnetic analysis of the radiator in the software package HFSS.

HFSS (High Frequency Structure Simulator) - is a powerful software package that calculates the multi-mode S-parameters and electromagnetic fields

for three-dimensional passive structures of arbitrary shape.

As a result of all the calculations was optimized shape microstrip balun transmitter and shoulder vibrators have selected another substrate material. Changing the substrate material due to the fact that the dielectric constant changes with fiberglass frequencies over 1.2 GHz, thus worsening the harmonization in the whole band. The results of the calculations are shown in Figure 4.

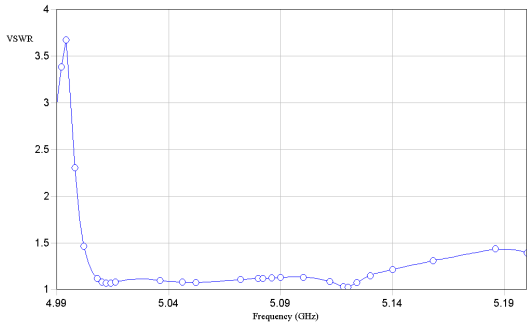

Figure 4 - VSWR optimized radiator

Figure 4 show that the VSWR of the radiator fully meet the requirements.

III Results prototyping

Was the prototype of the microstrip radiator, based on data obtained in the simulation. The material selected for the substrate FAF (Figure 5). Figure 6 shows the result of measuring the characteristics of manufactured radiator.

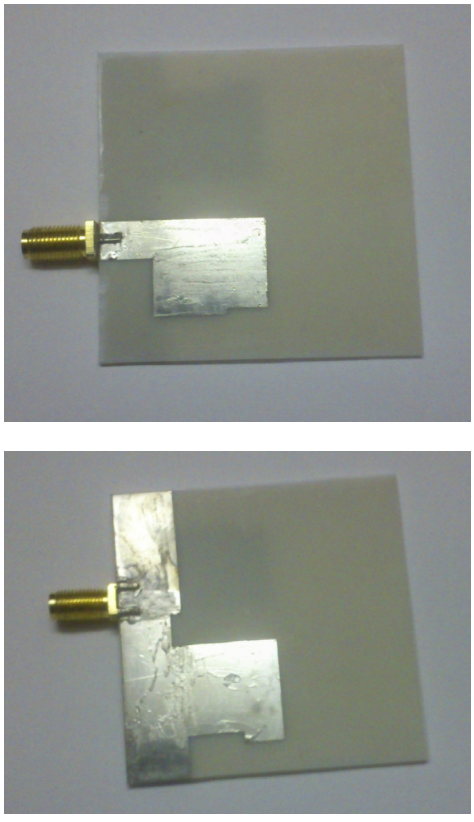

Figure – 5 The prototype antenna

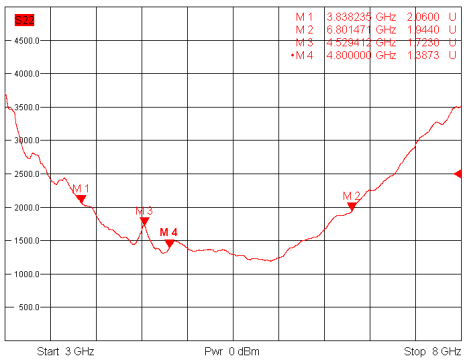

Figure - 6 VSWR antenna layout

Y-delayed VSWR, and the X-axis frequency in GHz.

IV. Formation NAM array

After receiving the required radiator with parametr, proceed to the construction phased c given NAM. To avoid interference between emitters spacing is chosen to be - the wave length. Number of emitters phased chosen equal to 8 to achieve the desired distribution of the NAM and receive antenna gain of 8 dB. Since the gain of a single radiator about 1.2 dB.

Required distribution of NAM can be obtained by forming a certain amplitude and phase distribution for each emitter. To obtain the desired amplitude and phase distributions was a mathematical model which, based on the Woodward-Lawson method (method of partial diagrams) [4], they were received.

Table 1 shows the number value of the amplitude and phase of each oscillator.

Table №1

№ oscillator	A_n , dB	φ_n , degree
1	-26.47	-101
2	-23.4	-109
3	-25.1	-98.7
4	-20.3	-142
5	-20.1	-122
6	-17.4	-168
7	-17.0	+142
8	-24.8	+105

Next, we substitute the distribution obtained in the model array antenna designed in HFSS. Each radiator is supplied on the basis of the received phase and amplitude distributions. As a result, we obtain the following DNA at a frequency f0 = 5.5 GHz (Figure 7)

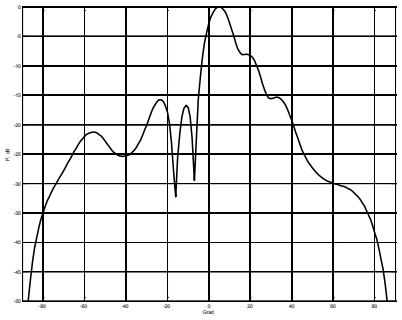

Figure 7 - The antenna pattern

V. Conclusion

A new design of microstrip radiator has working frequency band around 5 GHz. Amplitude and phase distributions for the array. On the basis of which was obtained the desired radiation pattern

VI. References

1. Mushnikov B. Electrodynamic models and research range from the combined microstrip radiators MaAntenny, 2008 № 7 (125), p. 11 - 17.

2. Kasyanov A.O., Obukhovets V.A., Mushnikov V.V., results of numerical and experimental studies of broadband emitters printed antennas. Antennas, 2007 № 5 (120), p. 9 - 15.

3. Kasyanov A.O., Obukhovets V.A., Mushnikov VV et al Radiation and scattering of electromagnetic waves. Electronic systems ranging and communication. monograph edited. V.A. Obukhov - Moscow Radio Engineering, 2007 -73 s.

4. Kasyanov AO, Mushnikov V.V., Numerical modeling of longitudinal printed radiators in planar phased arrays, Radiation and scattering of electromagnetic waves - IREMV - 2005. Intern. Nauchn. Conf. Taganrog, 20-25 June 2005.: Proceedings. - Taganrog publ TSURE, 2005. - With. 156 - 158.

5. Bart van Heck, Yap Sing Ho Design and modeling WLAN antenna for wireless network (Wireless № 1'2009)5. Bart van Heck, Yap Sing Ho Design and modeling WLAN antenna for wireless network (Wireless № 1'2009)

TRENDS IN GLOBAL AUTOMATION TO THE YEAR 2020

DR. GERALD W. COCKRELL CAP

PROFESSOR EMERITUS, INDIANA STATE UNIVERSITY
PRESIDENT OF ISA 2009

Introduction

Rapid changes in technology over the past 20 years has exhibited new modifications to the way we as humans act and think. No longer do we have to search for a coin operated phone to make calls to friends, family, and colleagues. Information is just a click away using the Internet. The methods used to educate young people have become nothing like teaching methods used just 10 years ago. It is possible to have renowned experts in a field teach students around the world. One field that has seen dramatic changes is manufacturing. Automation has become a method used to manufacture a wide range of products from cars to airplanes, to pharmaceutical products. Automated systems are used in many areas including manufacturing, transportation, environmental, and personal activities.

Automation used in industrial areas including design, manufacturing, quality, and delivery has advanced to a point where it is now possible to insure that a product is manufactured with high quality, increased efficiency, and lower cost over methods employed only a few years ago. It is now possible to build a product with minimal human interaction. Of course, the need for trained technicians and engineers to design, build, and maintain these systems is ever increasing.

Mike Caliel (ISA InTech, 2012) indicates that the scope of automation platforms has continually increased as the technology has been developed. Some of the automation developments that had the highest impact on the field include the single chip controller, the PLC, smart sensors and actuators, network technology, and improved operator interface products. The technology does tend to improve each and every day. This paper will outline some of the possible changes and new applications of technology to the automation field. Since technology changes so rapidly, the year 2020 will be the cut-off for our look into the future. It is important to remember that the changes presented are strictly the opinion of the author.

The four areas that will produce the greatest effect on automation include: wireless technology, system integration, smart devices, and artificial intelligence. We will discuss each area in terms of concept and future effect on automation in the world.

Wireless Technology

One technology that has changed the way people interact with their machines is the great advances in wireless. It is easy to see that with the wireless technology as exhibited in cell phone technology has produced a step-change in communications and the cultural effects of that it has brought about. The way people do business in the world has been advanced to a point where place and time is no longer a factor. People are afforded the opportunity to do business and communicate globally on a 24/7/365 basis. There are few limitations to the ability to solve problems, sell products, make decisions through the use of wireless technology. Automation is a main beneficiary of this wireless technology. It is possible to install a wireless enabled front-end or final control device into a system without the drawn out process of installing copper communication wire. An automation professional can essentially install the device in the process, power it up, and see the device connect to the wireless network. The hesitation that many automation professionals have concerning wireless is with security. They are concerned that hackers could intercept wireless signals for negative reasons. The security protocols should help minimize the concern in employing this technology in the future. The benefits in installing this technology should outweigh the limitations. Wireless technology is one technology that will help advance the effectiveness, efficiency, and cost of future automated systems.

System Integration

A second technology that should have profound effects on automation is in the continued development of methods to simplify the integration of systems. So much of automation is based in the interconnection of varied functional devices including front-end

transmitters, controllers, and final control elements. In many situations, the interconnections of these control elements are difficult if not impossible. The continued writing of standards and the improvement of plug-and-play technology will continue. To the automation professional, this will mean that designing and implementing control systems will continue to be more intuitive and straightforward. Just like one can expect to be able to trust that a USB device will transport from system to system, the automation system designer will be able to trust that individual devices may be interconnected into an automation system.

Smart Devices

The development of the single chip control device has brought about advances in the development of so called “smart devices”. A smart device has moved some of the computer processing from the central unit down to individual control elements. With the advances in network and wireless technology, we have seen great strides in the development of smart device technology. It is possible for a temperature measurement device using its own computer to complete measurement processes right at the device rather than using the time of the central controller. This make for a much more efficient system overall. The improvements and new developments in this field bodes well for the automation field.

Artificial Intelligence

A fourth and final technology that will have ramifications for the future is artificial intelligent (AI) systems. AI allows some decisions to be made by the system itself. For automation, this affords an opportunity to allow basic decisions about dynamic variables to be made at the device of by the central controller, without human intervention. AI technology will continue to find its way into automation systems.

Conclusion

There will be many additional innovations that have not even been thought of at this point that will produce increased effectiveness and efficiency by automated systems in the future. The future of automation is indeed one of continued development for the benefit of society. With and through automation, we will have the ability to have products and services that will exhibit the upmost quality, reliability, and benefit to everyone.

Reference

Caliel, Mike,”The Future of Automation” InTech, September/October 2012

SOFT COMPUTING IN INDUSTRIAL QUALITY CONTROL

Michail Krichevsky

Doctor of science, professor
Saint-Petersburg State University of Aerospace Instrumentation
Saint-Petersburg, Russia
mkrichevsky@mail.ru

Abstract

This paper discusses a quality control methods based on soft computing. The aim of the quality control in industrial application is to analyze the quality of industrial manufacturing activities. Signal processing systems can play a fundamental role in quality assessment since they can guarantee a high and constant quality inspection. The solution of quality control problems requires being able to tackle problems of different scientific areas (signal acquisition, signal preprocessing, feature selection and extraction, data fusion and classification). Soft computing techniques have been recognized in the literature as a good tool which can be used by the designer to achieve high quality.

Keywords – Quality control, Soft computing, Fuzzy logic, Neural networks, Quality assessment.

I. INTRODUCTION

The key element which is playing an important role in this research field is the family soft computing techniques: the techniques based on the usage of neural networks, fuzzy systems and evolutionary algorithms. The soft computing techniques offer new methods to make smarter, adaptive and intelligent the traditional signal processing systems and visual inspection systems. The soft computing methodologies can help the designer to compose quality control system modules in order to obtain more accurate and performing systems.

The main difficulty to solve the quality control problem consists in the need of being able to tackle problems of different scientific areas: the data acquisition (signal or image) requires knowledge of instrumentation and measurement systems, while the data preprocessing requires knowledge of image and signal processing. The proper quality control activities require knowledge of feature extraction, sensor fusion, system modeling and monitoring, data analysis and classification techniques. The research efforts led to the development of methodologies that try to integrate all the above activities to design visual inspection systems for the quality assessment.

Soft computing is an innovative framework for constructing intelligent hybrid architectures involving Neural Networks (NN), Fuzzy Inference Systems (FIS) and Evolutionary Computation (EC) [1]. In recent years, several adaptive hybrid soft computing frameworks have been developed for model expertise, decision support, image and video segmentation techniques, quality control and complicated automation tasks. Many of these approaches use a combination of different knowledge representation schemes, decision making models and learning strategies to solve a computational task. This integration aims at overcoming the limitations of individual techniques through hybridization or the fusion of various techniques.

In contrast with conventional techniques which only deal with precision, certainty and rigor, the guiding principle of soft computing is to exploit the tolerance for imprecision, uncertainty, low solution cost, robustness, partial truth to achieve tractability, and better rapport with reality. Table 1 lists the three principal ingredients together with their advantages [2].

Table 1. Comparison of different intelligent systems with classical approaches[1]

Model	**FL**	**NN**	**EC**
Mathematical model	SG	B	B
Learning ability	B	G	SG
Knowledge representation	G	B	SB
Expert knowledge	G	B	B
Nonlinearity	G	G	G
Optimization ability	B	SG	G
Fault tolerance	G	G	G
Uncertainty tolerance	G	G	G
Real time operation	G	SG	SB

[1] Fuzzy terms used for grading are good (G), slightly good (SG), slightly bad (SB) and bad (B).

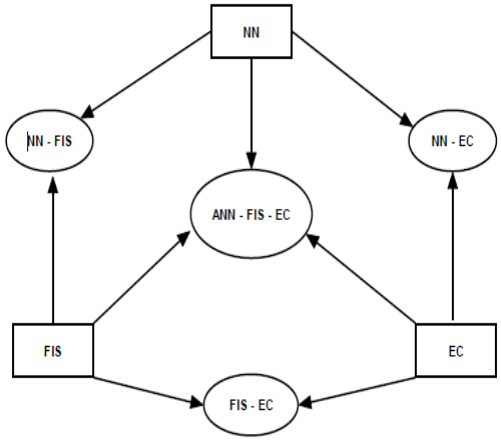

Fig. 1. General framework for hybrid soft computing architectures

To achieve a highly intelligent system, a synthesis of various techniques is required. Fig. 1 shows the synthesis of NN, FIS and EC and their mutual interactions leading to different architectures. Each technique plays a very important role in the development of different hybrid soft computing architectures. Experience has shown that it is crucial, in the design of hybrid systems, to focus primarily on the integration and interaction of different techniques rather than to merge different methods to create ever-new techniques. Techniques already well understood should be applied to solve specific domain problems within the system. Their weaknesses must be addressed by combining them with complementary methods.

II. QUALITY CONTROL IN INDUSTRIAL APPLICATIONS

The quality control systems aim to analyze and judge the quality of industrial manufacturing activities but these kinds of

activities involve repetitive tasks for the process control. The quality of the human visual inspection is thus typically subject to a progressive degradation to the visual fatigue and inattention. Recently the availability of reliable and visual acquisition devices and of high computing power hardware led to take into consideration the joint use of computers and machine vision for a non-invasive visual inspection. The automatic systems that perform visual inspection by means of machine vision are called automatic visual inspection system. These systems can play a fundamental role in quality control since they can guarantee a high and constant quality inspection. Reliable and high performance acquisition devices and microprocessors are nowadays available at low cost and the development of quality control systems is thus mainly limited by the capability of analysis and judging by the automatic inspection system (and not by the available hardware).

The design of a general quality control system must consider the following basic activities [3,4]:

1. ***Acquisition of data*** (signals or images) from sensors.
2. ***Preprocessing of data and feature processing*** in order to reduce the noise, compensate biases, correct aberrations in the images, enhance the signals.
3. ***Feature extraction and selection*** in order to better measure, describe and details the phenomena associated to the quality control problem.
4. ***Data fusion*** can be used to properly fuse the available features/sensors signals in order to obtain more significant and meaningful information concerning the quality of the observed industrial process.
5. ***Classification*** of the occurred situation in classes defined by the designer or production of a measure or an index of quality.

Hence the solution of quality control problems implies the need to manage techniques of different scientific areas: data
acquisition, data preprocessing and enhancing, feature extraction and selection, data fusion, approximation, and classification.

The last task is the most important among others problems because the production receive a measure of quality. Therefore we describe the tasks 1-4 briefly and devote the most attention to the problem of the classification.

Acquisition of data

The data acquisition (signal or image) is a typical problem of instrumentation and measurement systems. There are available techniques for sensor enhancement, sensor linearization, sensor diagnosis and sensor calibration (static and dynamic). The sensor modules can hence be more intelligent since they can self-calibrate and the undesired non-linearities can be reduced.

Preprocessing of data and feature processing

Signal preprocessing aims at correcting and enhancing the errors occurred in acquired data due to the acquisition devices. The preprocessing of a signal mainly aims to reduce the noise and to exploit the inherent information carried by the signal. Not only conventional but also computational intelligence techniques have been exploited for signal preprocessing.

1. *Feature extraction and selection*

Once the designer fixed all the features that will be processed from sensors, it is important to decide how to use them in order to obtain the quality

decision/measurement. For example, not of all of them can be necessary. The main reason to keep the dimensionality of the pattern representation (the number of features) as small as possible is to reduce the computational complexity of the system On the other hand, a reduction in the number of features may lead to a loss in the discriminant power that lowers the accuracy of the resulting quality control system. A limited yet salient feature set simplifies both the pattern representation and the classifiers structure that consequently will be faster and will use less memory.

Moreover, a small number of features can alleviate the "curse of dimensionality" problem when the number of samples in the available dataset is limited. The course of dimensionality problem refers to the requirement that the number of samples per feature increases exponentially with the number of features to maintain a given level of accuracy of the system. In other words, the more features will be used in the system, the larger must be the training dataset used to train the computational intelligence modules (for example the neural networks-based modules).

This important phase of the design of the quality control system is the *feature extraction* and *selection*. Very commonly, feature extraction precedes feature selection. The sequence of the two phases, whatever the order, represents a *dimensionality reduction phase*: the dimension of the final dataset is reduced, and therefore will be reduced the complexity of the computational intelligence module under training.

2. *Data fusion*

Soft computing techniques can be used to obtain meaningful information about the quality of the observed industrial process.

The first technique is called *sensor fusion*. Sensor fusion merges information from several sensors, possibly of different type, to create new combined measurements. The soft computing algorithms are commonly used in sensor fusion, where neural networks play a fundamental role.

Soft computing can be exploited also to create the so-called *virtual sensors*. The virtual sensors are systems capable to measure quantities without direct sensing the measured quantity, when direct sensing is not technically feasible or convenient by using indirect techniques, or incase of the desired quantity is difficult to be measured while other strictly related quantities can be measured. The soft computing techniques have been used to enhance and "virtualize" a great variety of sensors: image sensors, visual sensors, taste sensors, tactile and roughness sensors et al.

III. SOFT COMPUTING FOR CLASSIFICATION AND MEASUREMENT OF THE QUALITY

In this activity, the designer aims to produce a module that receives in input all the selected features and provides in output a value associated to the *classification* of the quality or an *index of quality*. The classification can be considered as the problem of partitioning the feature space into regions (one for each class). Ideally the classifier should take always correct decisions without ambiguous classifications or errors, but in practice we aim to reduce (or minimize) the classification error.

The key point of the transition from hard to soft computing is the observation that the computational effort required by conventional computing techniques sometimes not only makes a problem intractable, but is also unnecessary as in many applications precision can be sacrificed in order to accomplish more economical, less complex and more feasible solutions. Imprecision results from our limited capability to resolve detail and encompasses the notions of partial, vague, noisy and incomplete information about the real world.

In other words, it becomes not only difficult or even impossible, but also inappropriate to apply hard computing techniques when dealing with situations in which the required information is not available, the behaviour of the considered system is not completely known or the measures of the underlying variables are noisy. Soft computing techniques are meant to operate in an environment that is subject to uncertainty and imprecision. According to Zadeh [1], the guiding principle of soft computing is:

> exploit the tolerance for imprecision, uncertainty, partial truth, and approximation to achieve tractability, robustness, low solution cost and better rapport with reality.

All methodologies that constitute the realm of soft computing have been conceptualised and developed over the past fifty years. Each method offers its own advantages and brings certain weaknesses. Although they share some common characteristics, they are considered complementary as desirable features lacking in one approach are present in another. Consequently, after a first stage in which they were applied in isolation, the last decade witnessed an increasing interest on hybrid systems obtained by symbiotically combining the all components of soft computing. Fig. 3.1 shows some hybrid systems positioned in the corresponding intersection of soft computing techniques.

Among all methodologies NN and FL models are the relevance tools for the classification and the measurement of the quality. They perform in the same way after the learning stage of NN or the embedding of human knowledge about some specific task of FL is finished. They are two sides of the same coin [2]. Whether the more appropriate tool for solving given problem is an NN or an FL the availability of previous knowledge about the system to be modeled and the amount of measured process data.

The classical NN and FL system paradigms lie at the two extreme poles of system modeling (fig.2). At the NN pole there is a black box design situation in which the process is entirely unknown but there are examples (measurements, records, observations, samples, data pairs). At the other pole (the FL model) the solution to the problem is known, that is, structured human knowledge (experience, expertise, heuristics) about the process exists. Then there is a white box situation. In short, the less previous knowledge exists, the more likely it is that an NN, not an FL, approach will be used to attempt a solution, The more knowledge avail suitable the problem will be for the application of fuzzy logic modeling. On the whole, both tools are aimed at solving pattern recognition (classification) and regression (multivariate function approximation) tasks.

a) Neural Networks - Black Box
No previous knowledge, but there are measurements, observations, records

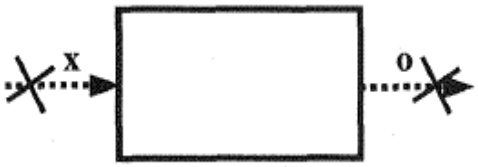

b) Fuzzy Logic Models - White Box
Structured knowledge (experience, expertise, or heuristics). No data required. IF-THEN rules are
the most typical examples of structured knowledge

*Fig.2 Neural networks (a) and fuzzy logic models (b) as examples of modeling approaches (**x**-input; **o** – output)*

In many instances, we have both *some knowledge* and *some data.* This is the most common *gray box* situation covered by the paradigm of neuro-fuzzy or fuzzy-neuro models.

In order to avoid too high (or too low) expectations for these new concepts of computing, particularly after they have been connected with intelligence, it might be useful to list some advantages and disadvantages that have been claimed for NNs and FL models. Table 2 summarizes the comparison between NNs and FL models [2]. To a large extent, the drawbacks pertaining to these two approaches seem complementary.

Table 2. Comparison between neural networks and fuzzy inference systems

Neural Network	Fuzzy Logic Models
Difficult to use prior rule knowledge	Prior rule-base can be incorporated
Learning from scratch	Cannot learn (linguistic knowledge)
Black box	White Box
Complicated learning algorithms	Simple interpretation and implementation
Difficult to extract knowledge	Knowledge must be available

IV. NEURAL NETWORKS FOR QUALITY CONTROL

Artificial neural networks are the software models inspired by the structure and behavior of biological neurons and the nervous system, but after this point of inspiration all resemblance to biological systems ceases.

Feedforward neural networks are the models used most often for solving nonlinear classification and regression tasks by learning from data. In addition, feedforward NN are mathematically very close, and sometimes even equivalent, to fuzzy logic models. NN and FL approximation techniques can be given graphical representation, which can be called a neural network or a fuzzy logic model.

Neural networks are composed of many computing units popularly called neurons. The strength of the connection or link, between two neurons is called the weight. The values of the weights are true network parameters and the subjects of the learning procedure in NNs. Depending upon the problem they have different physical meanings, and sometimes it is hard to find any physical meaning at all. Their geometrical meaning is much clearer. The

weights define the positions and shapes of basis functions in NN.

The neurons are typically organized in layers in which all the neurons usually possess the same activation functions (AF). The genuine neural networks are those with an input layer and at least two layers of neurons - a hidden layer (HL) and an output layer (OL) - provided that the HL neurons have nonlinear and differentiable AF. Such an NN has two layers of adjustable weights that are typically organized as the elements of the weight matrix **V** and **W**. The matrix **V** is the matrix of the hidden layer weights and matrix **W** comprises the output layer weights.

The nonlinear activation functions in HL neurons enable the neural network to be universal approximator. Thus the nonlinearity of the AF solves the problems of representation. The differentiability of AF in the hidden layer makes possible the solution of nonlinear learning.

Usually the input layer is not treated as a layer of neural processing units. Generally there will not be any processing in the input layer, and although in its graphical representation it looks like a layer, the input layer is not a layer of neurons. Rather, it is an input vector, eventually augmented with a bias tern, whose components will be fed to the next (hidden or output) layer of neural processing units. The neurons may be linear ones (for regression types of problems) or they can have sigmoidal AF (for classification). An elementary feedforward neural network is shown in fig.3.

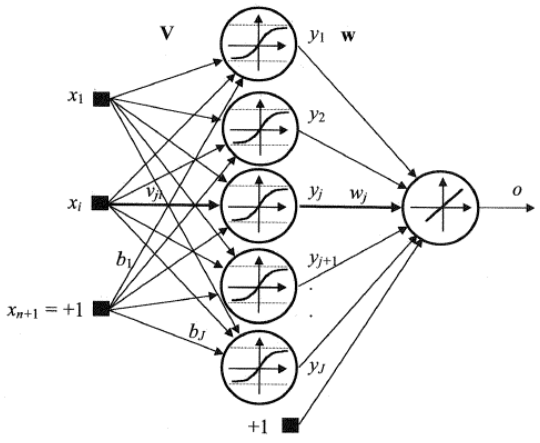

Fig.3. Feedforward neural network

Example 1. Tabl.3 contains the data about the two classes of objects: first (the fit class) and second (the defect class). This table is the base of examples for the training NN.

Table 3. Base of examples

	1 X1	2 X2	3 X3	4 X4	5 Class
1	40	15	1	53	1
2	43	5	1	52	1
3	35	6	0	41	2
4	27	6	1	70	1
5	36	3	0	28	2
6	30	12	1	48	2
7	41	13	1	38	1
8	35	4	1	42	1
9	27	7	0	42	1
10	38	18	1	61	1

There are all 60 examples in the table 3: 33 objects belong to the first class and 27 objects belong to the second class.

Fig. 4 displays the neural network for the base of examples of table 3. NN contains four neurons in the input layer, eight neurons in the hidden layer and one neuron in the output layer.

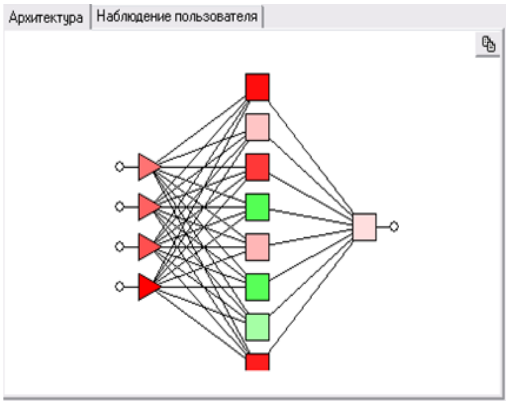

Fig.4 Architecture of neural network

The value of learning's quality of NN is showed in the table 4 (matrix of classification).

Table 4. Matrix of classification)

	Классификация (4) (Таблиц	
	STATUS.1.4	STATUS.2.4
Всего	33,00000	27,00000
Правильно	25,00000	21,00000
Ошибочно	8,00000	6,00000
Неизвестно	0,00000	0,00000
% правильных	75,75758	77,77778
% ошибочных	24,24242	22,22222
% неизвестно	0,00000	0,00000

Классификация (4) (Таблица_Кредитное_каче

The results of the learning aren't error-free: 8 objects of the first class and 6 objects of the second class are sorted wrong. Nevertheless we can use this NN for the classification of the new objects.

Table 5 shows the result of this sorting: the new object belongs to the second class.

Table 5. Result of sorting

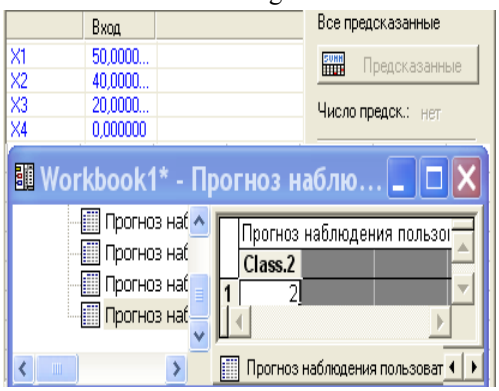

Thereby the neural network can use for the evaluation of the quality's measure: NN determines the label of the class.

V. FUZZY LOGIC FOR QUALITY CONTROL

Our understanding of most physical processes is based largely on imprecise human reasoning. This imprecision (when compared to the precise quantities required by computers) is nonetheless a form of information that can be quite useful to humans. The ability to embed such reasoning in hitherto intractable and complex problems is the criterion by which the efficacy of fuzzy logic is judged.

Fuzzy logic lies at the opposite pole of system modeling with respect to neural network methods. It is a white box approach (fig.2.b) in the sense that it is assumed that there is already human knowledge about a solution. Therefore, the modeled system is known (i.e., white). On the application level FL can be considered an efficient tool for embedding structured human knowledge into useful algorithms. It is a precious engineering tool developed to do a good job of trading off precision and significance. In this respect, FL models do what human beings have been doing for a very long time. **As** in human reasoning and inference, the truth of any statement, measurement or observation is a matter of degree. This degree is expressed through the membership functions that quantify (measure) a degree of belonging of some (crisp) input to given fuzzy subsets.

Fuzzy systems are universal approximators [6]. These proofs stem from the isomorphism between two algebras – an abstract algebra (one dealing with groups, fields, and rings) and a linear algebra (one dealing with vector spaces, state vectors, and transition matrices) – and the structure of a fuzzy system, which comprises an implication between actions and conclusions (antecedents and consequents). The reason for this isomorphism is that both entities (algebra and fuzzy systems) involve a mapping between elements of two or more domains. Just as an algebraic function maps an input variable to an output variable, a fuzzy system maps an input group to an output group; in the latter these groups can be linguistic propositions or other forms of fuzzy information.

The classical control methodologies developed mainly for engineering are usually based on mathematical models of the objects to be controlled. Mathematical models simplify and conceptualize events in nature and human activities by employing various types of equations which must be solved. However, the use of mathematical models gives rise to the question how accurate they reflect reality. In complicated cases the construction of such models might be impossible.

Fuzzy models will become more and more popular as solution schemes, and it will make fuzzy systems theory a routine offering in the classroom as opposed to its previous status as a "new, but curious technology." Fuzzy systems will be a standard course in any science or engineering curriculum. It contains all of what algebra has to offer, plus more, because it can handle all kinds of information not just numerical quantities.

After all the design steps and computation have been completed, this is final model is a very precisely defined nonlinear function [7]. By choosing the complexity of the rule basis, one can control the precision of the fuzzy model and trade that off against solution costs. Thus, one first defines the most relevant input and output variables for a problem. In fuzzy logic terns, one must define the universes of discourse, i.e., the domains and the ranges of relevant variables. Then one specifies what is *low, medium, high, cold, hot* and so on, in a given task. In fuzzy logic terns, one defines the fuzzy membership functions (fuzzy subsets or attributes) for the chosen input and output variables. Then one structures the knowledge in form of IF-THEN rules, that is, fuzzy rule. The final stage is to perform the numerical part (applying some inference algorithm) and to defuzzify the resulting fuzzy subsets.

Fuzzy sets and fuzzy logic applied to control problems form a field of knowledge called fuzzy logic control. The goal of control in engineering is action. It might be also evaluation, instruction, conclusion, forecasting. A block diagram for control processes is depicted in fig. 5.

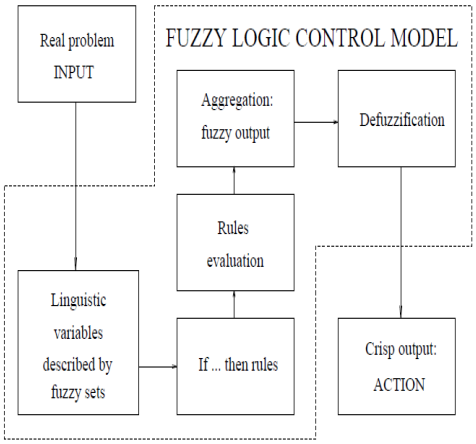

Fig.5 Block diagram for fuzzy logic control process

Example 2. Fig.6 displays fuzzy logic control for 4 input variables and one output parameter. This system is destined for the assessment of the object's quality. The quality of this object is described by four input features.

The output parameter determines the value of quality by means of the continuous scale.

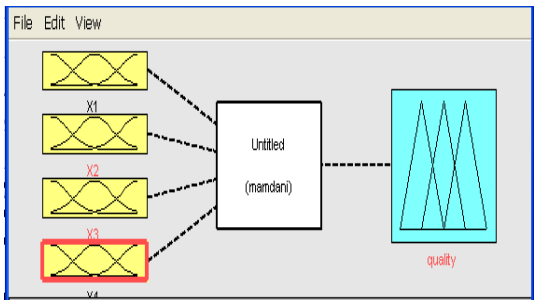

Fig.6. System of fuzzy logic control

The control objective is for any given set of input variables to find a corresponding output – quality of object. Each of input parameters is the linguistic variable with three terms: *small, middle, high*. As example fig.7 shows membership functions for the first variable.

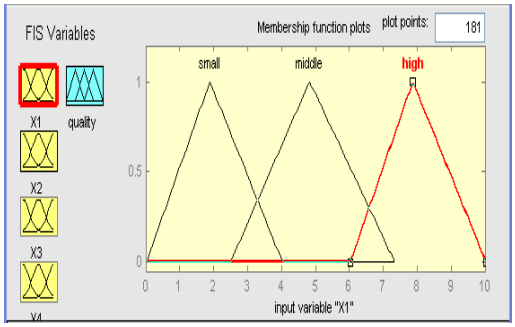

Fig.7. Membership functions for the first input variable

After the forming base of rules the system of fuzzy logic control gives the value of quality as conditional units. Fig.8 displays the value of quality equal 83 points for given set of input variables: *X*1 = 9,2; X2 = 8,4; X3 = 9,2; X4 = 9.

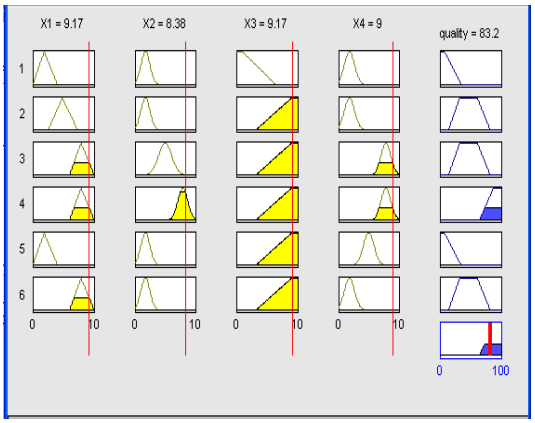

Fig.8. Result of system of fuzzy logic control (1)

For another set of input variables the value of quality equal 13 points (fig.9).

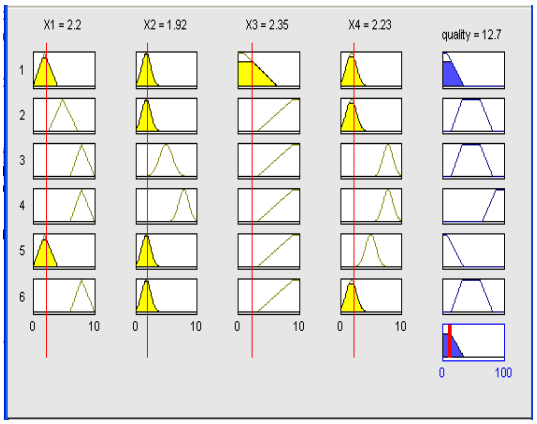

Fig.9. Result of system of fuzzy logic control (2)

VI. CONCLUSION

This paper presents a opportunity of use the soft computing methods in the problem quality control. The neural networks and fuzzy logic models show the ability to get the measure of quality: discrete and continuous. Performed examples emphasize the reality of decision of the quality control's problem.

REFERENCES

1. Заде Л.А. Роль мягких вычислений и нечеткой логики в понимании, конструировании и развитии информационных интеллектуальных систем. - Новости искусственного интеллекта, 2001, №2-3, с.7 – 11.

2. A. Abraham. Adaptation of Fuzzy Inference System Using Neural Learning, StudFuzz. 2005, 181, p.53–83.

3.V.Piuri ,F. Scotti, M. Roveri. Computational Intelligence in Industrial Quality Control. Intelligent Signal Process., IEEE International Workshop, Faro, Portogallo, 2005. p.4-9.

4. Y. Dote, S. J. Ovaska. Industrial Applications of Soft Computing: A Review. Proc. of IEEE, v. 89, 9, 2001.p.1243-1265.

5. V.Kecman. Learning and Soft Computing - Support Vector Machines, Neural Networks, and Fuzzy Logic Models. The MIT Press, London, 2001. - 576p.

6. T.J.Ross. Fuzzy Logic with Engineering Applications. John Wiley & Sons Ltd, United Kingdom. 2010. - 607p.

7.V.Bojadziev, M.Bojadziev Fuzzy logic for business, finance and management. World Scientific, New Jersey, 2007. - 232 p.

AN ARCHITECTURE FOR BIKE TO INFRASTRUCTURE COMMUNICATION.

Turi Gagliano, Alberto Giuffrida

Department of Electrical, Electronics and Informatics Engineering
University of Catania
Viale Andrea Doria, 6 -95125 Catania, Italy

Abstract

In this work, we discuss the architecture a system for bike to Infrastructure communications. This system allows us to capture data inherent to the transit of bicycles along an established path and makes such information available through the internet. The system detects the speed of the bike, temperature of the ambience, bumps on the road, accidents and position of the bikes in the group.

1. Introduction

The technological evolution in progress and the availability of pervasive network has enabled the development of mobile communications between vehicles and between vehicles and infrastructure for the exchange of information in support of mobility. This type of communication has been developed especially for cars and is aimed to increase safety in traffic [1]. Through the exchange of information concerning the speed of the vehicles, their distance and the traffic conditions, the driver can react in a timely manner upon the occurrence of abnormal conditions and avoid accidents [2].

The communication between a vehicle and infrastructure can also be very useful in a different context from cars. In this paper we propose a communication architecture suitable to the monitoring of bicycles that move in extra-urban areas in order to check their position and take action quickly in the event of accidents. In several countries, where bicycles are widely used, dedicated Bike paths are available, often far away from high-traffic roads, enabling cyclists to move without the danger of a collision with some car. On the one hand, these routes are very comfortable, on the other cyclists often travels alone and in case of an accident due to an illness or a fall, it can take up to a long time to get help. For this reason, the availability of a suitable communication infrastructure that allows to detect the position of the cyclist, monitor its condition and acquire also information on the state of the path may be very useful [3].

Consider the case of travel agencies that organize trips on bike paths particularly beautiful, who need to take action if any of its customers has some problems. In addition, if information about the biker can be made available on an appropriate server on the Internet, it can be monitored from anywhere in the world and therefore in the event of an organized trip to faraway places, the family may have information on the evolution of the journey by simply logging in to the server.

The structure is composed by three main elements:

- Dynamic entity: the sensor located on the bike;
- Static entity: a network of receivers along the route;
- Remote entity: the web server that stores the data in a Sql database and displays information about the bikers.

The bikes move along the track and continuously send information to the fixed nodes along the road, which are in turn provided with 3g modules, or connected by a wire network; These nodes then send their data to the web server.

2. Data acquisition

The main data to be acquired are the speed of the bike, the temperature of the track, the presence of bumps on the road, and accidents. The position of the bike in a group, the distance traveled and the average speed are calculated by the web server , whereas the fixed nodes only collect data and transfer them through the network to the web server.

The measurement of the speed is obtained using an odometer installed on the bike, querying it every two seconds. This should allow a continuous detection of the position of the bike on the path. The knowledge of the speed of the bike allows to compute its position

between a fixed node and the following and therefore have an accurate localization of the position of the rider. This information is useful not only for remote monitoring of the rider but also to allow other bikers of a group to know the position of each of them. Temperature of the track is acquired by fixed nodes, with the possibility to split the path in climatic zones (flats, hills, mountains). Those measurements are done every 10 minutes and are available to the biker which can organize his travel according to the weather conditions.

The presence of holes or irregularities of the bottom along the road can be detected by a mems accelerometer, as bumps and holes make impulsive acceleration which are easily recognizable. In this way, the cyclist during his trip can collects valuable information on the state of the road and communicate them the web server. This information can be used to plan maintenance or to warn other riders of the potential hazards. In the rare case of an accidental acceleration, we can assume a bump or a hole, and using the bike speed and the time of the event notification, the server can allocate the hazard and notify it.

Accidents are recognized using acceleration and rotation (as a fallen bike has its slope of about $\pi/2$ from the vertical).

3. Data transmission

For communication between the nodes fixed bicycles and we have chosen to use the ZigBee protocol [4], which has allowed us to create nodes of small size, light weight and low power consumption. ZigBee (802.15.4 standard) has the following features:

Frequency	Number of Channels	Band	Max Devices Supported
2.4 – 2.4835 GH/z	16	250 Kb/s	65000

We use variable length frames during communication, which allow us to optimize the throughput.

The technology we adopt operates on a different band from that of cellular phones or radio devices which can be used by the bikers, for this reason there is no interference with this type of devices. However, we can have shadow areas along the track created by the electromagnetic noise produced by Wi-Fi networks used to communicate between the fixed nodes. The Wi-Fi carrier frequency, defined by the standards, is 22 MHz; a ZigBee can occupy 5MHz, so every channel of Wi-Fi network we lose 4 ZigBee channels. In the case a biker goes through a shadow area, and a bike sensor can't send its data, it memorize those data in a buffer

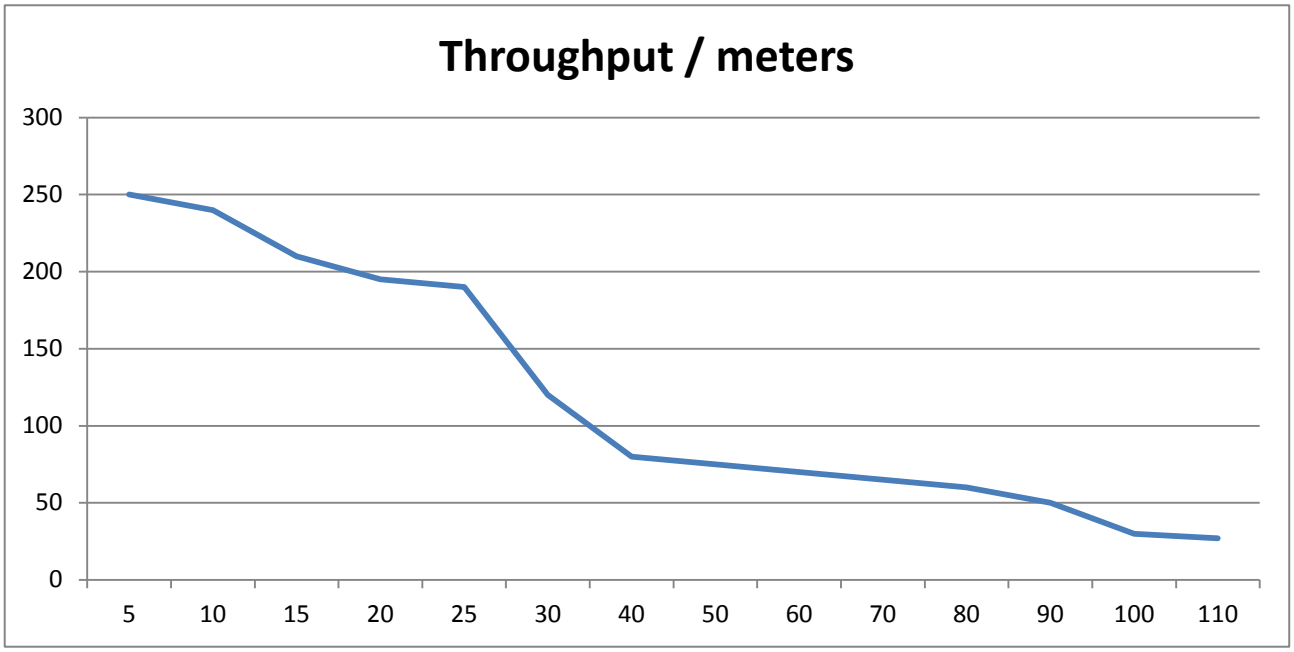

and send as soon as possible, when the biker leaves the shadow area.

The positioning of fixed nodes along the track must be done with attention to the electromagnetic noise and to the distance which can be covered by ZigBee nodes. The diagram above shows how the throughput of ZigBee transmitters decreases gradually increasing distance from them; those values are observed in a residential area, a good biking course. In an unpopulated area, the total absence of noise improves the measurement.

It is interesting to calculate the maximum communicating distance between two MB950 ZigBee modules, the ones we used in our testing. In eyesight condition, the distance is very good, in the order of 300 meters (about 984 feet), optimum for sending alarm signals. On the other side, adding obstacles the maximum distance strongly decreases in presence of angles like perimetral walls or similar. So the graph shows the throughput variation along a track with trees and little buildings. So the positioning of the course sensors should be done every 300-350 meters (984-1148 feet) in straight areas, and to be lowered when near a turn.

4. Data storage

To store data preserving the temporal order, we used a transmitter FIFO buffer. So in case we lose the signal, the bike sensor store the data in exact sequence, so they can be downloaded to the next track sensor when it will be in range. Normally every stored data is quickly sent leaving the pile empty, so the server can have updated and fresh data.

In case a track sensor is broken, like in Fig. 1, (showing in green two working sensors, and in red the faulty one), a bike, represented by an arrow, leave the left track sensor. The bike is now in the faulty sensor area, indicated by the red arrow, so the bike sensor store the data in its pile, until it reach the third working sensor, were it will download all the data; in case of a great number of bikers, and to avoid both very long frames and a big Frame Error Rate (FER), we established a 40 byte maximum length for every frame: in case not all the data fit a frame, it will be send another frame.

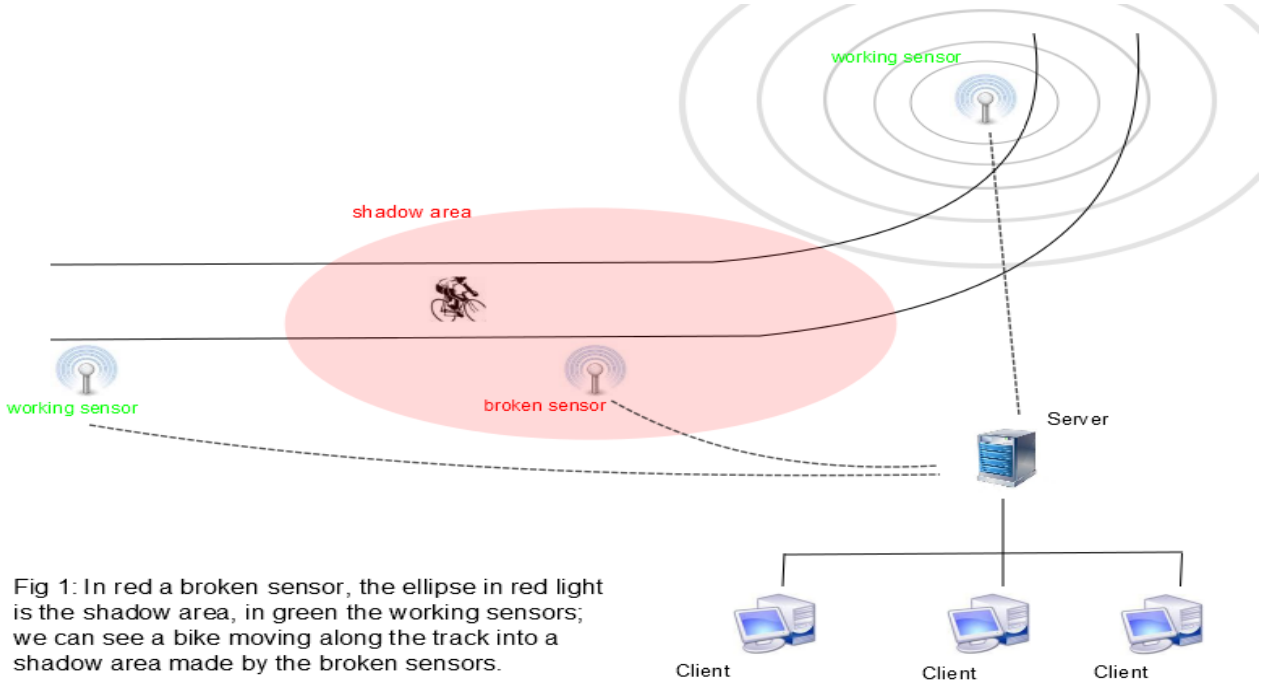

Fig 1: In red a broken sensor, the ellipse in red light is the shadow area, in green the working sensors; we can see a bike moving along the track into a shadow area made by the broken sensors.

5. Bump and accident recognition

To recognize acceleration caused by falls and bumps, we used a three axis accelerometer. These axes could be measured in positive and negative values depending on the verse of the acceleration. In normal and resting position, only the Z (vertical) axis will be moved, because every body, on the terrestrial surface, is attracted by the ground because of the gravity force. The accelerometer is build to measure static acceleration (like a wrist rotation) or a dynamic rotation (like a running car). For tilt sensing application we use the static acceleration: we assume that in every body the only constant and always present acceleration force is the gravity force. To let the sensor recognize falls, first thing was measuring axis rotation, and express them with these formulas:

Rotation angle towards Y axis:

$$\theta = \arctan\left(\frac{A_x}{\sqrt{A_y^2 + A_z^2}}\right)$$

Rotation angle towards X axis:

$$\varphi = \arctan\left(\frac{A_y}{\sqrt{A_x^2 + A_z^2}}\right)$$

With an accelerometer is not possible to measure the yaw angle, but we can use as a reference the horizontal vector and the gravity acceleration vector and using the formulas we can calculate the angle between two different references:

Horizontal Vector Angle:

$$\Phi = \arctan\left(\frac{A_z}{\sqrt{A_x^2 + A_y^2}}\right)$$

Gravity Vector Angle:

$$\Phi = \arctan\left(\frac{\sqrt{A_x^2 + A_y^2}}{A_z}\right)$$

Using a cheap sensor coupled with a simple processor (in the experiment, we used a MB950, coupled with a STM32W108 ARM processor), the calculation time would be too long to, so we used another way : a simple check on the norm of the acceleration vector and a simple analysis of the three axis component vectors. After have fixed a threshold, for example an acceleration of 2g, we use the classical physic formula:

$$\text{Acceleration} = \sqrt{|x_i - x_f|^2 + |y_i - y|^2 + |z_i - z_f|^2}$$

If a threshold is exceeded, a bump is detected and the values of axes X, Y and Z are stored. If after a time interval those X and Y values are high, and Z value is minimal, then the bike is not in balance anymore, but it will be laid in the ground. So the sampling function are stopped, the formulas are calculated again to see if the bike is really fallen. If after the time interval normal values for X, Y and Z are read, a bump is recorded.

6. Conclusions

In this paper we have presented the architecture of a Bike-to-Infrastructure communication system and discussed its possible applications. Although cars are now the most popular mode of transport, and they focused all efforts to increase the safety and functionality, should not be overlooked that the decrease in non-renewable resources is pushing other means of transport. Among all the bicycle is certainly the most eco-friendly and has the least impact on the environment and for this reason its use is growing. Therefore it is important to begin to design systems to support the mobility by bike. Our paper has aimed to provide a small contribution in this direction.

References

[1] KyungBok Sung, JaeJun Yoo, DoHyun Kim, "Collision Warning System on a Curved Road using Wireless Sensor Networks", IEEE 66th Vehicular Technology Conference, VTC-2007 Fall.

[2] F. Ye, M. Adams, and S. Roy, “V2V wireless communication protocol for rear-end collision avoidance on highways,” in Proc. IEEE International Conference on Communications, pp. 375–379, May 2008.

[3] Eisenman, S. B., Miluzzo, E., Lane, N. D., Peterson, R. A., Ahn, G.-S., and Campbell, :”BikeNet: A mobile sensing system for cyclist experience mapping”. ACM Trans. Sensor Netw. 6, 1, Article 6 (December 2009).

[4] Homepage of ZigBee™ Alliance, http://www.zigbee.org/

EVOLUTION OF INTEL MICROPROCESSORS

Denis Ikonnikov

Saint-Petersburg State University of Aerospace Instrumentation,
Saint-Petersburg, Russia

denis-ikonnikov@mail.ru

ABSTRACT

A microprocessor is an essential part of a personal computer. Intel is the leading producer of microprocessors in the sector of desktop and mobile computers. The advent of computers on integrated circuits has transformed modern society. General-purpose microprocessors in personal computers are used for computation, text editing, multimedia display, and communication over the Internet. Intel has done significant work to make these features available to the world and Intel continues to improve its technology.

I. ERA OF INTEGRATED ELECTRONICS

To start with, it is essential to state what microprocessor is. A microprocessor combines the functions of a computer's central processing unit (CPU) on a single integrated circuit (IC) or no more than a few IC. It is an all-purpose, programmable device that accepts digital data as input, processes it according to commands stored in its memory, and provides results as output.

Intel produces microprocessors starting from the first, released in 1971. Many of them presented new significant improvements that are described below.

The 4004 microprocessor appeared in 1971 and was Intel's first microprocessor. This invention started the era of integrated electronics.

1972 was the year of the 8008 microprocessor. It was two times more powerful than the 4004 microprocessor. The 8008 became the brains of the device called the Mark-8 that is considered to be one of the first computers made for the home use.

1974 was marked by the 8080 microprocessor. It became the part of the first personal computer—the Altair. Intel 8080 is thought to be the first true general-purpose processor. Thanks to The Intel 8080 microprocessor video games and home computers became possible.

In 1978 Intel presented the 8086 microprocessor that was the first 16 bit processor and it was about ten times more efficient than its predecessors.

In 1979 Intel sold the new computer to IBM. The 8088's success raised Intel into the ranks of the Fortune 500, and the company was called by Fortune magazine as one of the "most successful in the Seventies."

The Intel 286 that is originally known as the 80286 was presented in 1982. All the software that was written for previous models could be run on this processor. This software compatibility remains a specialty of Intel's family of microprocessors.

In 1985 Intel introduced the Intel386 microprocessor. It was 32-bit and was "multi-tasking". It meant it could run multiple programs at the same time.

The next Intel's milestone was the Intel486 microprocessor. The Intel486 processor was the first microprocessor that allowed going from command-level computer to point-and-click computing. The Intel486 processor was the first processor that presented a new feature—built-in math coprocessor, which increased the speed of computing because it offloaded complex math functions from the central processor.

The advent of Intel's fifth generation processors was set in 1993 with the introduction of the Intel Pentium processor which made possible to easier process data from the "real world" such as graphics procession, sound and multimedia in particular.

Next generation of microprocessors was introduced in 1995 when Intel launched The Pentium Pro processor. It owes its greater performance to an innovation called Dynamic Execution. This technology made possible greater 3D visualization and interactive technologies.

The successor of the Intel Pentium—the Intel Pentium II, presented in 1997, featured serious improvement in performance in comparison with previous Intel Architecture processors. It was based on the combination of the P6 microarchitecture and Intel MMX.

Intel continued its line of Pentium microprocessors, introducing in 1999 the Intel Pentium III processor. It featured 70 new instructions that significantly improve multimedia applications. It utilized a low-power state to conserve power during idle times.

The seventh generation of microprocessors owes to the Intel Pentium 4 processor, introduced in 2000, that brought us in the age of the nanotechnologies. Intel's first microprocessor, the 4004, ran at 108 kilohertz (108,000 hertz), compared to the Intel Pentium 4 processor's initial speed of 1.5 gigahertz (1.5 billion hertz). If automobile speed had increased similarly over the same period, you could now drive from San Francisco to New York in about 13 seconds. [1]

II. TRANSISTORS AND MOORE'S LAW

Transistors are the main components of microprocessors. Transistors are miniature electronic switches. They are the blocks of the microprocessor that are the basis of the computer. As the light switch, transistors have two positions, on and off. This process of on/off allows transistors to process information in a computer.

In 1965, Intel co-founder Gordon Moore predicted that the number of transistors on a chip would double about every two years. [2] This point was called Moore's Law. Since then, Moore's Law has made revolution as Intel exponentially increased the number of transistors in processor.to increase productivity and energy efficiency.

Moore's Law and code names of microprocessors that Intel produced in different periods of time are shown in fig.1. Those, who brought significant changes are described in history above. It is clearly seen that the number of transistors doubles about every two years.

Moore's Law is the starting point for new technological capabilities and improved energy efficiency. It is the engine of semiconductor industry.

It is interesting that in 1978, the flight from New York to Paris cost around $900, and the flight lasted for about 7 hours. If the airline industry had developed in accordance with Moore's Law, now your ticket on the same route would cost less than a cent, and the flight would take less than one second.

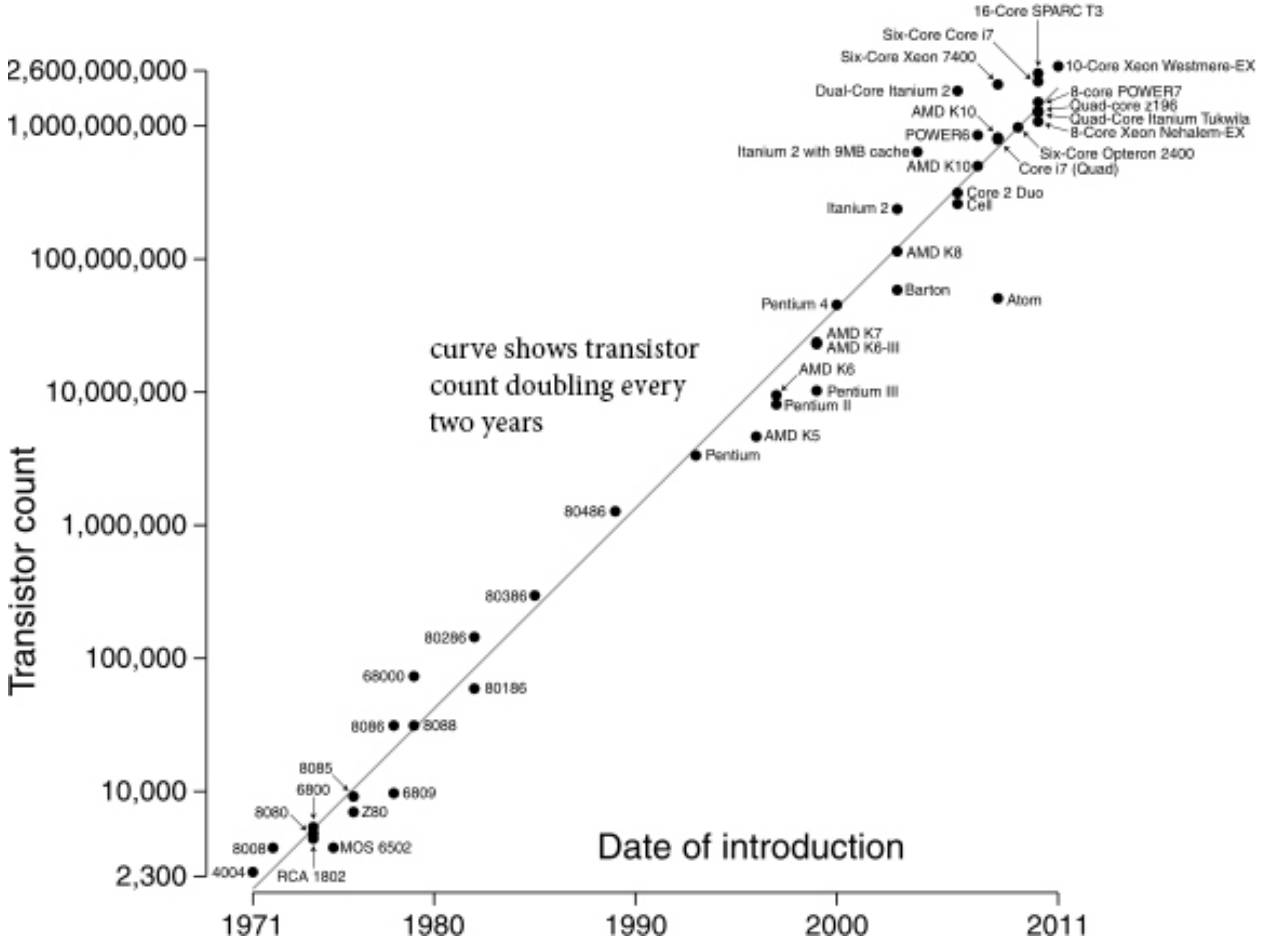

Fig. 1. Moore's Law

III. "TICK-TOCK" MODEL

"Tick-Tock" is a model that was approved by Intel in 2007 aimed at the control of every change in microarchitecture with a shrink of the technological process. Every "tick" corresponds to the shrinking of the process technology based on the previous microarchitecture and every "tock" creates a new microarchitecture. Every year, there will be either "tock" which is a derivative architecture or "tick" with a new architecture.

Intel's "tick-tock" model guarantees that the development of the future microprocessors is determined and Intel will deliver new outstanding features in accordance with this model.

A tick advances manufacturing technology.

A "tick" cycle occurs every two years: Intel advances manufacturing process technology and continues follow Moore's Law. So, increase in transistor density gives new capabilities, higher performance, and greater energy efficiency within a smaller, more productive version of the previous "tock" microarchitecture.

For example, the introduction of Tri-Gate transistors for the 22nm manufacturing process technology corresponded to a “tick”. This new technology brought better performance and extended the battery life of smartphones, tablets.

It is important to mention that Intel's microprocessor “ticks” are usually very conservative on the architecture side, which limits the performance improvement. [3]

A tock delivers new microarchitecture.

Using the previous “tick” Intel presents the next greater innovations in microarchitecture of microprocessor. This big innovation falls on alternating “tock” cycles. The main goal of Intel microarchitecture advancements is to improve energy efficiency and performance, as well as functionality, encryption/decryption, video transcoding, and other integrated capabilities.

In general, the Tick-Tock model is shown in Fig. 2.

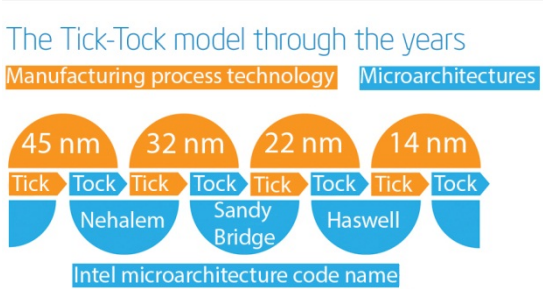

Fig. 2. The Tick-Tock model through the years

As it can be seen in fig. 2 the first Intel microarchitecture in “Tick-Tock” model had code name Nehalem. It considerably advanced computing and it was based on the 45nm manufacturing process technology. In the subsequent “tick”, Intel made even faster computing speeds, reduced power consumption, and introduced more advanced applications with the release of Intel Core processor family on 32nm. In the “tock” that followed Intel improved performance in games, HD video, Web, and many more with introduction of Intel new microarchitecture code name Sandy Bridge based on 32nm process technology. Ivy Bridge was the next “tick” which was a mild upgrade that shrunk technological process to 22nm and dropped power consumption.

Currently, the most advanced microarchitecture has code name Ivy Bridge. The next microarchitecture called Haswell is to be released in May-June 2013.

IV. SHAPING THE FUTURE

Intel continues to shrink transistor sizes, develop new technologies, and release new microarchitectures according to the "tick-tock" model. This approach is the basis of today’s industry and it will continue to be it in the future.

The evidence of Moore’s Law is everywhere, in all devices that people use today, such as personal computers, laptops, mobile phones, and home appliances, and also inspires on new technological innovations in automobile industry, medical devices, and spacecrafts.

Researchers in Intel Company think that they solved the problem of 10nm manufacturing process. On this stage new chips will consume very little power. The 10nm solution may rely on a number of experimental technologies as photonics, graphene, materials synthesis, dense memory, nanowires, extreme ultra violet lithography (EUV) and updated tri-gate transistors. [4]

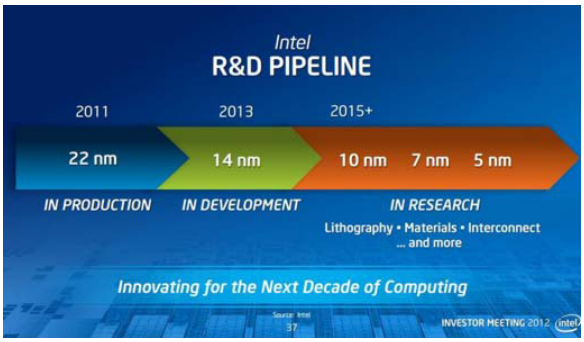

Fig. 3. Intel R&D pipeline

It follows from fig. 3 that Intel already has ideas for 10nm, 7nm and 5nm processes. Taking the timeframe into consideration, Intel says 10nm chips will appear in 2015, with work on 5nm technology beginning that same year.

The company is preparing fabs in the USA and Ireland to make chips using the 14nm fabrication method. Fabs are shown in fig. 4.

Fig. 4. Intel future fabs

There are also negative standpoints. Currently, all technological process is based on the usage of silicon. In about 10 years it will be impossible to use silicon. Intel has already admitted that it becomes harder and harder to sustain Moore’s Law as it was firstly predicted by Gordon Moore. That is why Moore’s Law cannot be named the “Law”. It can be treated as a point that was previously considered to be the “Law”. For all technological process is shrinking it is harder to use silicon, that is why we are seeing Tri-Gate transistors used in Ivy Bridge CPUs. It is an effort to extend the effective life of silicon.

The problem is two-fold: heat and leakage. Today’s Intel processors have a layer that is almost down to 20 atoms across. When the technological

process is down to 5 atoms than it is “all over”. In this case, the heat that is generated in chip will be so high that the chip will be simply melt. The other concern is leakage. We simply wouldn’t know where the electron is anymore.

In the next 10 years scientists will change Moore’s Law in order to extend its life. After that, we will be seeing the appearance of molecular computers that will be followed by quantum computers later in the 21st century. [5]

V. CONCLUSION

Intel has made many significant changes in their microprocessors since the beginning. It will contunue to follow “Tick-Tock” model and shrink the manufacturing process technology as it was predicted my Gordone Moore but Intel will have to think of a new point as Moore’s Law cannont be named the “Law”. In the coming decades Intel will face new challenges that will have to be solved to continue to improve its technologies and remain the leader.

REFERENCES

[1] Intel processor history. Retrieved January 22, 2013 from http://download.intel.com/pressroom/kits/IntelProcessorHistory.pdf

[2] Moore’s Law inspires Intel innvotations. Retrieved Frebuary 1, 2013 from http://www.intel.com/content/www/us/en/silicon-innovations/moores-law-technology.html

[3] AnandTech - The Ivy Bridge Preview: Core i7 3770K Tested. Retrieved February 16, 2013 from http://www.anandtech.com/show/5626/ivy-bridge-preview-core-i7-3770k/

[4] Intel: we know how to make 10nm chips | ZDNet. Retrieved Ferbuary 6, 2013 from http://www.zdnet.com/intel-we-know-how-to-make-10nm-chips-7000004170/

[5] Physicist predicts Moore’s Law will collapse in about 10 years – TechSpot. Retrieved March 1, 2013 from http://www.techspot.com/news/48409-physicist-predicts-moores-law-will-collapse-in-about-10-years.html

OVERVIEW OF IMAGE PROCESSING METHODS IN IRIS BIOMETRIC SYSTEMS

Kinderknecht Regina

Saint-Petersburg State University Of Aerospace Instrumentation,
Saint-Petersburg, Russia
mykinderknecht@yandex.ru

Abstract

The paper provides an overview of the image processing methods in biometric systems for identification of iris. Are general requirements applicable to such methods to meet specialized needs.

I. Introduction

Now systems of identification of the person to unique biometric indications actively develop. Biometric identification is used in enterprise systems of identification of employees, security, payment systems, are applied to carrying out of passport control and many other things.

The most widespread biometric systems are systems on the basis of fingerprints. But the most protected from spoofing are such indications of the person as DNA and an eye iris. DNA usage inconveniently for wide application. Usage for identification of an individual of an iris of an eye possesses following advantages:

- High informative;
- Genetic independence and uniqueness;
- Reflex response to exterior stimuli;
- A non-contact method of registration.

The general scheme of identification of the person on an iris of the eye consists of following stages:

1. A taking of the source image of an eye;
2. Iris localization on the image;
3. Normalization (transfer in pseudo-polar co-ordinate system);
4. Parameterization (selection of indications on an iris);
5. Compilation of the binary code;
6. Comparing of the received code with the codes which are available in a database of system.

Format Iris-code is standardized. However the codes received by different systems, are not identical. This results from the fact that different systems implement various approaches to selection of unique signs on the iris image.

In paper some algorithms used for the analysis of the image for the purpose of detection of unique indications of an iris (specks, grooves, etc.) are considered.

II. Requirements

Uniqueness of each iris consists in its unique picture. The iris image can be considered as the two-dimensional nonstationary signal defined on a finite co-ordinate space.

Transformation Fourier in tasks of the analysis of the arbitrary signals gives the information only about global frequency properties of a signal, but does not allow to estimate local frequency singularities of a signal. For example, it does not distinguish the stationary signal which is the total of two sine, from a nonstationary signal in the form of two sine following one after another. Window transformation Fourier is only partial solution of this problem.

Therefore it is convenient to apply wavelets to the analysis of properties of the nonstationary localized signal. Wavelets are convenient that:

- They are well localized in the frequency and co-ordinate areas;
- As their bases the basic functions solving special tasks in specific application can be used;
- They allow to carry out the multiscale analysis of structure of the image;
- They are simple for the discrete implementation.

Hence, in the task of the analysis of the image of an iris wavelets possess advantage in comparison with transformation Fourier.

III. Review

The exposition of the several transformations used for allocation of signs on the image of an iris is more low reduced.

Transformation of Haar

Is the system of the elementary orthogonal functions consisting from piecewise constant on [0,1] functions. Basis function of Haar has structure:

$$\psi_{m,k}(x) = a^{m/2}\psi(a^{m/2}x + k),$$

$$\psi(x) = \begin{cases} 1, & 0 < x < 1/2 \\ -1, & 1/2 < x < 1 \\ 0, & x < 0,\ x > 1 \end{cases}$$

Two-dimensional transformation of Haar is realised by application of one-dimensional transformation at first along lines of the image, after that along columns.

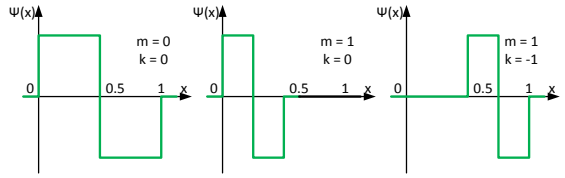

Figure 1 - Functions of Haar

As a result of one-dimensional transformation it turns out two signals. The first is the oblate version, the second represents detailing information.

For the first and second signals accordingly:

$$a_k = \frac{I_{2k-1}(x) + I_{2n}(x)}{\sqrt{2}},\ d_k = \frac{I_{2k-1}(x) - I_{2k}(x)}{\sqrt{2}},$$

$$k = 1,2...N/2$$

where $I(x)$ - value of pixel lengthways ,

k - pixel number.

Transformation of Haar allows to part high-pitched and low-frequency components in the image.

Disadvantage is that in frequency area of function of Haar are not absolutely localized.

Transformation of Gabor

Functions a Gabor possess property of localisation in frequency and co-ordinate area and look like:

$$\psi(x,y) = \exp\left[-\frac{1}{2}\left(\frac{x_\varphi^2}{\sigma_x^2} + \frac{y_\varphi^2}{\sigma_y^2}\right)\right]\cos(2\pi f_0 x_\varphi + \theta),$$

$$x_\varphi = x\cos(\varphi) + y\sin(\varphi),\ \ y_\varphi = -x\sin(\varphi) + y\cos(\varphi),$$

where σ_x, σ_y - the parameters setting a size of a window,

f_0, θ - parameters of modulation of the kernel of the filter,

φ - an angle of orientation of a window.

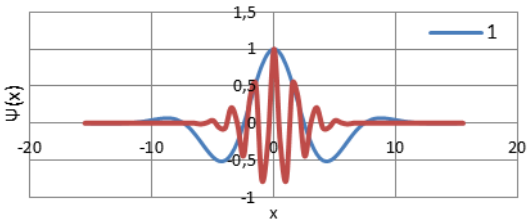

Figure 2 - One-dimensional functions a Gabor

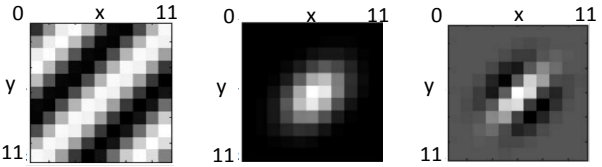

a) b) c)

Figure 3 - a) a two-dimensional spectrum of a signal; b) a gauss a signal turned on 45 °; c) result of a filtration

As the informative indications received with use of filters a Gabor, the local phase of the image received by convolution of the image by the filter starts. Value of a phase then is quantized.

Basis functions a Gabor are not orthogonal. Therefore outcome of convolution of the image with the filter the Gabor is presence of a constant component that hampers the image analysis.

Transformation of Hermite

Functions of Hermite organise orthonormal system of functions, possess property of localisation both in frequency, and in co-ordinate areas.

Basis one-dimensional functions of Hermite have structure:

$$\psi_n(x) = \frac{(-1)^n \exp\left[-x^2/2\right]}{\sqrt{2^n n!\sqrt{\pi}}} \cdot H_n(x),$$

$$H_0(x) = 1,\ \ H_1(x) = 2x,$$

$$H_n(x) = 2x \cdot H_{n-1}(x) - 2(n-1) \cdot H_{n-2}(x),$$

where $H_n(x)$ - polynomials of Hermite.

Functions of transformation of Hermite are defined through functions of Hermite:

$$\Psi_n(x) = \psi_0(x) \cdot \psi_n(x) = \frac{(-1)^n \exp\left[-x^2/2\right]}{\sqrt{2^n n!\sqrt{\pi}}} \cdot H_n(x).$$

Two-dimensional functions of Hermite out by multiplication one-dimensional:

$$\Psi_{n,m}(x,y) = \psi_n(x) \cdot \psi_m(y).$$

Transformation of Hermite consists in image convolution in each point with functions of Hermite for the set gang of indexes $[n,m]$

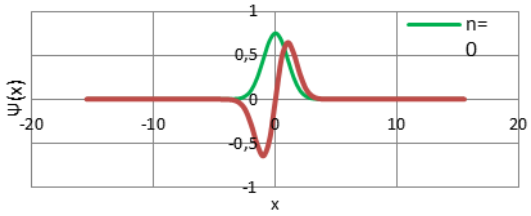

Figure 4 - One-dimensional functions of Hermite

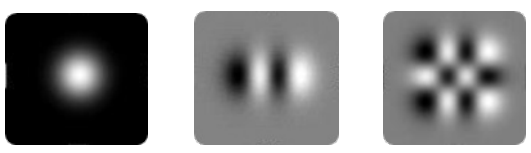

a) b) c)

Figure 5 - Two-dimensional functions of Hermite:

a) $\psi_{0,0}$; b) $\psi_{3,0}$; c) $\psi_{3,2}$

IV. Conclusion

The image received at registration in system, will differ a little from the images shown afterwards at identification of the same person. Therefore an important problem is the threshold choice at which differing images of the same iris will be apprehended by system as identical. For transformation of Haar it will be defined by compression degree. For transformation a Gabor resolving capability of a method depends on number of bits by which the phase is coded. For transformation of Hermite resolving capability depends on the chosen base functions. The choice of threshold value at a stage of deriving of a binary code of an iris is important.

VI. References

1. Волошин Н.В., Кузьмук В.В., Тараненко Е.А. Моделирование и распознавание информативных участков в автоматизированных системах иридодиагностики // Восточно-Европейский журнал передовых технологий. – 2011. – №2. – с. 65 – 69
2. Коланкех А.К., Спицын В.Г., Хамкер Ф. Нахождение параметров и удаление постоянной составляющей фильтра Габора для обработки изображений // Известия Томского политехнического университета. – 2011. – Т. 318. – №5. – с. 57 – 59
3. Павельева Е.А., Крылов А.С. Поиск и анализ ключевых точек радужной оболочки глаза методом преобразования Эрмита // Информатика и её применения. – 2010. – Т. 4. - №1. – с. 79 – 82

THE DEVICE OF PROCESSING SPECTRAL-EFFICIENT SIGNALS.

Kryachko Mikhail

Saint-Petersburg State University of Aerospace Instrumentation,
Saint-Petersburg, Russia
mike_kr@mail.ru

Abstract

This paper describes digital spectral efficient system that allows increase both speed of signal generation and protection of information transmission. The system is composed from two parts: matched filter and feedback unit. The feedback unit is a main part of system, which allows multiple repeat the convolution of input signal and the impulse response of a matched filter.

I. INTRODUCTION

Currently used signals and modulation provide either not high specific speed or unsatisfactory spectrum rate decrease or have large energy losses.

Due to the rapid development of discrete messages radio transmission systems it is scarce of spectrum resources, increasing the volume of information transmitted, increasing requirements for quality of communication. Extend the frequency range is complicated problem, in this connection have to find ways to improve the efficiency of existing systems designated portions of the spectrum. Especially important is the need to effectively address this problem in developing multi-channel radio systems, such as both satellite and cellular, as well as in the translation of large data volumes during transmission of video images in digital television, high quality videoconferencing, as the most advanced telecommunications and communications media. Various methods are used for these purposes, for example, re-use of frequencies by providing space-time division multiplexing (multipath onboard antennas, antennas with switched beam polarization applications, etc.), special types of modulation, spectral-efficient code, and etc.

Standards for the width of the spectrum emitted from the output of a radio transmitter oscillation and the decay rate of the level-of-band emissions suggest a significant narrowing of the bandwidth (see [1]). It is essential to provide for the restriction of bandwidth occupied by the signals and increase the rate of the level-of-band emissions decrease.

Narrowing of the spectrum and a decrease in the level of-band emission is used for example in existing cellular standard GSM (see [1]). In such systems, narrowing of the spectrum is achieved by using a narrow-band signal with a Gaussian low-pass filter frequency response at the input of the modulator. The use of such characteristics gives both the decay rate of the level-of-band emissions no higher than $1/f^4$, where $f-$ frequency and low concentration of energy within the occupied bandwidth.

II. THEORETICAL JUSTIFICATION

Optimal shape synthesis of the envelope signals, which have both a high rate of drop-band emission levels and low occupied bandwidth, can be made on the basis of atomic functions or near-functions [2].

Atomic functions are both finite and the solution of differential equations of the form:

$$y^{(n)}(t)+a_1 y^{(n-1)}(t)+\ldots+a_{n-1}y'(t)+a_n y(t)=\sum_{k=1}^{N}C_k y(at-b_k) \quad (1)$$

The simplest and most important atomic functions are made up of infinite convolutions of rectangular pulses.

Using the Fourier rectangular pulse can be represented in the form (as it is known, its spectrum is $\frac{\sin x}{x}$):

$$\varphi(t)=\frac{1}{2\pi}\int_{-\infty}^{\infty}e^{jut}\frac{\sin(u/2)}{u/2}du. \qquad (2)$$

$N-$fold convolution of $(N+1)$ identical rectangular pulses $\varphi(t)$ is a finite spline $\theta_N(t)$.

To obtain continuous finite function, consider the convolution of variable length pulses $\varphi_n(t)$ (Fig. 1):

$$\varphi_n=\begin{cases}2^{n-1}, & |t|\le 2^{n-1}\\ 0, & |t|>2^{n-1}\end{cases} \qquad (3)$$

For even more of a smooth function the process can be repeated, and for infinitely smooth

function must be repeated an infinite number of times.

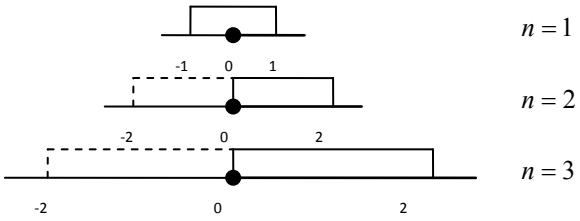

Figure 1. Convolution impulses of variable length

To finite carrier such an infinite convolution, it is necessary to take convolution of contractions such functions $\varphi_1(t)*\varphi_2(t)*\ldots*\varphi_n(t)*\ldots$ so that the series $\sum_{n=1}^{\infty} a_n < +\infty$ is converged. The simplest convergent series is the sum of infinitely decreasing geometric progression with ratio 2. So the result of such an infinite convolution is a new finite function defined on the interval $[-1;1]$. It is easy to show that it satisfies the equation (1) in its simplest form [3]:

$$y'(t) = 2y(2t+1) - 2y(2t-1) \qquad (4)$$

with conditions $\sup p = [-1;1]$, $y(-1) = y(1) = 0$, $y(0) = 1$.

Not difficult to show that it is at most one solution of equation (1) with the boundary conditions $up(t)$:

$$up(t) = \frac{1}{2\pi}\int_{-\infty}^{\infty} e^{iut}\prod_{k=1}^{\infty}\frac{\sin\left(u2^{-k}\right)}{u2^{-k}}du. \qquad (5)$$

III. DESCRIPTION OF THE SYSTEM

To solve the problem of increasing the speed of the formation of the spectral-efficient signals and increase the security of the transmitted information, the device was implemented spectral efficient signal on the basis of atomic functions (Fig. 2) [4].

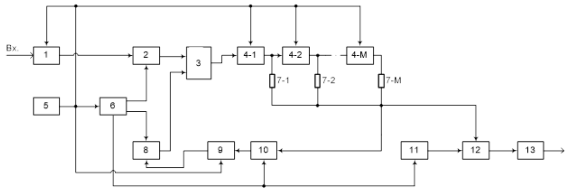

Figure 2. Block diagram of the signal generation

1 – Sampling unit, 2 - First electronic key, 3 – Adder, 4 - Multipoint delay line, 5 - Clock generator, 6 - Generator of control pulses, 7 - Weighing elements

8 - Second electronic key, 9 – Delay, 10 - Third electronic switch, 11 – Inverter, 12 - Fourth electronic switch, 13 - Low Pass Filter

The basis of the device is the introduction of the feedback loop, which allows create random impulse response and many times to repeat the convolution of input signal and the impulse response of a matched filter. These factors lead to smoothing of the input signal and, as a result, first, to increase the rate of decrease of-band emission, and secondly, to reduce the frequency bandwidth.

The timing diagram of the device is shown in Figure 3.

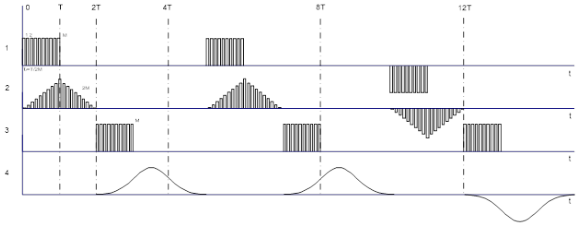

Figure 3. Timing diagram of the device signal generation.

Input information sequence (Diagram 1, 3), passing procedure matched filtering, forms a triangular signal at the output of weighing elements (Diagram 2). This signal is sent on the reverse link back to the input of the matched filter. Passing another procedure of matched filtering, the output device generates signals with increased durability and rounded shape of the envelope (Diagram 4).

IV. CONCLUSION

Increasing the duration narrows occupied bandwidth, and rounding the envelope fluctuations increases the decay rate-of-band emissions. In this way it is possible to increase the number of partial channels in a multichannel communication system with frequency-division multiplexing, and consequently, an increase in volume of transmitted information in a designated band.

REFERENCES

[1] Dr. Kamilo Feher. Wireless digital communications. Modulation and spread spectrum applications. Prentice-Hall PTR. Upper Saddle River, New Jersey 07458.

[2] Цифровая обработка сигналов и изображений в радиофизических приложениях. / Под ред. В.Ф. Кравченко. – М.: ФИЗМАТЛИТ, 2007. – 544 с.

[3] Рвачев В.Л. Теория R-функций и некоторые ее приложения.- Киев: Наукова думка, 1982. - 552 с.

[4] Патент RU .№ 2468525, МКИ H-01, опубл. 27.11.2012, Крячко М.А., Крячко А.Ф., Макаров С.Б. Устройство формирования спектрально-эффективных сигналов.

MODELING THE FLOW OF FISH

Malofeeva Marina

Saint-Petersburg State University Of Aerospace Instrumentation,
Saint-Petersburg, Russia
marina-al-90@mail.ru

I Task Deskription

In all northern rivers around the world valuable fish species swim upstream for spawning. During that period they are an easy prey for poachers, which catch them in large quantities in a very short time period. It is very difficult to predict this moment, so to avoid massive population reduction the spawning fish is counted. There are many ways of counting the fish but all of them are largely inaccurate. It was offered to develop a system with two video cameras arranged at different angles to the passing fish. The two cameras need to record images which are then processed by software. In order to plan the development of this software, it is necessary to model the fish flow and analyse limitations and effectiveness of counting the fish. Modelled fish stream should move with speed V in a narrow place with depth h, width d, length a and corresponding width of display output on which the flow happens. Modelled fish stream should flow from one side of display to another without breaking limits of depth and width. Also the movement of fish models should be very close to natural, which requires setting the turning angle of each fish on both displays.

II Model deskription

For creation of the modelled system we used the Poisson distribution to form fish flow along the X coordinate. Characteristic of the flow is defined by the following velocity parameter:

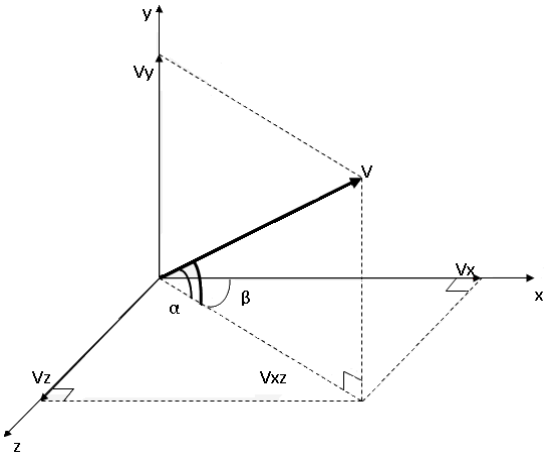

Diagram 1 – Position of velocity vector on the coordinate axes

V_{xz}: can be found via angle α and velocity vector by using right angle triangle formula:

$$\frac{V_{xz}}{V} = \cos\alpha \Leftrightarrow \quad (1)$$
$$V_{xz} = V * \cos\alpha$$

Then knowing V_{hz} as hypotenuse of two right angle triangles we can also find V_z and V_x

$$\frac{V_x}{V_{xz}} = \cos\beta \Leftrightarrow$$
$$V_x = V_{xz} * \cos\beta = V * \cos\alpha * \cos\beta; \quad (2)$$
$$\frac{V_z}{V_{xz}} = \sin\beta \Leftrightarrow$$
$$V_z = V_{xz} * \sin\beta = V * \cos\alpha * \sin\beta$$

Similarly, we find Vy:

$$\frac{V_y}{V} = \sin\alpha \Leftrightarrow \quad (3)$$
$$V_y = V * \sin\alpha$$
$$\Rightarrow V_x = V * \cos\alpha * \cos\beta;$$
$$V_y = V * \sin\alpha; \quad (4)$$
$$V_z = V * \cos\alpha * \sin\beta,$$

where common velocity is calculated as:

$$V = randn(1,n) * \sigma + V0 \quad (5)$$

Following these formulas we can find the coordinates along X,Y and Z axis.

Movement of fish is given by set law of motion with random variable distribution. In this case it is the usual law of distribution which is given by the following formula:

$$V = randn(1,n) * \sigma + V_0 \quad (6)$$

where sigma is defined as:

$$\sigma = 1 \quad (6.1)$$

In order to bring the motion of each fish close to natural, it is necessary to define the turning angle with which the fish constantly changes the direction of its motion. The angle is defined based on the current position and an arbitrary random angle. When turning, the fish can also move towards the top of the display, as well as towards the bottom. In order for the fish not to cross the display borders and "turned" away from them in the opposite direction, we need to define how to generate the arbitrary random angle.

$$\alpha(k) = \alpha(k) + delta, \quad (7)$$

where delta is defined based on the position of the fish.

To get that we need to divide the depth h in half:

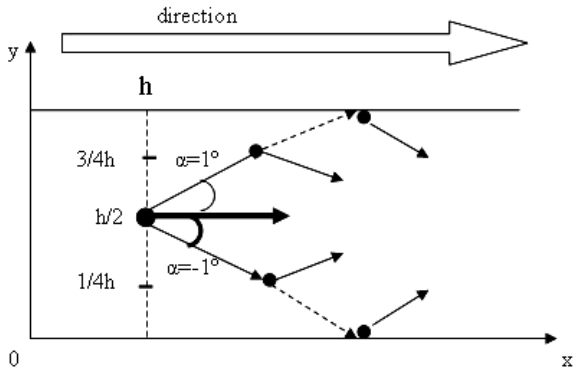

Figure 2 – Restriction on the Y axis

Similarly for axis Z. Each time the fish will be on one side or the other h/2 and d/2, the variable angle will be generated in different ways. The closer the fish is to the top or to the bottom of, the greater the probability that a random variable will fall so that the fish will turn in the opposite direction. These h/2 (d/2) should also be split on 2 halves to increase the chance turning fish.

Thus, if the fish is above h/2, but less than 3/4h, random variable delta, which is added to the previous position of the fish, is composed as follows:

$$delta = rand * (b - a) + a, \quad (8)$$

where $a = 0$, and $b = -0.5$ (Figure 3).

With these data, the delta is formed in such a way that the fish are likely to either float in the same direction, or will turn down. Similarly happens when the fish will be above 1/4h, but below h/2: $a = 0$, and $b = 0.5$. If the fish will be near the edge of the screen, the parameters are as follows: for the upper bound h $a = -1$, and $b = -0.5$, for the lower limit of 0 $a = 0.5$, and $b = 1$. These calculations are similar to the angle of rotation for the height d on the axis Z.

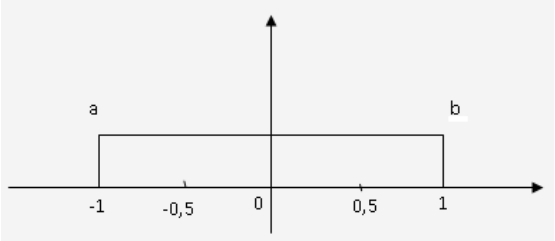

Figure 3 – The values of the parameters a and b

Placing restrictions on the parameters of the angle X and Y not to fish swam in the opposite direction. Fish will swim in the opposite direction, if the angle is too large or too small. To limit the angle you would enter:

$$alfa = sign(alfa) * 30, \quad (9)$$

which allows you to reduce the angle. Thus a positive angle is equal to one, and negative - minus one. Then rounded up to 30 degrees.

III Conclusion

During the movement managed to simulate the flow of fish on the internet.

It should be noted that the program starts running slower with increasing density parameters and the speed of the flow, increases the amount of computation per unit of time. On-screen fish can fuse with the flux n = 10000. image has significantly distorted by the flow rate increases with the size of the sample - in this case the visibility of images displayed on the screen, is deteriorating, fish movement is erratic and intermittent, some can "jump" from one location to another, to which it must be later .Therefore, under certain parameters increased Matlab can not cope with the task: output stream to the screen just will not have time to be produced.

When modeling a large flow of fish required to compress the model time, is increase the speed of the fish. In this situation, you can create a video that would give when playing normal playback picture of the flow of fish. According to the results of modeling the flow of fish you want to find the relationship between the flux density of fish and some integral characteristics of the images on the projection of the flow. To study this relationship field experiments are too costly.

IV References

1. http://www.exponenta.ru/
2. Ануфриев И. «Самоучитель Matlab». «БХВ-Петербург», СПб, 2004. 710 стр.

AN EMBEDDED SYSTEM FOR PRECISION FARMING

Salvatore Monello, Sebastiano Pulvirenti, Emanuela Ventura

Department of Electrical, Electronics and Informatics Engineering
University of Catania
Viale Andrea Doria, 6 - 95125 Catania, Italy

salvo.monello@gmail.com, sst.pulvirenti@gmail.com, venturaemanuela88@gmail.com

Abstract

The optimization of the resources to increment the productivity of a Greenhouse is one of the most discussed problems in the precision farming field. Product quality and production are increased with an accurate control of the variables in the system. This paper describes an embedded system, for the remote monitoring of the greenhouse climatic conditions, that through automatic controls permits to improve the quality of the environment, concurring in that way to optimize the production. The developed system is based on the use of the board STM32L152 for the data acquiring and a PC for the data elaboration.

1. Introduction

The new technologies of wireless communication have given a precious contribute to the precision farming development, pointing to a more sustainable and resources-sensitive agriculture [1]. In addition the improvement of the environment conditions has become an important choice for the agricultural production. An accurate control of the production contributes to solve one of our times problems, that is the reduction of energetic waste and water consumption. Even if the greenhouses are protected from the external atmospheric agents, without an opportune control system is possible the happen of conditions that cause the waste of resources and damage the production.

The proposed system in this paper (showed in Fig. 1) acquires the main environmental parameters of the greenhouse that is the measurement of the rate of humidity, the temperature, and luminosity of the production environment through the use of opportune sensors [2], [3]. Depending on the acquired values it will decide if open the windows to air the environment, turn on the fans to circulate the air or heat the greenhouse. The data read from the sensors are pre-elaborated by the STM32L152 board, that is heart of the proposed system, and are then sent to user PC through Xbee technology [4]. The user, by the graphic interface, can send remote commands and know in any moment the status of the greenhouse and the temporal trend of the temperature, humidity and luminosity values.

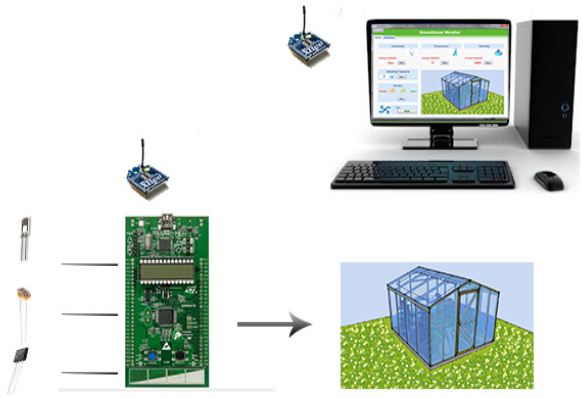

Figure 1 GreenHouse and GreenHouse Monitor

The PC has two functions. On one hand it offers a graphic interface that permits the user, operating locally, to display opportunely the variables and to send the appropriated commands when requested. In addition, its calculation power will allow it to implement sophisticated a control algorithm for an optimal greenhouse management and will be able to communicate with several embedded systems (each one controls one greenhouse) to manage more complex system, also formed by more than one greenhouse. On the other hand, the PC can be configured as web server to permit remote access to the informations and permit the monitoring through a smartphone, tablet or palmar computer.

The heart of the system is represented by the STM32L152 microcontroller, that owns a high number of analogic and digital inputs and a powerful microcontroller, and is well suited for creating control embedded systems.

The paper is organized as following:

The sect.2 describes the issues related to hardware components design of the system and their resolution. The Sect.3 describes the software architecture and the logic implemented. Finally, the sect.4 outlines the functionalities given by the Green house monitor.

2. Hardware Design

This section gives a description of the main hardware modules and the solved problem for their design.

- STM32L1XX is a family of Microcontroller produced by STMicroelectronics and based on 32-bits Risc ARM cores with the primary goal of the low-power usage. The boards includes two SPI, two I²C, three USART, eight 16-bit timers, two watchdog timers, temperature sensor, 16 to 24 channels into one ADC, two DACs, 37 to 83 GPIOs, seven DMA, real-time clock (RTC), cyclic redundancy check (CRC) engine.

- Bipolar stepper motors: they are usually used for applications where high precision and reliability is required. In this application they were used to control the windows opening in the greenhouse. Even if a normal DC could be used for this function, it would have permitted only ON/OFF operation with a total opening/closing of the windows. In that case, if a partial opening was necessary, then the use of opportune encoder and sophisticated control system were requested. The use of a Stepper Motor instead permits an accurate control of the window opening, without using sophisticated feedback devices. But this implies a more complex electronic scheme compared to a normal DC motor. In the case of Bipolar Stepper Motors is necessary to polarize in the correct way the winding according to an appropriate sequence. Such rotation sequence is produced by 4 digital I/O ports of the STM32L152 board that therefore can change the motor rotation speed at any time and implement simple algorithmic to minimize the problem related to the window inertia. The power supply circuit of the motor is represented in fig.2, and uses the L298/N integrated circuit.

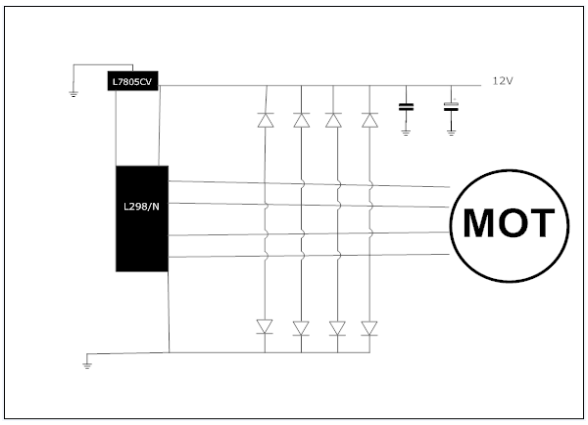

Figure 2 Stepper Motor power supply circuit

- The humidity sensor used, model HCZ-J3, needs an alternate voltage based on 1 KHz and $1V_{rms}$ sinusoidal wave input. The wave form was generated by the integrated DMA of the SMT32L152 that transfers the digital samples from the RAM memory to the DAC. The converted samples are thus outputted. The result is a squared wave form with a sinusoidal trend, 1 KHz frequency and $3V_{pp}$ because such is the board output voltage.

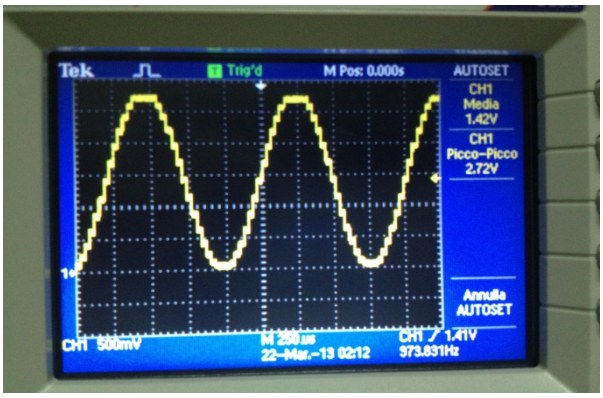

Figure 3 Wave form in output from DAC

To smooth the edges, it was used a low-pass filter. In the figure 3 and figure 4 is shown respectively the wave form before and after the filter application. Since the sinusoidal wave has $3V_{pp}$ in output from the board it was used a voltage divider to reduce it at $1V_{rms}$.
The sensor output is still sinusoidal therefore to read a constant value of voltage it was used half-wave rectifier and a capacitive filter.

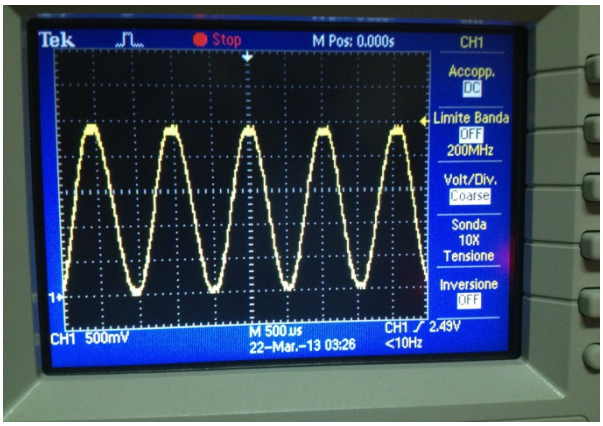

Figure 4 Wave form in output after the low pass filter

- The temperature sensor used is the LM35, a precision sensor based on integrated circuit, whose output is linearly proportional to the Celsius temperature (Fig.5).

.

- To measure the luminosity in the greenhouse it was used a photoresistance, model LDR07, with a voltage divider.

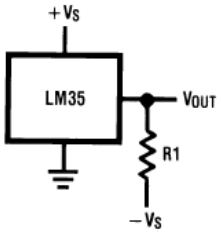

Figure 5 LM35

- For the communication were used the Xbee series 1 modules, engineered to meet IEEE 802.15.4 standards and support the needs of low-cost and wireless low power sensor networks.

3. Software Architecture

For the development of the application were used the following technologies:

- IAR Embedded Workbench: a high-performance C/C++ compiler and debugger tool suite for applications based on 8-, 16-, and 32-bit microcontrollers.
- X-CTU: is Windows-based application provided by Digi. The software was written to interact with the firmware files found on Digi's RF products and to provide a simple-to-use graphical user interface to them.
- Xbee API for C#: is an API Xbee for C#. It is realized for the serie 2 of Xbee, but they were appropriately modified to be used in the serie 1 modules.
- Microsoft Visual Studio 2010
- Microsoft Expression Blend 2

Application initializes all the registers with the configuration initial values and a Timer starts periodically that will generate an interrupt managed from the respective handler. The period length can be set remotely. Once the configuration is over it remains listening to new commands from the PC. The following commands can be received:

- Set the readying sensors frequency.
- Set the threshold of the temperature sensor
- Set the threshold of the luminosity sensor.
- Set the threshold of the humidity sensor.
- Start the fan.
- Stop the fan.
- Open or close the window to a certain position (0, 1, 2, or 3).

The following operations will be executed in the handler according to the sequence represented in fig.6:

- Enable sensors, convert values read from sensors and save in a 16-bit array.
- Disable sensors. It includes the power off of the DMA, DAC and ADC peripherals used for the sensors. This is made for reasons of energy saving and a better use of the resources.

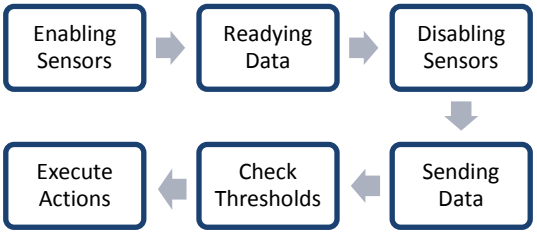

Figure 6 Operations executed by the Handler of the main Timer

- The values obtained are then translated to meaningful values according some calibration algorithm.
- Send to PC the read values through the ZigBee and Xbee Serie1 modules. A 16 bit address was assigned to these modules and they are set in API mode thus in facts a frame will be sent. API operation is an alternative to the default Transparent operation; this option facilitates many operations such as the examples cited below:

-Transmitting data to multiple destinations without entering Command Mode

- Receive success/failure status of each transmitted RF packet
- Identify the source address of each received packet

A host application can interact with the networking capabilities of the module; it can send data frames to the module that contain address and payload information instead of using command mode to modify addresses. The module will send data frames to the application containing status packets; as well as source, RSSI and payload information from received data packets. The frame sent from the STM32L152 is showed in the Fig.7. It contains the read values of each sensor, the current status (thresholds values, readying sensors frequency, fan status, and current window position).

In addition to send such frame at any main timer interrupt, the firmware of the board keeps listening for any new command from PC; a state machine is used to get the command received. The data transfer was optimized for band saving.

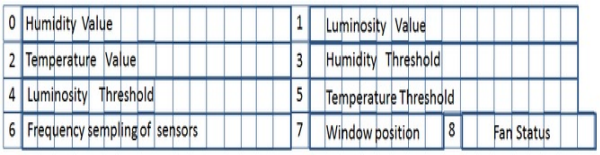

Figure 7

- Check the thresholds and execute the respective actions. (i.e. Opening Window Fig 5)

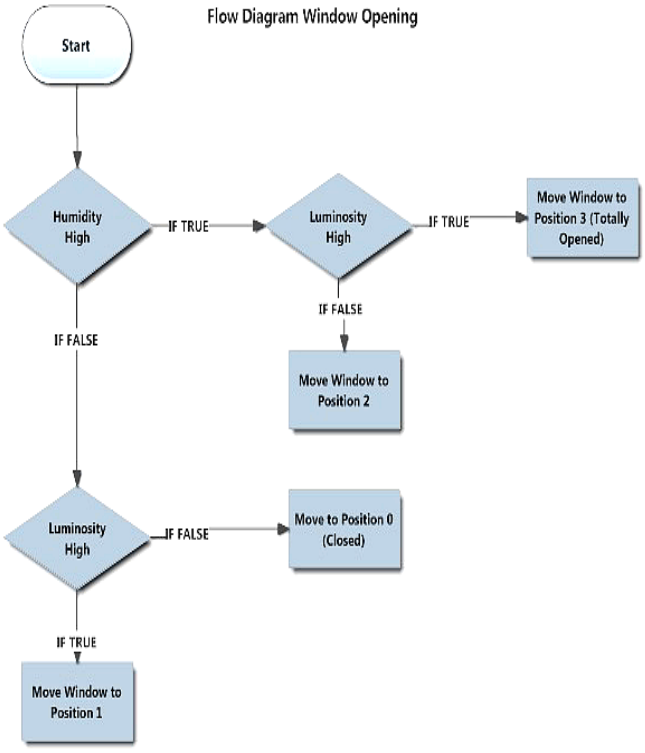

Figure 8

4. GreenHouse Monitor

The user has an application realized in Wpf, with a graphic interface (shown in fig.9), where is possible to:

-Display the data of the last readying of the sensors (temperature, humidity, luminosity).
-Set the threshold of each component.
-Set the frequency of readying/sending data of the microcontroller.
-Start the fan manually.
-Open the window to the indicated position (0, 1, 2, 3).
-Display the charts of the last hour of monitoring (Fig 7).

Regarding the communication of PC it was used the libraries Api-xbee-C# [5] that was adapted to the used series 1 modules.

Conclusions

This paper was described the design and construction of a low-cost system for monitoring and controlling a green house. The system has a low-power usage through the use of energy saving technology as the board low power and the Zigbee protocol. The automatic control of the environment variables allows keeping under control the microclimatic variations and assures those favorable conditions to the productive process.

REFERENCES

[1] Romanov, V.; Artemenko, D.; Galelyuka, I.; Kovyrova, O.; Sarakhan, Y.; Fedak, V., "Computer devices for precision agriculture," Intelligent Data Acquisition and Advanced Computing Systems (IDAACS), 2011 IEEE 6th International Conference on , vol.1, no., pp.26,29, 15-17 Sept. 2011

[2]Luciano Gonda, Carlos Eduardo Cugnasca – "A Proposal of Greenhouse Control Using Wireless Sensor Networks", Proceedings of the 4th World Congress Conference Computers in Agriculture and Natural Resources, 24-26 July 2006 (Orlando, Florida USA)

[3] Lei Xiao; Lejiang Guo, "The realization of precision agriculture monitoring system based on wireless sensor network," Computer and Communication Technologies in Agriculture Engineering (CCTAE), 2010 International Conference On , vol.3, no., pp.89,92, 12-13 June 2010

[4] Homepage of ZigBee™ Alliance, http://www.zigbee.org/

[5] XBee API for C# http://code.google.com/p/xbee-api-sharp/

Figure 9

DEVELOPMENT PROCESS OF PROCEDURE FOR EVALUATING SCIENTIFIC AND TECHNICAL STUDIES

Stanislav Nazarevich

Saint-Petersburg State University of Aerospace Instrumentation,
Saint-Petersburg, Russia
albus87@inbox.ru

ABSTRACT

The paper describes the main results of scientific and technological research. A scheme of management assessment process of scientific and technological research for the various activities is presented. The characteristics of the different type of activity in forming of the capacity of scientific and technological research are presented.

I. INTRODUCTION

In line with the model of the life cycle of the formation of scientific and technological research get thought several stages. The first stage of the life cycle is the identification and analysis of problem areas to assess the complexity and magnitude of the problem. Through research and analysis of topical issues and assessment of key stakeholders, the motivation, the quality of which depends on the decision taken to reduce the difference between the desired state and the current situation. As a result of the first stage of developing the terms of reference are worked out, which should clearly define further movement towards the development of process solutions. The second step is the generation of ideas, solutions, and best practices for the problem under investigation. Through a review of the many information resources one can obtain a broad base with turnkey solutions, taking into account the specificity of each company. The third stage depends on the choice of activities within the Scientific and Technical Research [1]: innovation, science, engineering and manufacturing activities.

II. DESCRIPTION OF THE MODEL

For each of the activities certain processes are specific that result in the conversion of various resources in innovation. Figure 1 shows a diagram of the management assessment process of scientific and technological research (STI), which describes the main processes characteristic of innovation, science and engineering and production activities. The third phase for engineering and manufacturing activities begins with the formation and development of rationalization proposals, based on the data of the previous process of database generation of ideas and solutions. Any technical change or the introduction of non-standard ways of performing manufacturing operations, original methods for the organization of work, may be related to the engineering solutions aimed at streamlining the process and organizational production processes. When successful engineering solutions, are made the object becomes a rationalization proposals innovation that pass the verification process to the requirements laid down at the stage of requirements specification for innovations. As for innovation is characterized by mutual way for engineering and for science, it should be noted that to obtain the basic innovation the results of basic research must be presented. Scientific activity also begins with the choice of direction and database generation of ideas and solutions, if the chosen direction recognizes promising, the process of making a decision about the initialization of research (R & D) in this area [2]. During the course of research formed "innovation" - new knowledge, method or principle derived from research and development. After conducting research to evaluate the impact of research in the case of achieving the goals of work, research results take the form of some scientific innovation potential. Innovation is the conformity assessment requirements specification, then moves on to the next stage. After checking for compliance with the terms of reference to make the analysis of internal capacity of innovation.

III. FORMS OF STI

This analysis is a collection of data on innovations, structures, characteristics, and functions necessary for the detection and subsequent analysis of the unique properties of the object. Structuring properties of an object in order of importance, are evaluation criteria, with which it is possible to carry out the process of identifying the results of STI. System of criteria for assessing STI also includes criteria that are used in the examination of innovations

for the right to obtain a patent. So for the assessment of the capacity of STI can be patentable innovations indicate that claims to shape.

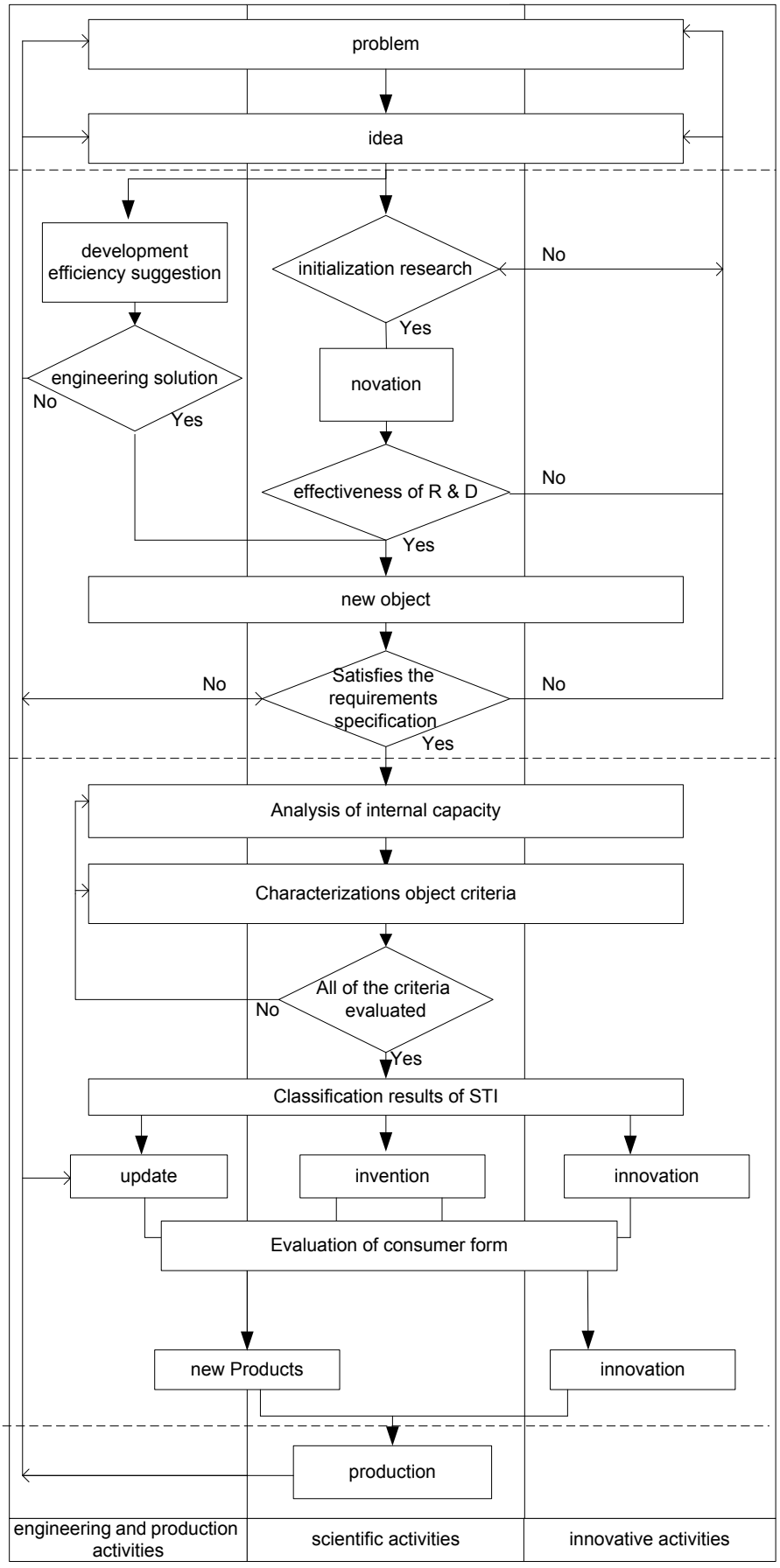

Fig.1 - Scheme of the process evaluation of scientific and technological research

Estimating the results of STI as intellectual property for subsequent patenting a reduction in the time spent in the trajectory of the life cycle of a product and a competitive advantage. The next stage is the classification of objects to the evaluation of the intrinsic properties and the definition of the relevant group of results of STI. Through the analysis and evaluation of consumer form of objects can be concluded on the market attractiveness of the object, and to plan activities for the promotion of this product. Thus, the appraisal form is the consumer division of the results on the basis of STI indicators inner potential. This data forms are easily perceived by the market, because of the known methods of promotion and replication of similar objects in perspective, or not yet covered market segments. Finally, the results take the form of STI products already known to the market, with a certain technical level, on the basis of which the participants concluded the segment about the competitive position of the product, thus triggering mechanism of the strategy of differentiation of products, in some sense filling segment goods substitutes or analogues of the competitive product. Under the influence of these factors in the presented there scheme is feedback of existing products with the upgrade process and improvements in order to achieve a sustainable competitive position of the company.

IV. CONCLUSION

Control scheme assessment process of scientific and technological research is suitable for the analysis and classification of potential innovations in some sense. In the evaluation process significantly reduces the time not only to determine the scope and the target segment of the market, but the timing on the study and evaluation of the patentability of innovations as a result of intellectual activity. Thus, as a result of the developed scheme of the management procedure of evaluation of scientific and technological research appears, the ability to predict and plan the results of STI, both existing and potential, and the future needs of the market and production in general.

REFERENCES

[1] Nazarevich S.A. Integrated indicator of the results of scientific and technological research. "Issues of Radio Electronics", a series of general engineering, 2013.

[2] Nazarevich S.A. Development of criteria for the identification of innovative facilities. V International Scientific and Practical Conference" Legal protection, economics and management of intellectual property"

ANALYSIS OF CANONICAL FORMS OF LINEAR DYNAMICAL SYSTEMS

Vadim Nenashev

Saint-Petersburg State University of Aerospace Instrumentation,
Saint-Petersburg, Russia

granat89@mail.ru

At computer modeling of dynamic systems there is a need for a choice of concrete realization of system for space of conditions. Most often for these purposes choose one of canonical forms [1].

Canonical Forms (CF) are characterized by simple structure and the minimum number of varied parameters. Set of CF can be considered, how a set of standard models of dynamic systems. The knowledge of properties of these models and their characteristics allows to choose CF convenient for the solution of specific objectives of simulation and analysis or synthesis of systems [2, 3].

CF are classified on accompanying, modal, chain and balanced. It is considered on one CF from each class below, namely: Frobenius canonical form (FCF); Jordan canonical form (JCF); balanced canonical form (BCF) and Raus's canonical form (RCF). For their construction m-functions in a package of computer simulation of Matlab were developed and debugged.

In this work the problem of comparison of characteristics of specified CF, in particular their analysis about providing the smallest computing relative error when entering small distortions into matrix A and descriptions in space of conditions is considered.

In a general view the solution of an objective quite volume and non-trivially therefore we will be limited to one test example. As a test example the passive electric chain (EC) of the third order containing two resistors, two capacitors and one coil of inductance was chosen.

The passive electric chain is described by description matrixes in space of the conditions, given in table 1:

Table 1.
Description matrixes in space of conditions of EC

A	b	c
$\begin{matrix} -1 & 0 & -1 \\ 0 & -1 & 1 \\ \frac{1}{5} & -\frac{1}{5} & 0 \end{matrix}$	$\begin{matrix} 1 \\ 0 \\ 0 \end{matrix}$	$0 \quad 1 \quad 0$

From this description of an electric chain transition to similar matrixes for four studied CF was carried out.

For the comparative analysis of sensitivity of CF to computing errors distortions were brought in them. For this purpose values of elements of a matrix A for ±10% changed. In a Matlab package it can be carried out by means of expression:

$$Ad = A \cdot * \begin{bmatrix} 0.9 & 1.1 & 0.9 \\ 1.1 & 0.9 & 1.1 \\ 0.9 & 1.1 & 0.9 \end{bmatrix}, \qquad (1)$$

where $\cdot *$ - operation of bit-by-bit multiplication of matrixes. Elements of matrixes of b and c remained invariable.

Frobenius Canonical form

Matrixes of the reference model (RM) and the distorted model (DM) of FCF EC are given in table 2.

Table 2.
Description matrixes in space of conditions of RM and DM of FCF

A_f	b_f	c_f
$\begin{matrix} 0 & 0 & -0.4 \\ 1 & 0 & -1.4 \\ 0 & 1 & -2 \end{matrix}$	$\begin{matrix} 1 \\ 0 \\ 0 \end{matrix}$	$0 \quad 0 \quad 0.2$

Ad_f	bd_f	cd_f
$\begin{matrix} 0 & 0 & -0.36 \\ 1.1 & 0 & -1.54 \\ 0 & 1.1 & -1.8 \end{matrix}$	$\begin{matrix} 1 \\ 0 \\ 0 \end{matrix}$	$0 \quad 0 \quad 0.1366$

The results of computer simulation of RM and DM are presented in Figures 1 and 2.

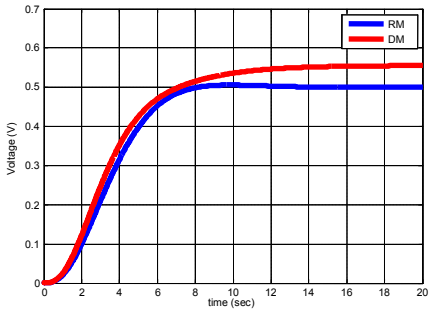

Fig. 1. Schedules of transitional characteristics of the FCF electric model

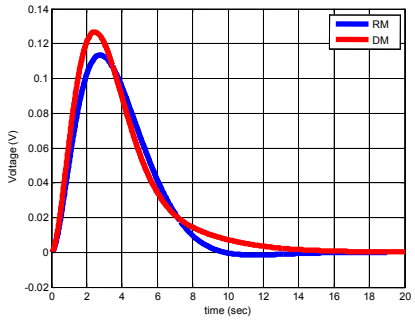

Fig. 2. Schedules of weight characteristics of the FCF electric model

From schedules of figures 1, 2 it is visible that the error of an output signal of the distorted model made about 10%.

Jordan canonical form.

Matrixes of the RM and the DM of JCF EC are given in table 3.

Table 3.
Description matrixes in space of conditions of RM and DM of JCF

A_j			b_j	c_j
– 0.5	– 0.3873	0	1	-0.5 0.6455 0.5
0.3873	– 0.5	0	0	
0	0	– 1	1	

Ad_j			bd_j	cd_j
– 0.45	– 0.426	0	1	-0.5 0.6455 0.5
0.426	– 0.45	0	0	
0	0	– 0.9	1	

The results of computer simulation of RM and DM are presented in Figures 3, 4.

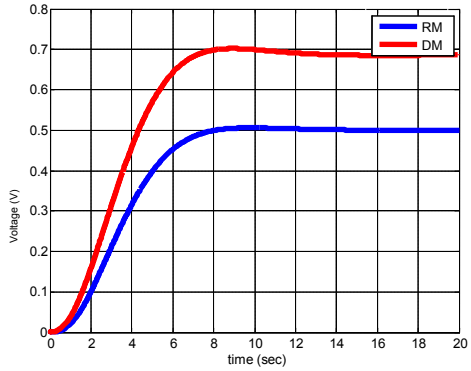

Fig. 3. Schedules of transitional characteristics of the JCF electric model

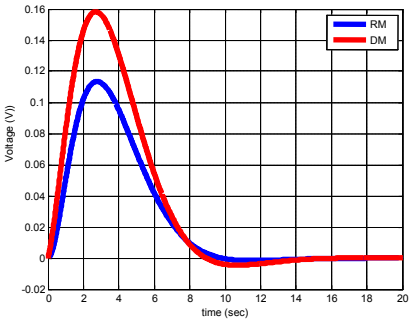

Fig. 4. Schedules of weight characteristics of the JCF electric model

After carrying out similar experiment with FCF, according to the schedule of the transitional characteristic (figure 3) we observe that an error of an output signal of the DM on a site from [0; 1] it is insignificant, and on a site (1; + ∞] makes about 25%. From figure 4 it is visible that an error of an output signal of the DM on a site from [0; 1] ∪ [6; + ∞] is insignificant. On a site (1; 6) makes about 25%.

Balanced canonical form.

Matrixes of the RM and the DM of BCF EC are given in table 4.

Table 4.
Description matrixes in space of conditions of RM and DM of BCF

A_b			b_b	c_b
– 0.1171	– 0.4024	– 0.1386	0.28	0.29 0.33 0.17
0.4024	– 0.5047	– 0.5842	-0.33	
– 0.1386	0.5842	– 1.3782	0.17	

Ad_b			bd_b	cd_b
– 0.1053	– 0.4427	– 0.1247	0.28	0.29 0.33 0.17
0.4427	– 0.4543	– 0.6426	-0.33	
– 0.1247	0.6426	– 1.2404	0.17	

The results of computer simulation of RM and DM are presented in Figures 5 and 6.

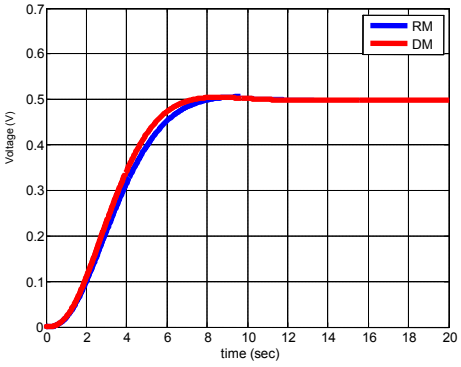

Fig. 5. Schedules of transitional characteristics of the BCF electric model

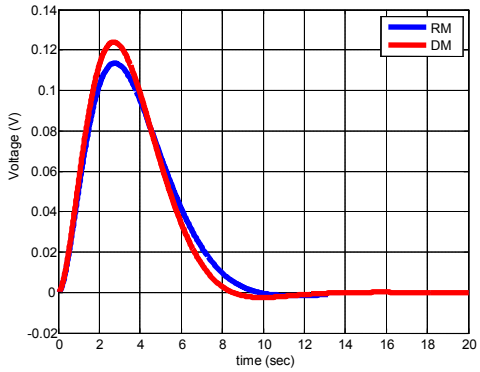

Fig. 6. Schedules of weight characteristics of the BCF electric model

From schedules of figures 5, 6 follows that the output signal of the distorted model changed slightly that illustrates small sensitivity of BCF to distortions.

Raus's canonical form.

Matrixes of the RM and the DM of RCF EC are given in table 5.

Table 5.

Description matrixes in space of conditions of RM and DM of RCF

A_r			b_r	c_r
−2	1.0954	0	1.09 0 0	0 0 0.373
-1.0954	0	0.4472		
0	-0.4472	0		

Ad_r			bd_r	cd_r
−1.8	1.205	0	1.09 0 0	0 0 0.373
-1.205	0	0.4919		
0	-0.4919	0		

The results of computer simulation of RM and DM are presented in Figures 7 and 8.

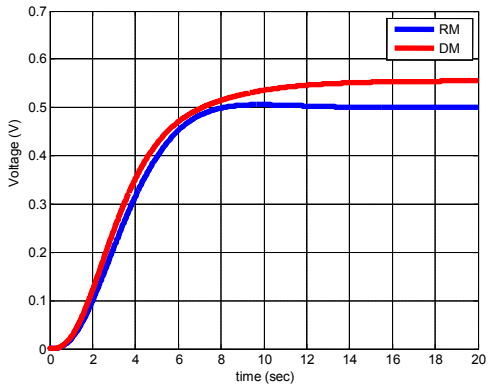

Fig. 7. Schedules of transitional characteristics of the RCF electric model

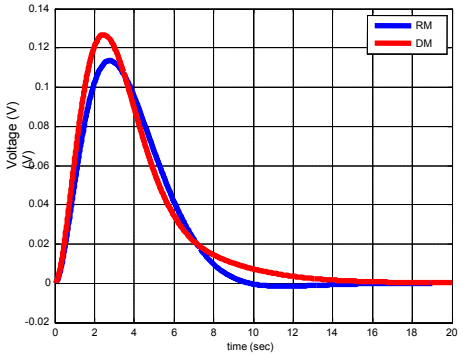

Fig. 8. Schedules of weight characteristics of the RCF electric model

From figures 7, 8 it is visible that the error of an output signal of the distorted model made about 10%.

For comparison of errors of studied canonical forms on the basis of the received results we will use calculation of norms of a difference of the corresponding functions:

$$\begin{aligned} nrp &= \|p(t) - pd(t)\| = \sqrt{\int_0^\infty (p - pd)^2 dt}; \\ np &= \|p(t)\| = \sqrt{\int_0^\infty p^2 dt}; \\ nrq &= \|q(t) - qd(t)\| = \sqrt{\int_0^\infty (q - qd)^2 dt}; \\ nq &= \|q(t)\| = \sqrt{\int_0^\infty q^2 dt}, \end{aligned} \qquad (2)$$

where $p(t)$, $pd(t)$ – transitional function of the reference and distorted model, respectively; $q(t)$, $qd(t)$ – weight function of the reference and distorted model, respectively.

Using a formula (2), we will calculate a relative error for transitional and weight functions:

$$Kp = \frac{nrp}{np}, \quad Kq = \frac{nrq}{nq}.$$

Estimates of a relative error of canonical forms are given in table 6.

Table 6.

Assessment of a relative error

	FCF	JCF	BCF	RCF
Kp	0.0879	0.3875	0.0260	0.0879
Kq	0.1532	0.4075	0.1018	0.1532

By results of computer modeling and to estimates of a relative error of an output signal (table 6) it is possible to draw a conclusion that the smallest

error is provided by BCF; further FCF and RCF follow; and the output signal of system in JCF appeared the most sensitive to introduction of distortions.

REFERENCES

[1] Mironovsky L. A. Functional diagnosing of dynamic systems: Scientific edition. M - SPb. : prod. The Moscow State University - the REEF, 1998. 256 pages

[2] Mironovsky L. A. Analogovye and hybrid models of dynamic systems. Scalar systems//Manual. 1985

[3] Gerasimov A. N., Isakov V. I., Shepeta A. P., etc. Linear systems of automatic control. Scientific edition. – SPb. : SUAI, 2009.

EVOLUTIONARY PREDATOR-PREY MODEL WITH STOCHASTIC DISTURBANCE

Mark Polyak

Saint-Petersburg State University of Aerospace Instrumentation
Saint-Petersburg, Russia
markpolyak@gmail.com

Abstract

In this article a pair of first order coupled, continuous, time invariant, ordinary differential equations are considered for modeling predator-prey systems. An approximate solution to Lotka-Volterra equations is proposed and the effect of stochastic disturbance of its parameters is analyzed. Phase trajectory of proposed solution is mathematically described by means of level-crossing theory of random processes.

Keywords: ordinary differential equations, ode, Lotka-Volterra equations, predator-prey equations, phase plane, phase trajectory, stochastic process, level-crossings.

I. Introduction

Ecological systems usually consist of two or more interacting species whose population dynamics are influenced by many factors. There are numerous methods for mathematically describing the various biological phenomena. The model might consist of a system of difference, integral or differential equations. The differential equations may be partial or ordinary, deterministic or stochastic.

Many differential equations don't have a known analytic solution. Although such equations can be solved numerically, the absence of analytic solution makes it difficult to further analyze models based on those equations. Nevertheless systems of differential equations remain one of the most widely used mathematical apparatus for describing complex dynamical systems.

II. Predator-Prey Model

One of the most well known mathematical models in biology is the predator-prey model used to describe population dynamics. The model was proposed by A. Lotka and V. Volterra in the first part of 20th century. In its simplest form the model is described by a pair of first-order non-linear differential equations

$$\begin{cases} \dfrac{dx}{dt} = x(\alpha - \beta y) \\ \dfrac{dy}{dt} = -y(\gamma - \delta x) \end{cases}, \qquad (1)$$

where $x \geq 0$ is the population size of prey; $y \geq 0$ is the population size of predator; $\alpha \geq 0$, $\beta \geq 0$, $\gamma \geq 0$ and $\delta \geq 0$ are model parameters describing interaction between two species x and y; finally, derivatives dx/dt and dy/dt denote the rate of change of prey and predator populations respectively.

Differential equations (1) are used to model dynamical systems behavior in biology, chemistry, economics and other fields of science. In biological interpretation of Lotka-Volterra equations the terms $(\alpha - \beta y)$ and $(\delta x - \gamma)$ are called global growth rates of prey and predator as they denote the rate of change of both populations.

To be more precise, the term αx represents exponential growth of prey as it is assumed to have an unlimited food supply. The rate at which predator and prey meet (the rate of predation) is denoted by coefficient β and term βxy in equation (1). So changes in the number of prey population are expressed as prey's own growth minus the number of prey eaten by predators.

Similar reasoning can be applied to the second equation of system (1). The term $-\gamma y$ denotes the exponential decay in the number of predators caused by their death from such reasons as old age or not having enough food supplies (low prey population). The prey species are not supposed to die of old age as they are assumed to be eaten by predators as soon as they become old and easy to catch. The δ constant is used as the rate at which the predator population grows. It is not necessarily equal to the rate β at which predators consume their prey. The change in predator population is given by the growth of the predator population minus natural death.

It should be mentioned that the predator-prey system of equations (1) can be easily extended to a more general class of Lotka-Volterra system by assuming that global growth rates $f(x, y)$ and $g(x, y)$ are polynomials of degree higher than one

$$\begin{cases} \dfrac{dx}{dt} = xf(x, y) \\ \dfrac{dy}{dt} = yg(x, y) \end{cases}. \qquad (2)$$

Further generalization of Lotka-Volterra system (2) that accounts for more than two species may be written as follows

$$\frac{dx_i}{dt} = x_i f_i(\vec{x}), \vec{x} = \begin{bmatrix} x_1 \\ \vdots \\ x_n \end{bmatrix}, \qquad (3)$$

where x_i is the population size of species i, $i = \overline{1,n}$, and $\vec{x}$ is a column vector of population sizes of all n species.

III. Solving Lotka-Volterra Equations

Lotka-Volterra equations (1-3) are long known and well studied. Nevertheless due to the non-linearity of the system its analytical solution is unknown and numerical methods must be applied.

The solutions of system (1) are periodic functions that cannot be exactly expressed in terms of standard trigonometric functions. This fact is illustrated on figure 1, which shows a solution of system (1) with parameters $\alpha = 1.5$, $\beta = 0.4$, $\gamma = 3$ and $\delta = 0.2$. Solution is found by a Runge-Kutta ODE solver using Dormand-Prince numerical method implemented by MatLab `ode45` function.

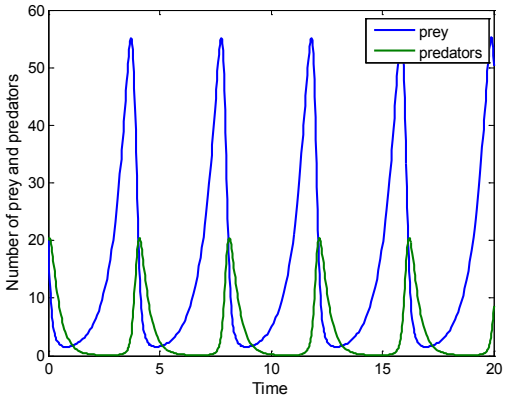

Figure 1. Numerical solutions of predator-prey equations, $\alpha = 1.5$, $\beta = 0.4$, $\gamma = 3$ ***and*** $\delta = 0.2$

Phase plot of the predator-prey evolutionary model with the same parameters as above is shown on figure 2. Closed shape of phase trajectory confirms periodicity of the solution. Dynamical system (1) follows this trajectory counter-clockwise in phase space.

Figure 2 clearly shows the so called "atto-fox" problem [1] which is one of the most serious drawbacks of Lotka-Volterra equations. It is about the number of predators (e.g. foxes) being too small. In fact it may be a fractional number close to zero. In real world it would mean extinction, while the model suggests that a population can survive and fully recover after its number is reduced to 10^{-18} species.

Solution of Lotka-Volterra equations with a different set of parameters $\alpha = 1$, $\beta = 0.05$, $\gamma = 0.5$ and $\delta = 0.02$ is shown on figure 3. This solution looks more like a standard harmonic motion

$$s(t) = A\cos(\omega t + \varphi) \qquad (4)$$

with A being the amplitude, φ — the phase and ω — the angular frequency of oscillating in time t variable s. Phase plot of this solution is shown on figure 4.

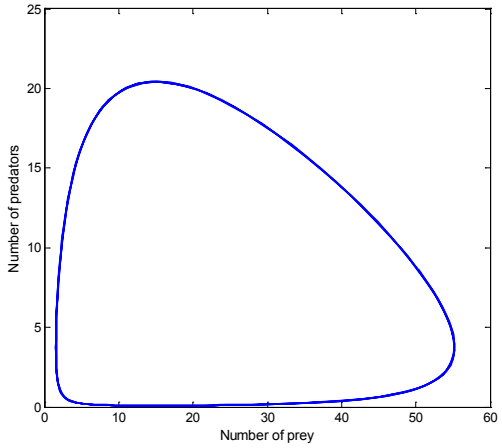

Figure 2. Phase portrait of the numerical solutions of predator-prey equations, $\alpha = 1.5$, $\beta = 0.4$, $\gamma = 3$ ***and*** $\delta = 0.2$

Harmonic motion takes a form of a closed oval (or a circle) in phase space [2] while phase plot on figure 4 has the form of an egg. This phase plot is clearly much closer to an oval than the phase trajectory on figure 2. The egg-like shape of phase trajectory may be explained by minor amplitude and phase fluctuations in equation (4).

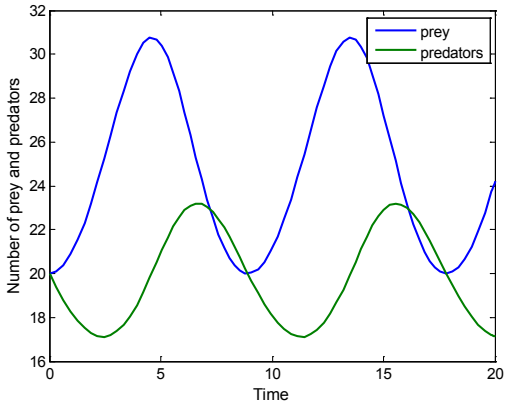

Figure 3. Numerical solutions of predator-prey equations, $\alpha = 1$, $\beta = 0.05$, $\gamma = 0.5$ ***and*** $\delta = 0.02$

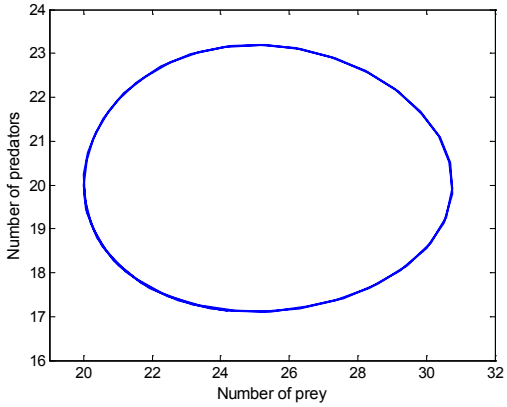

Figure 4. Phase portrait of the numerical solutions of predator-prey equations, $\alpha = 1$, $\beta = 0.05$, $\gamma = 0.5$ ***and*** $\delta = 0.02$

A traditional approach to obtain approximate analytic solution of system (1) is linearization, which simplifies the system of equations. Linearization of Lotka-Volterra equations results in a set of differential equations used to describe harmonic oscillation which have the general solution

$$\begin{aligned} x(t) &= A_1 \cos(\omega t + \varphi_1) \\ y(t) &= A_2 \cos(\omega t + \varphi_2) \end{aligned}, \qquad (5)$$

where A_1, A_2, φ_1 and φ_2 are parameters of harmonic oscillation depended on α, β, γ and δ. It is clear from figures 1 and 3 that solution (5) is just an approximation to the unknown analytic solution of system (1). This approximate solution will be discussed in more detail in the next section below.

Another approach to obtaining analytic solutions to the Lotka-Volterra problem is to analyze the invariant, or first integral, of the system (1), since the existence of a first integral reduces the system to a one-dimensional problem [3; 4]. The form of the first integral of equation (1) is known

$$\Lambda = \alpha \ln y + \gamma \ln x - \beta y - \delta x , \qquad (6)$$

where Λ is the conserved quantity — a constant value dependent on initial conditions and not on t.

Equation (6) has natural logarithms of x and y as well as their linear terms which makes it difficult to separate variables. A simple workaround is to analyze this equation in a 3D-space by introducing a function $E(x, y)$ such that

$$E(x, y) = \alpha \ln y + \gamma \ln x - \beta y - \delta x = \Lambda . \qquad (7)$$

A visualization of equation (7) is presented on figure 5. It resembles a surface bended downwards towards XOZ and YOZ planes, with the bends being caused by the logarithms in equation (7). The value of $E(x, y)$ is color coded.

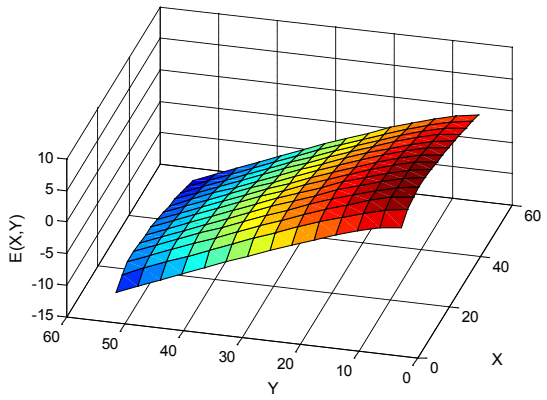

Figure 5. 3D plot of the first integral of Lotka-Volterra equations with parameters $\alpha = 1.5$, $\beta = 0.4$, $\gamma = 3$ and $\delta = 0.2$. Third axis corresponds to different values of conserved quantity Λ

Equation (7) describes the connection between variables x and y. And so do phase trajectories on figures 2 and 4. This means that equation (7) is an analytical form of describing the phase trajectory of system (1). A contour plot of $E(x, y)$ presented on figure 6 reveals that phase trajectories of numerical solutions to Lotka-Volterra equations with different initial conditions are isoclines of function $E(x, y)$. This fact is easy to explain as conserved quantity $\Lambda = E(x, y)$ corresponds to a constant of integration of system (1) and thus is dependent on initial conditions.

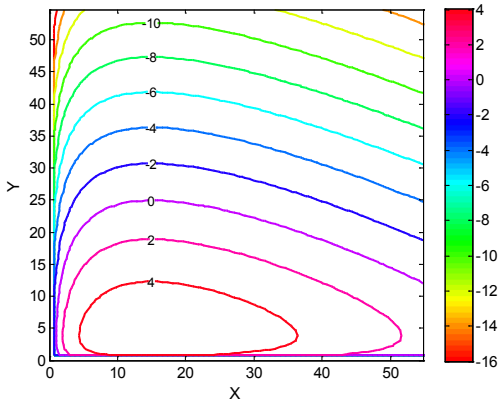

Figure 6. Contour plot of $E(x, y)$ with the same parameters as on the previous figure. Isoclines are color coded and correspond to different values of conserved quantity Λ

IV. Random Fluctuation of Parameters of Lotka-Volterra Equations

Lotka-Volterra equations do not take into account many different factors that together make a significant contribution to the process describing population dynamics. Those factors include death of both prey and predators from illnesses, deficit in prey's food supply, existence of alternative food sources for predators, seasonal, regional and different temporary factors affecting population growth and many other impossible to predict random events. Some of those factors may be accounted for by a more complex model based on systems of differential equations (2) or (3) but the random nature of events suggests that a stochastic model should be used instead.

By substituting some terms in equation (1) with stochastic processes we will receive stochastic differential equations (SDEs). SDEs are difficult to solve, hard to understand; even ordinary numerical methods for solving ODEs usually perform badly on SDEs. Those facts lead to a conclusion that it is better not to deal with SDEs.

An alternative approach is first to obtain a solution of an ordinary differential equation and then parameterize algebraic function of this solution with stochastic processes. This method allows avoiding main difficulties of SDE but requires non-numerical analytical solution of ODEs.

Let us consider solution (5) in the manner described above. If parameters A_1, A_2, φ_1 and φ_2 are stochastic processes than each equation in solution (5) is a Gaussian narrow-band random process [5; 6]

$$s(t) = A(t) \cos\left[\omega_0 t + \varphi(t)\right], \qquad (8)$$

where $A(t)$ and $\varphi(t)$ are some slowly varying relative to $\cos\omega_0 t$ random functions of time; $s(t)$ is either a number of predators $y(t)$ or a number of prey $x(t)$.

Representation of a Gaussian narrow-band random process in the form of equation (8) is general for many different domains of science. Random functions $A(t)$ and $\varphi(t)$ are usually called an envelope and a phase of process $s(t)$. $A(t)$ and $\varphi(t)$ are statistically independent [5]. Random phase $\varphi(t)$ is uniformly distributed over interval $\varphi(t)\in[-\pi,\pi]$ while random envelope $A(t)$ has a Rayleigh probability distribution function, $A(t)\in[0,\infty)$.

For simulating process (8) it is important that $A(t)$ and $\varphi(t)$ remain slowly varying functions relative to $\cos\omega_0 t$. To achieve this a uniform and a Rayleigh random noises have to be smoothed in order to make their maximum spectral frequencies significantly less than ω_0. Unfortunately low-pass filters used for smoothing affect not only the frequency domain of processes $A(t)$ and $\varphi(t)$ but also their distribution functions, making them approach Gaussian distribution instead of their original uniform and Rayleigh distributions.

This problem can be solved by a different representation of random process $s(t)$ by means of quadrature components $A_c(t)$ and $A_s(t)$

$$s(t)=A_c(t)\cos\omega_0 t-A_s(t)\sin\omega_0 t, \qquad (9)$$

where $A_c(t)=A(t)\cos\varphi(t)$ and $A_s(t)=A(t)\sin\varphi(t)$. Components $A_c(t)$ and $A_s(t)$ are connected with functions $A(t)$ and $\varphi(t)$ by simple formulas

$$\begin{aligned} A(t)&=\left[A_c^2(t)+A_s^2(t)\right]^{1/2},\ A(t)\ge 0\\ \varphi(t)&=\operatorname{arctg}\left[A_s(t)/A_c(t)\right],\ \varphi(t)\le|\pi| \end{aligned}. \qquad (10)$$

The advantage of equation (9) is that slowly varying quadrature components $A_c(t)$ and $A_s(t)$ both have Gaussian distribution and low-pass filters don't affect it. The algorithm of smoothing of a random process is described in [7].

Phase portrait of solution (5) with $x(t)$ and $y(t)$ taking the form (8) is given on figure 7. In this case phase trajectory of the system can be thought of as a two-dimensional vector random process $\xi(t)=\{x(t),y(t)\}$ [5; 8]. Behavior of trajectory $\xi(t)$ on phase plane (x,y) could be described in terms of level-crossing theory of stochastic processes [2; 5; 9].

Let's estimate the number of excursions of this two-dimensional process outside a predefined area Ω which satisfies the conditions $x(t)\in[H_1,H_2]$, $y(t)\in[H_3,H_4]$. A general formula for an average number of excursions $N_\xi(\Omega,T)$ of phase trajectory $\xi(t)$ outside a predefined area Ω during time interval $[t_0,t_0+T]$ is written as follows

$$\begin{aligned} &N_\xi(\Omega,T)=\\ &=\left[N_x^-(H_1,T)+N_x^+(H_2,T)\right]\times\\ &\times P\{y(t)\in[H_3,H_4]\}+\\ &+\left[N_y^-(H_3,T)+N_y^+(H_4,T)\right]P\{x(t)\in[H_1,H_2]\} \end{aligned}, \qquad (11)$$

where $N_*^\pm(H_i,T)$ is an average number of positive or negative excursions of one-dimensional process $x(t)$ or $y(t)$ outside level H_i during time interval $[t_0,t_0+T]$.

Average value $T_\xi(\Omega)$ of relative duration of process $\xi(t)$ staying in a predefined area Ω would be expressed by formula

$$\begin{aligned} T_\xi(\Omega)&=P\{\xi(t)\in\Omega\}=\\ &=P\{x(t)\in[H_1,H_2],\ y(t)\in[H_3,H_4]\} \end{aligned}. \qquad (12)$$

Finally an average duration of an excursion of two-dimensional process $\xi(t)$ outside area Ω can be obtained from the following formula

$$\tau_\xi(\Omega)=\frac{1-T_\xi(\Omega)}{T^{-1}N_\xi(\Omega,T)}. \qquad (13)$$

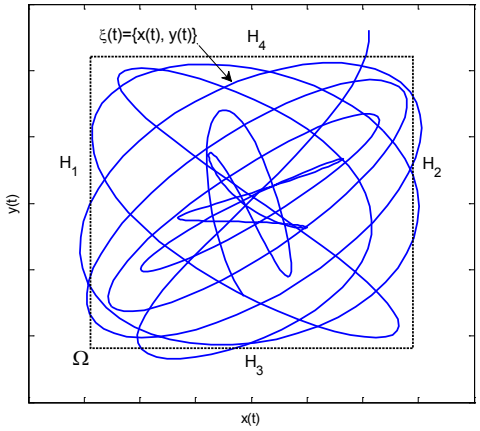

Figure 7. Phase trajectory of a two-dimensional vector random process $\xi(t)=\{x(t),y(t)\}$ on a phase plane (x,y)

For Gaussian processes $x(t)$ and $y(t)$ values $N_*^\pm(H_i,T)$ and $P\{*(t)\in[H_i,H_{i+1}]\}$ can be easily estimated. That is for a zero mean Gaussian process $\eta(t)$

$$P\{\eta(t)\in[H_i,H_{i+1}]\}=\Phi\left(\frac{H_{i+1}}{\sigma_\eta}\right)-\Phi\left(\frac{H_i}{\sigma_\eta}\right), \qquad (14)$$

where Φ is the Laplace function and σ_η is the standard deviation of $\eta(t)$; and

$$\begin{aligned} &N_\eta^+(H_i,T)=N_\eta^-(H_i,T)=\\ &=\frac{T}{2\pi}\left[-r_\eta''(0)\right]^{1/2}\exp\left(-\frac{H_i^2}{2\sigma_\eta^2}\right), \end{aligned} \qquad (15)$$

where $r_\eta''(0)$ is the value of second derivative of normalized correlation function $r(t_1,t_2)$ at zero point.

V. Conclusion

Phase trajectory of a solution to Lotka-Volterra equations with random parameters shown on figure 7 reveals that this solution corresponds to real species evolution in a much better way than the deterministic solution, obtained by numerical integration. Indeed there are an uncountable number of known and unknown factors (in other words visible and hidden variables) that affect population dynamics in nature and a good mathematical model must take that fact into account by means of statistics and random variables.

It is shown that stochastic disturbances of parameters of solution to predator-prey equations could be described by level-crossing theory. Analytic expressions for calculating level-crossing statistics are presented in equations (11-15).

With the help of analytical and graphical techniques, the Lotka-Volterra equations reveal useful information about the dynamics of a predator-prey system. Despite some limitations, they serve as a decent model for many two-species environments.

References:

1. D. Mollison. "Dependence of epidemic and population velocities on basic parameters", Math. Biosci., 107, 1991, Pp. 255-287
2. M. Polyak. "Analysis of phase trajectories of a random process", *International Forum "Modern information society formation – problems, perspectives, innovation approaches": Proceedings of the Forum*, St. Petersburg, June 6-11 / SUAI, SPb, 2010. Pp. 75–80
3. C.M. Evans, G.L. Findley. Analytic Solutions to the Lotka-Volterra Model for Sustained Chemical Oscillations // S.G. Pandalai, ed., Recent Research Developments in Chemical Physics, 2000. Pp. 1-32
4. D Hyde. Predator-Prey Modeling with the Lotka-Volterra Equations, 2011. URL: http://onlinemathcircle.com/wp-content/uploads/2012/03/Lotka-Volterra-Equations.pdf (visited on 22/03/2013)
5. V. I. Tikhonov, V. I. Khimenko, *Excursions of the Trajectories of Random Processes*. Moscow, Nauka, 1987.
6. V. I. Khimenko, D. V. Tigin, *Statistical acousto-optics and signal processing*, St.-Petersburg, Published by St.-Petersburg University, 1996.
7. M. Polyak. "Smoothing interval estimation for a random process in real time", *International Forum "Information and communication technologies and higher education – priorities of modern society development": Proceedings of the Forum*, St. Petersburg, May 26-30 / SUAI, SPb, 2009. Pp. 72–75
8. M. Polyak. "Phase-plane method: a practical approach", *International Forum "Modern information society formation – problems, perspectives, innovation approaches": Proceedings of the Forum*, St. Petersburg, 30 May – 3 June / SUAI, SPb., 2011. Pp. 55-59
9. V. I. Tikhonov, V. I. Khimenko, "Level-crossing problems for stochastic processes in physics and radio engineering: A survey", *Journal of communications technology & electronics*, vol. 43, No 5, Pp. 457-477, 1998

DESIGN AND DEVELOPMENT OF AN EMBEDDED ORIENTED FRAMEWORK FOR THE CONTROL AND MONITORING OF REMOTE SYSTEMS

Guglielmo Seminara

Department of Electric Electronic and Computer Engineering
University of Catania, Italy

1. Introduction

Imagine a world where is possible to control everything is around us from whatever places and where anyone can monitoring the data from real world using small devices, easy to configure and to install. Internet is the key to realize it. Today, computers and mobile devices are part of our life. All activities occur by them: work, fun, communication and content sharing. We can imagine that inside them there is all that we use more frequently or that makes life easier. But this is not enough. I must be able to perform all my activities using different devices in different places. In order to do this is required a net, a system that allows to link together more executors.

With the development of nanotechnologies, high computing powers and different functionalities are available in tight spaces inside integrated circuits whose behaviour is defined by a program. The language used for its definition evolves with the computing powers and this allows to converge complicated functionalities in a single device, for example a server web inside them. A server is a component that provides a service to another component named client that makes requests. To communicate, the two entities, must talk using the same language, they must have a common communication protocol that ensures performance and reliability. Today is possible to implement web server in very small and cheap devices, so we can monitoring or enable its I/O from remote.

Data presentation in Internet environments occurs through web pages. They are developed using different technologies, the most widespread, standard and lightweight is HTML. The language offer the possibilities to create graphical interfaces without difficulties that are visualized on a browser.

Graphical processing is delegated to client devices, accordingly the computation also. Since also small devices have high computing powers, it is possible to implement graphical interfaces that allows better data visualization. With HTML5 [1], a new version that introduces features that before were only present in the operative systems, it was released a component that allows to draw using programming, Canvas. Drawing and event handling allows to realize more imaginative graphics, animations and games whose market was exclusively of Flash.

2. Virtual Instruments

For many years the electronic instrumentation was the only solution at the measurement problem. Although they ranged in size and functionality, they all tended to be box-shaped objects with a control panel and a display. They are very powerful, expensive and designed to perform one or more specific tasks defined by the vendor. The user generally cannot extend or customize them. The knobs and buttons on the instrument, the built-in circuitry, and the functions available to the user, all of these are specific to the nature of the instrument.

Widespread adoption of the PC over the past twenty years has given rise to a new way for scientists and engineers to measure and automate the world around them. One major development resulting from the ubiquity of the PC is the concept of virtual instrumentation. A virtual instrument consists of an industry-standard computer or workstation equipped with application software, cost-effective hardware such as plug-in boards, and driver software which together perform the functions of traditional instruments. Today virtual instruments are used in many application with faster development, higher quality products and lower costs. Virtual instruments replace the traditional panel equipped with buttons and display by a virtual front panel on a PC monitor.

Actually the most known tools are as follows:

- Labview [2]. Is a highly productive graphical programming language for building data acquisition and instrumentation systems.
- LabWindows [3]. Is a Windows based, interactive ANSI C programming environment designed for building virtual instrumentation applications.
- HP Vee [4] . Allows graphical programming for instrumentation applications. It is a kind of Visual Engineering Environment, an iconic programming language for solving engineering problems.
- Measurement Studio. Provides a collection of controls and classes designed for building virtual instrumentation systems inside Visual Basic or Visual C++.
- Labview Web. Allows to develop web based applications through graphical programming. A GUI enables the user to control and monitor labview based measurement system through web browser.

- Dundas dashboard software [5]. Is a platform used to create dashboards. The web version allows to be integrated in web applications that use silverlight, while the standard version borns for .NET.

Fig.1 Electronic Instruments.

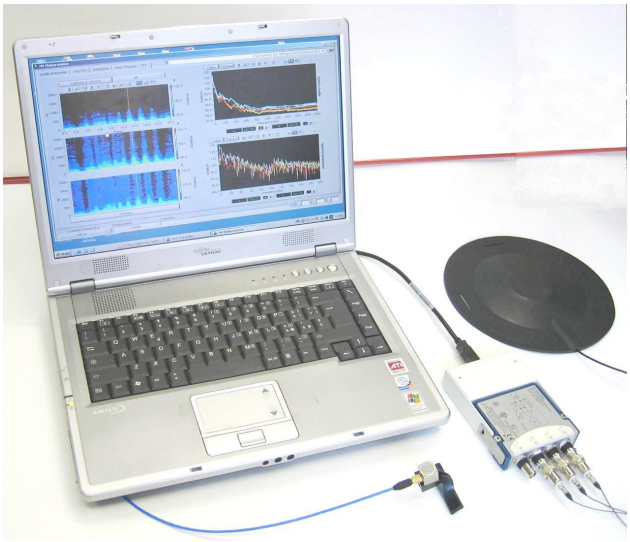

Fig.2 Virtual instruments.

3. Limits of current technologies

Although current technologies provide a high level functionalities, they present some limitations which prevent a wider use. Some of these technologies aren't available for the web so it's not possible to share information. Others use Flash or Silverlight, which are strongly dependent from the operating system used in microsoft environments and not accessible from mobile devices. Moreover often they use a proprietary language which is hardly extendible. They limit the use of a server with specific technology and they are hard to insert in embedded devices. At last they aren't open source. These reasons have led us to the realization of a framework that allows to define virtual instruments, simply and in the majority of the devices: Drinks.

4. Drinks

It hasn't a proprietary language but uses the power of Javascript and HTML to interface it with the browser and it is a framework wherewith we can create and use some widget. Drinks is a web technology and accessible from whatever part of the world and not dependent from system operative like Flash or Silverlight. It allows to integrate the components with other Javascript libraries and in any websites using any server side technology, also it is an open source project released under New BSD license. To demonstrate the completeness of the toolkit we have realized a comparison between Labview and Drinks showed in Fig.3 and Fig.4.

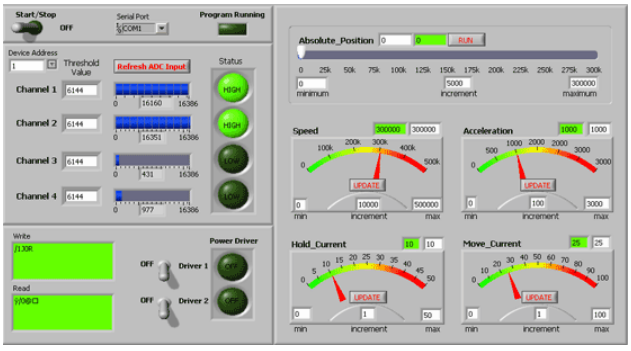

Fig.3 A panel created using Labview.

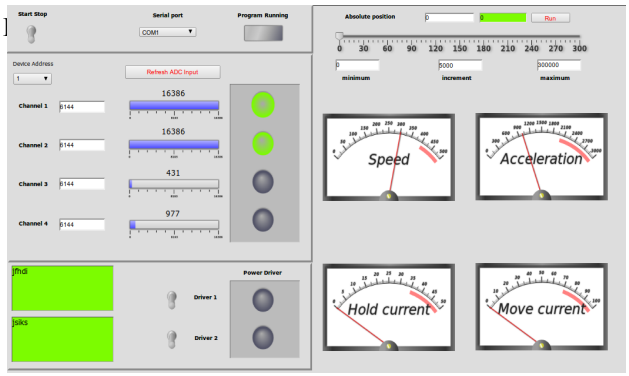

Fig.4 The same panel created using Drinks.

In the first version Drinks implements 20 instruments. They are divided into categories and to each one is associated a tag. The categories are Knob, Display, Switch, LED and Slider. The toolkit is showed in Fig.5.

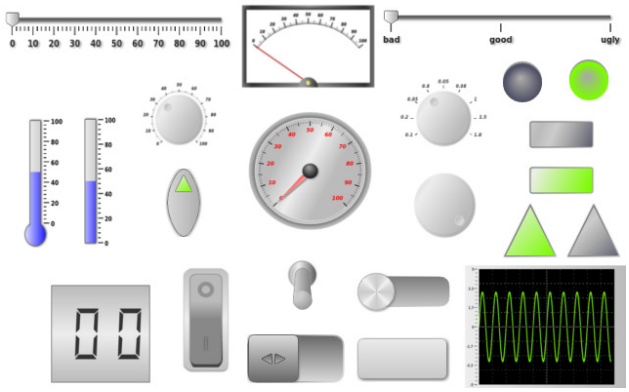

Fig.5 Drinks toolkit 1.0

The components have a series of attributes that can be configured. Some of these are for example width, height and radius for the sizes, value, min_range and max_range to set the range of the instrument, align for the alignment, divisions and precision.

We have designed some events to define procedures that trigger when some conditions occur for example: onchange, when the instrument changes its value, onload, when it is loaded and onalert, onleavealert when the instrument enters or leaves from an alarm range.

Instruments can be also created and its properties manipulated using Javascript. Two important features are the Ajax support and the instruments compositing. Ajax is transparent to the user using two attributes href and refresh that indicate respectively the file that the request must contact and the seconds that must pass from a request and another. Drinks also provides an Ajax class that implements functionalities like GET and POST requests. Instruments can be composited from the base components to advanced simply inserting their tag inside the parent instrument. Also we can associate a tag to the advanced component just created. For example a gauge with a seven segments display and a led.

Fig.6 A gauge with a Led and a 7segments Display.

One of the possible applications of Drinks is the digital oscilloscope. It can be created using an important component: the Display Graph. It is a widget that render a series of point as a function of time. The most important attributes are sweep, frequency, amplitude and position x, y. Also we can set the mode of render selecting from CH1 (channel 1), CH2 (channel 2), dual (both channel), X/Y (one as a function of the other). So combining the display graph with other components like sliders and knobs we achieve a digital oscilloscope.

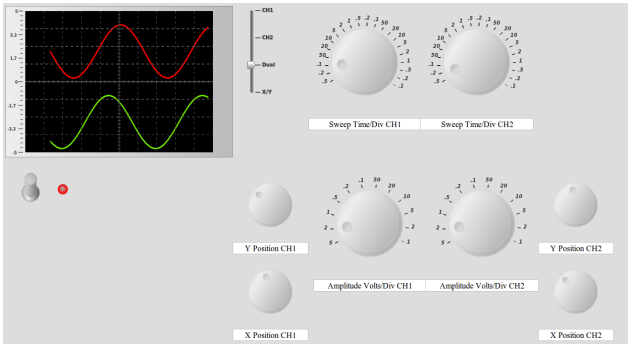

Fig.7 Digital Oscilloscope made with Drinks.

5. A case study: AgriNET

Thinking to the possible applications we have designed a system for the Precision Agriculture [6] area. For example we can be interested to monitor parameters as PH, conductivity, temperature, salinity or light in order to grow up our plants in the better of the ways. So we have developed an embedded system oriented to the remote control of sensors and actuators linked to a microcontroller with a server web: AgriNET.

The hardware used is FlyPort. It is developed From OpenPicus team and its features are:

- Microchip 16 bit processor PIC24FJ256
- 16K Ram
- 5 Volt power supply.
- Digital and analog I/O.
- 4 UARTs.
- RTC 32.768 Khz
- RJ45 connector.

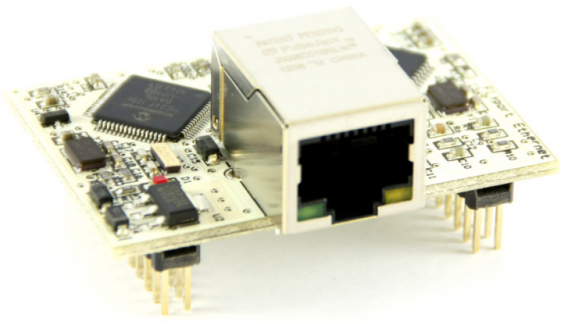

Fig.8 Flyport board provided by OpenPicus team.

The TCP/IP stack is implemented by microchip and

provided for free. The protocols that are supported are ARP, IP, ICMP, TCP, UDP, DHCP, SNMP, HTTP, FTP, TFTP. We have also provided the board of an eeprom to store data, and an XBEE to have scattered sensors without wired connections.

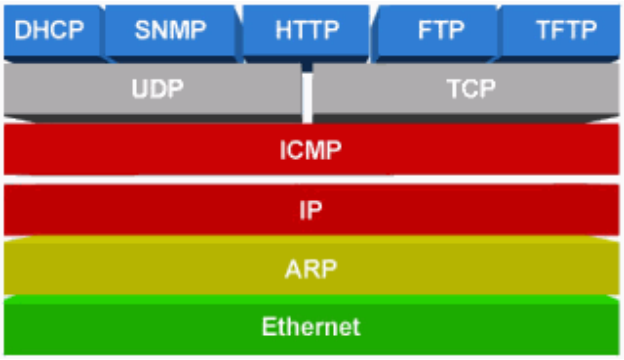

Fig.9 Microchip TCP/IP stack.

In the main page we can see the temperature of the board, the state of digital inputs, digital outputs and analog inputs. The user can set a series of parameters like net and port configurations. We can define a description for each port, a max and min threshold that if is exceeded, the system triggers an alarm, time parameters and others.

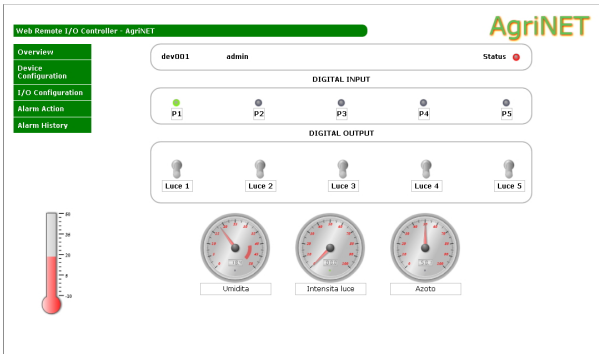

Fig.10 AgriNET main page.

User can also define an action to do when the alarm occur like an email, an sms or an output enabled or disabled. There is also a section where the user can see a report of the alarms occurred.

6. Conclusions

The framework presented in this paper lends itself optimally to be included in embedded environments, thanks to the AJAX support, the update times of the values taken from the hardware can be configured and driven at high speeds. The integration in FlyPort allowed us to implement an embedded system which has shows very good functionalities. The components of the system can be viewed from mobile devices and the language adopted is simple and standard.

References

[1] Chen Li-Li; Liu Zheng-Long, "Design of Rich Client Web Architecture Based on HTML5," Computational and Information Sciences (ICCIS), 2012 Fourth International Conference on , vol., no., pp.1009,1012, 17-19 Aug. 2012

[2] Swain, N.K.; Anderson, J.A.; Ajit Singh; Swain, M.; Fulton, M.; Garrett, J.; Tucker, O., "Remote data acquisition, control and analysis using LabVIEW front panel and real time engine," SoutheastCon, 2003. Proceedings. IEEE , vol., no., pp.1,6, 4-6 April 2003

[3] Xue Qing; Jia Luo; Yonghong Liu; Changwei Zheng, "Research and application of virtual instrument for tank integrated simulator based-on LabWindows," Quality, Reliability, Risk, Maintenance, and Safety Engineering (ICQR2MSE), 2012 International Conference vol., no., pp.1458,1460, 15-18 June 2012

[4] Klinger, M., "Reusable test executive and test programs methodology and implementation comparison between HP VEE and LabView," AUTOTESTCON '99. IEEE Systems Readiness Technology Conference, 1999. IEEE , vol., no., pp.305,312

[5] http://www.dundas.com/dashboard/

[6] Qingyuan Ma; Qiang Chen; Qingsheng Shang; Chao Zhang, "The Data Acquisition for Precision Agriculture Based on Remote Sensing," Geoscience and Remote Sensing Symposium, 2006. IGARSS 2006. IEEE International Conference on , vol., no., pp.888,891, July 31 2006-Aug. 4 2006

BREADBOARD OF MINIATURE ELECTRONIC SYSTEM OF PRESSURE CONTROL FOR GAS PIPELINE

Shabashev D., Daletskiy A.

Saint-Petersburg State University Of Aerospace Instrumentation,
Saint-Petersburg, Russia
dshabashev@gmail.com

Abstracts

Pressure is one of key technical parameters of technological process. Sensors of pressure provide the most important information about technological process and ensure its safety. In the paper we propose breadboard for studying of parameters of modern electronic pressure sensors. Technical description and appearance of breadboard are given.

I. Introduction

Today the sphere of application of sensors of pressure covers many industries, such as: food, pharmaceutical, chemical, oil processing power, mechanical engineering, water purification etc. For measurement of various parameters of pressure specialized sensors are used. The list of parameters measured by these devices isn't limited only to pressure and pressure difference. Level of liquids, consumption of liquids and gases also can be indirectly measured by them [1]. By the principle of functioning sensors of pressure are subdivided on mechanical and electronic. The most widespread mechanical pressure sensors are manometers, but in connection with their shortcomings electronic sensors of pressure come to change by it. It is obvious that for the students who are studying in "Industrial Electronics" research of electronic sensors of pressure, their characteristics and the physical processes connected with their work is very important. The developed breadboard of research electronic pressure sensor is for course "Sensors of measurement equipment".

II. Choice of sensors

Pressure sensors can be classified in a following way:

1. By the type of measured pressure (absolute, relative, differential).
2. By type of fluid (gas, liquid, vapor, aggressive).

There are several criteria for the selection of pressure sensor:

1. Sensor type that is determined by the type of pressure applied to the sensor (absolute, relative, differential).
2. The error in the temperature range (from 5% to 10%).
3. Type of work environment for pressure sensor (dry gas).
4. The value of the supply voltage (5V, 12V).
5. Simplicity of the device (the minimum number of additional components to be included).

Following the criteria set out above, in this laboratory model was selected pressure sensor of dry gas MPX4250AP by Motorola. This sensor has the following features:

1. Measurement range is 0 to 250 KPa;
2. Small size and weight (3x2.8sm);
3. Supply voltage 5V;
4. An interface to a variety of microprocessor.

III. Schematic diagram

As with most existing electronic pressure sensors there is a direct dependence of output signal with the sensor supply voltage. The appearance of the selected sensor is shown in figure 1.

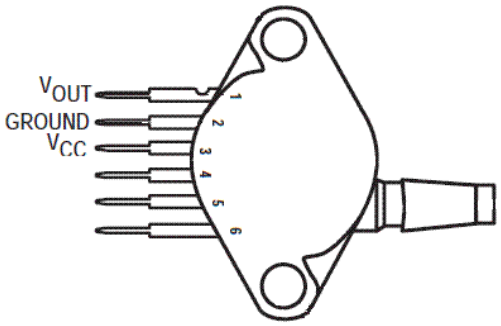

Figure 1– The appearance of the sensor MPX4250AP

The sensor has six pins, three of which are not used in this laboratory breadboard. The other three are used to supply power, ground and output signal. Schematic diagram of the inclusion of the sensor is shown in the figure 2.

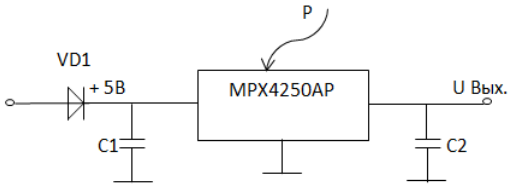

Figure 2 – Electric scheme

In this circuit, the diode VD1 is designed to protect circuits against reverse polarity Capacitor C1 filters the supply power and C2 - smoothing the output signal.

IV. Capabilities of breadboard

The laboratory equipment consists of two parts. The first step is the research of the static characteristics in order to study the dependence of the output signal from the current pressure. According to the datasheet graph of this dependence is shown in figure 3 [2].

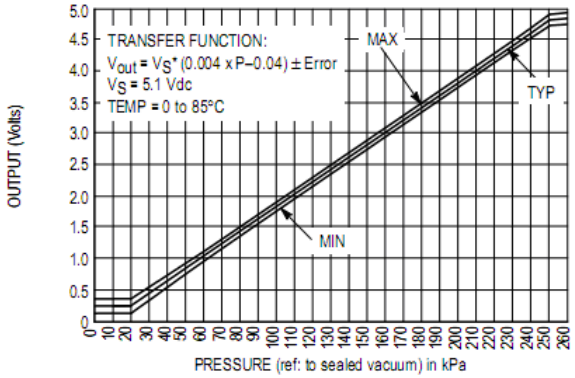

Figure 3 - Static characteristic of the sensor

The second step is to analyze the dependence of the accuracy of the sensor by the stability of the supply voltage.
The design of breadboard is shown in figure 4.

V. Construction of the breadboard

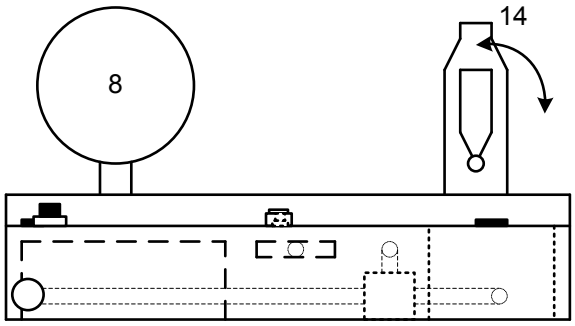

Figure 4 - The design of the breadboard (in front view).

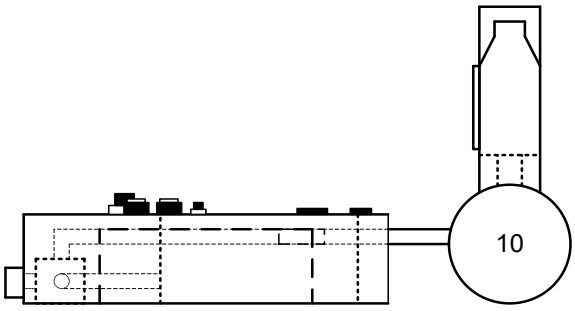

Figure 5 - The design of the breadboard (side view).

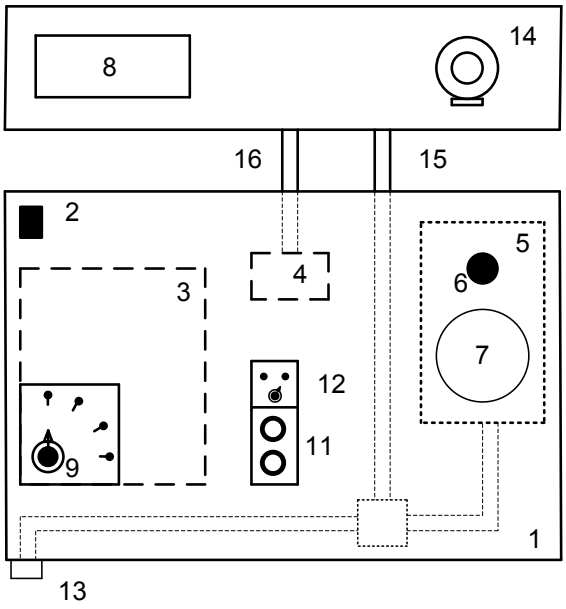

Figure 6 - Design of the breadboard (top view).

Proposed construction of the layout has the following components:

1. Case of breadboard.
2. Switch on button.
3. Power supply plugin.
4. Electronic pressure detector.
5. Compressor.
6. Compressor switch on button.
7. Basic manometer.
8. Precise manometer.
9. Supply voltage control.
10. Working volume
11. Clamp of external Multimeter.
12. Mode switcher
13. Draw off valve №1.
14. Draw off valve №2.
15. Pipe from compressor to useful capacity.
16. Pipe from useful capacity to detector.

VI. Appearance of breadboard

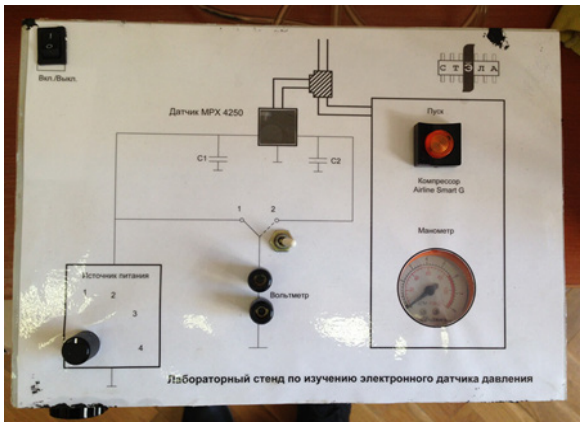

Figure 7 – Control panel.

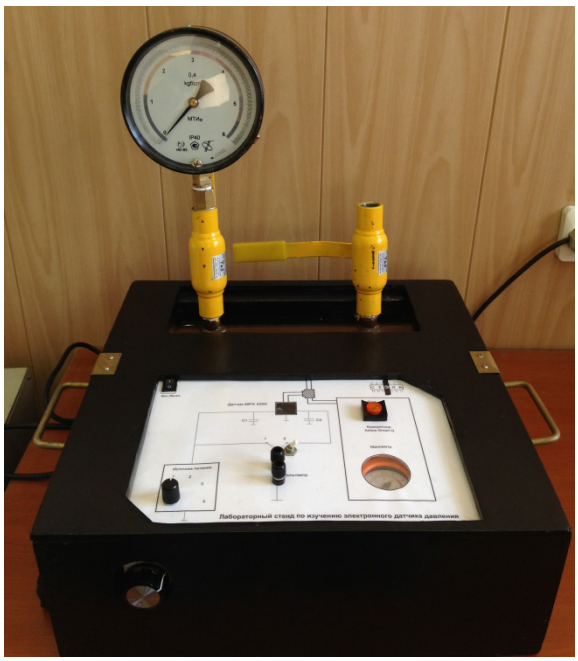

Figure 8 - Appearance of the breadboard.

Figure 9 – Working volume, draw off valve and precise manometer.

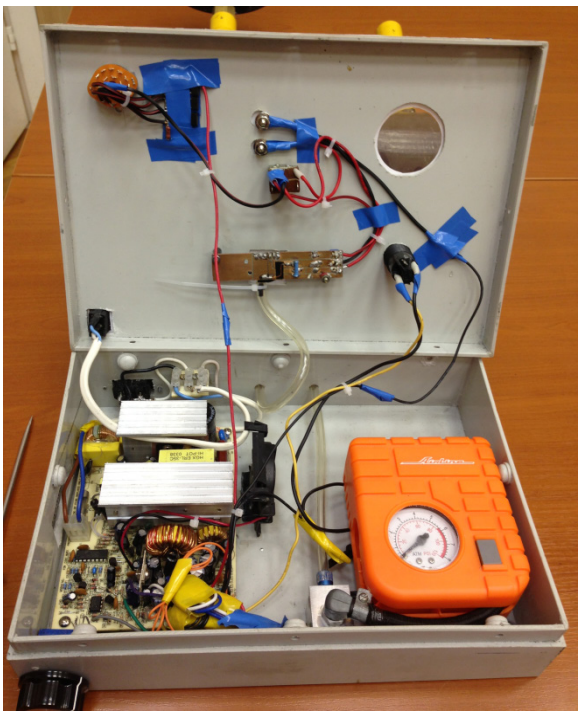

Figure 10 – Internal view of breadboard.

Conclusion.

This breadboard has the following advantages:

1. Visualization of physical processes.
2. Easy to use.
3. Cheap.

The next upgrades are possible:

1. Changing of gas temperature
2. Connecting the breadboard with PC

References

1. www.pressure.ru/sensors.shtml
2. Datasheet MPX4250APFREESCALE SEMICONDUCTOR
3. http://gendocs.ru/v5429/конспект_лекций_современная_элементная_база_систем_управления_ла?page=7

OPTIMIZATION OF THE PRODUCTION-ENGINEERING PROCESSES FOR PRECISION FIGURINE DESIGNS

Oleg Vasilyev
Saint-Petersburg State University of Aerospace Instrumentation,
Saint-Petersburg, Russia
innfri@gmail.com

Abstract

Purpose - to improve the quality of manufacturing precision figurine designs that meet the best standards and requirements of international, industry and government standards by creating an automated system of hardware and software. In the process we used the method of the situational approach of quality management, SWOT-PEST-analysis and the methodology for functional simulation in the standard IDEF0 and computer-aided design AutoCad. As a result, a model of complex automated manufacturing of precision figurine design waveguide systems was developed.

Keywords: electrochemical shaping, contingency management, infrastructure support, waveguide system, electroplating, quality control, IDEF0, workflow, integrated automated system tenzoimpuls regulation.

I. INTRODUCTION

Fabrication of waveguides by galvnoplastiks seems most appropriate in terms of accuracy, complexity, and cost effectiveness.

Electroplating is widespread as a method to produce thin-walled parts with precise internal profile that are not economically inefficient or impossible to get any other way. These details include the waveguides. Main working surface of the waveguide are internal. The purity of the inner surfaces of channels depend attenuation radio waves and stability of the individual components of the waveguide system. Using the method of electroplating, one can accurately reproduce the complex micro-and macro-geometrical relief by electroplating a metal layer on the model, the shape, size and surface roughness of which correspond to the interior of the waveguide channel. The thickness of the deposited layer is determined by the required mechanical strength and can range from 0.5 to 5 mm. The deposited metal can be copper, nickel, nickel-cobalt. When choosing the design of rational mandrel can completely eliminate machining, since the deposition process provides sufficient accuracy and base surfaces abutting nodes [1].

In previous works of the author has developed and presented a model described above technology, the methodology for functional modeling IDEF0. The outcome of the study was to identify bottlenecks process, streamlined functionality, define the control points, and identified the criteria to optimize the system as a whole. Deposition of a metal or alloy is in the need for control and management of the potential difference, current, temperature, agitation, electrolyte composition, etc. All these factors affect the speed, frequency, regularity and quality of the deposition of copper particles on the mandrel. Such processes are difficult to monitor and control, not to mention the introduction of complex systems, the aim of which is to obtain new the quality and reduce the time of manufacture.

II. PROCESSES AND CONNECTIONS

There are plenty of waveguides, which are currently produced by mechanical means of brass, copper, nickel and alloys, a wide variety of structures that define the parameters of the product. The more complex the product design and more release program, the economically expedient to translate it into galvanoplastic method of manufacture.

Manufacture of precision components figurine waveguide systems is the combined process, which include a number of complex sub:

- models design,
- models production,
- cnc mechanical and chemical treatment models,
- the actual process of deposition of metals and alloys,
- separating products from the model,
- final cnc machinating products, etc.

Connection between them depends on the extent of the production management system, the organization providing the infrastructure and availability of quality management system.

Maintaining the stability of process parameters during manufacture of the product, the optimal transition from one subprocess to another, and thereby minimize the risk of mistakes and defines marriage in the long run, the quality of the product and, most importantly, the quality of the whole process.

Thus, electroplating is the most complex physical and chemical process in the chain of sub-manufacturing products. Defining parameters can be

considered as the amount of current, the form and frequency of the voltage, the chemical composition of the electrolyte, the weight, density and configuration of the location of the cathode-anode system in the bath, etc. The stability of these parameters determines the stability (repeatability) of quality of the products, which is essential in the manufacture of high-precision, precision parts waveguides complex configurations.

That the enterprise quality management system based on the principles of Total Quality Management and process-oriented approach within the requirements and recommendations of the series of standards ISO 9001-2008, is to ensure that the manufactured precision figurine design (PFD) waveguide systems will exactly match the requirements of the specification and, therefore, will reduce the cost of production.

III. WAY FOR IMPROVEMENT

Advantage and definition of customer satisfaction makes it possible to measure, analyze and improve the result of the manufacturing process PFD.

Relying on "continuous improvement" process-oriented approach, a model was developed technological process of PFD methodology IDEF0. This allowed the process to identify bottlenecks and focus on the modernization of the technological base of production and laboratory.

From the analysis of the model that is necessary to create a more thorough and comprehensive study:

- Detailed specification;
- Design of equipment;
- The creation of an experimental model;
- Calculation of cost-effectiveness;
- Upgrading of laboratory facilities;
- Find and attract investment in the project;

In drawing up the terms of reference should be tailored to suit a typical production process of manufacturing products using electroforming, which include the following, the basic process:

- Design and production of the model;
- The application of the conductive layer in the case of models of dielectric materials;
- Electrolytic deposition of active layer;
- The application of the structural layer;
- Machining massing;
- Extraction model.

Compared with other processes the deposition of metal on the model is much longer vulnerable to power surges and difficult to control. The need was to stabilize the current intensity with a minimal pulse in the range of 0 to 50 Amps. Must maintain a constant temperature of the electrolyte, read acidity, provided mixing. There are also some disadvantages of this method:

- Uneven distribution of electrolytic deposits on the surface of the relief model, complicating production of parts with square corners, grooves and channels;
- A limited number of metals and alloys that can be used in the manufacture of parts;
- Relatively low deposition rate.

All identified indicators highlighted the need to formalize the specification and design of complex automated system of manufacturing PFD with all deficiencies and requirements of the key standards.

IV. Conclusion

According to the results of the research methods of background acoustic resonance self-regulation processes and electrochemical formation, using AutoCad CAD system developed and offered to the consideration of 3D-model of Universal installation electroforming (Fig. 1).

Fig. 1 - 3D-model of the universal automated installation electroforming

This work requires continuous improvement and testing of new systems to qualitatively improve the final result. Especially because this is required by ISO 9001.

References

[1] Vasiliev, O.I. Quality assurance processes of manufacturing precision figurine designs of waveguide systems / O. Vasiliev, E. Semenova // Questions electronics. Ser. General engineering. 2011. No. 3. P. 8-36

[2] Kudryavtseva, O.V. Tech electroforming / O.V. Kudryavtseva. SPb.: Polytechnic, 2010. 148.

[3] Vasiliev, O.I. Innovation effect of the regulation in the process of manufacturing precision figurine designs / O. Vasiliev, IA Vasilyev. / Scientific. SUAI session: Sat. Report: Part 1, Part 3: Engineering. SPb.: SUAI, 2012. C.

NEW FUNCTIONAL MATERIALS BASED ON LaF_3-SrF_2 HETEROSTRUCTURES

Tikhon Vergentyev

Saint-Petersburg State Polytechnic National Research University
Saint-Petersburg, Russia

I. INTRODUCTION

Last years the active development science direction is investigations of thin films and heterostructures based on MF_2, where M = Ca, Sr, Ba, Cd and RF_3, where R – rare-earth elements and ionic solid solutions $R_{1-x}M_xF_{3-x}$. Based on it the models of fluoride sensors [1], oxygen sensors [2], batteries [3] and transistors [4] are proposed. These functional materials are an integral part of the industry nano instrumentation. However the question about modification active component of these devices is open.

The new approach to modification fluoride materials was offered by Joachim Maier and co-workers [5]. Creation of heterostructures BaF_2-CaF_2 has allowed changing the conductivity of samples by two orders of magnitude higher than the conductivity of pure component. The authors made the assumption about the mechanism of ion transport F^- to boundary interfaces increasing the in-plane conductivity.

The purpose of this experimental work is growing of heterostructures LaF_3-SrF_2 with total thickness 200nm and the different thicknesses per layer varying from 100nm to 5nm on the substrates MgO (100) and investigation their planar conductivity. Also compare the results with thin films of pure materials LaF_3, SrF_2 and solid solutions $La_{0.5}Sr_{0.5}F_{2.5}$, $La_{0.95}Sr_{0.05}F_{2.95}$.

II. SAMPLE PREPARATION AND EXPERIMENTAL TECHNIQUE

The thin films are grown into modified vacuum system with oilless vacuum 10^{-8} Pa and equipped RHEED methodic. Epi-ready substrates MgO (100) with size 3x10x0.5 mm^3 are used, which are fixed on the electrical heater. The thicknesses are measured with quartz sensor with 5% precision. The density of SrF_2 is estimated according to the ratio of the growth rate $\frac{\upsilon_{SrF2}}{\upsilon_{SrF2}+\upsilon_{LaF3}}$.

After exposure to air, the gold electrodes are deposited on the end of samples for further measurements conductivity of thin films. The electro-physical parameters were measured with dielectric spectrometer Novocontrol BDS'80 in the wide temperature (300-570K) and frequency ranges (10^{-1}-10^6Hz). The magnitude of field strength is V_{rms}=50V/cm. The relative errors of the impedance and capacity do not exceed ~$3*10^5$. The stability of temperature is less than 0.1K.

III. RECEIVED RESULTS AND DISCUSSION

The Nyquist's plots of investigated samples consist of a semicircle and a sloped line that is typical for systems of solid electrolytes [6]. The figure 1 shows a hodograph of impedance with N=10 (in further N is total number of layers LaF_3 and SrF_2 includes in the heterostructures) and corresponding to it an equivalent circuit, where R_v – bulk response of the sample, C_{dl} – capacity of double layer of boundary "electrode/electrolyte" and $Z_w=(1-j)W\omega^{-0.5}$ – Warburg impedance describing diffusion processes in investigating systems, where W – Warburg constant [7]. The intersection of the semicircle with the horizontal axis is equal the direct current (DC) resistance of solid electrolytes (R_v). Thus DC-conductivity of measured electrolyte is $\sigma_{DC} = \frac{1}{R_V}\frac{d}{S}$, where d – distance between electrodes, S – square of end part of heterostructure under the electrode.

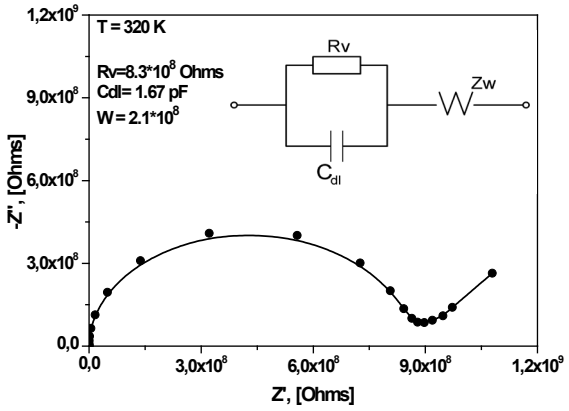

Figure 1. The hodograph of impedance for structure with N = 10 at the temperature 320K. The insert: the equivalent circuit describes the migration process in this sample.

The temperature behavior are shown in the figure 2 according to Arrhenius-Frenkel's law $\sigma T = \sigma_0 \exp(-\frac{E_a}{kT})$. The insert of figure 2 shows the energy activation behavior of investigating samples. It is seen that the lowest energy activation demonstrates heterostructures with N from 6 to 10 and it equals ~430meV. The general form of planar conductivity has a peak of conductivity near N=10 for all measured temperatures (fig. 3).

For samples with N≥20 are observed gradual modification the form of hodographs namely the semicircle moves below the x-axis Re(Z) and the circuit are describes by equivalent circuit with CPE-element (constant phase element) and it has impedance $Z^*_{CPE} = Z_0(j\omega)^n = \left(\frac{Z_0}{\omega^n}\right)\left[\cos\left(\frac{\pi n}{2}\right) - j\sin\left(\frac{\pi n}{2}\right)\right]$, where $0 \le n \le 1$; at limited case when n = 0 Z^*_{CPE} does not depend from frequency and $Z_0 = R$, when n = 1 value Z_0 is capacitance $Z_0 = \left(\frac{1}{C}\right)$ and $Z^*_{CPE} = -\frac{1}{\omega C}$ [7].

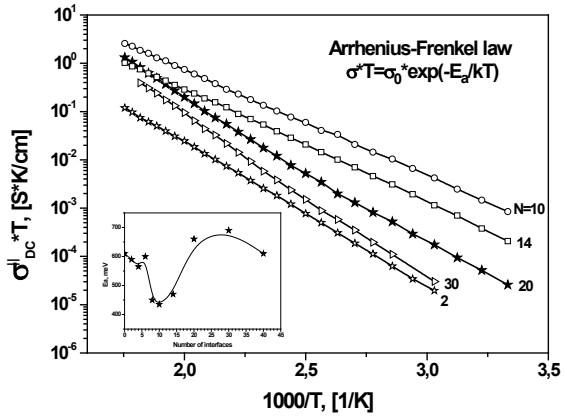

Figure 2. Temperature behavior of the planar conductivity for several super lattices, where N is number of layers. The insert - the activation energy of the samples taken from the Arrhenius-Frenkel's law.

Thus semicircle displacement below x-axis by an angle φ satisfies $\varphi = (1 - n)90^0$. In other words the similar equivalent circuit broadens out the Debay spectra $\sigma(\omega) = \sigma_\infty + \frac{\sigma_0 - \sigma_\infty}{1+j\omega\tau}$ and it is described by Cole-Cole spectra $\sigma(\omega) = \sigma_\infty + \frac{\sigma_0 - \sigma_\infty}{1+(j\omega\tau)^n}$ [8]. Deviation Debay spectra for samples N≥20 is not pronounced and n ≈ 0.85 in all measured temperature range.

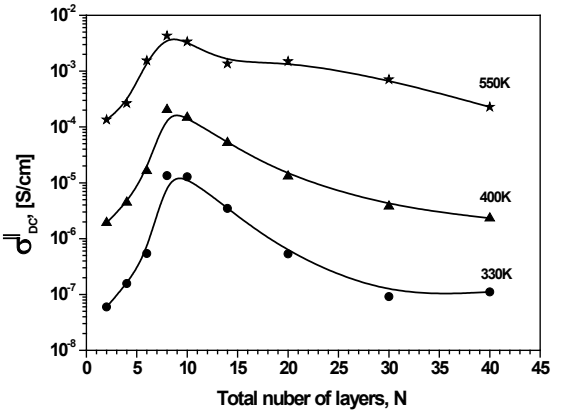

Figure 3. The conductivity behavior of the heterostructures with different number of layers of layers, but total thickness is 200nm (in other words if N=20 than the thickness of each layer is 10nm).

For comparison figure 4 shows temperature behavior of planar thin films conductivity of pure LaF_3, SrF_2 and solid solution $La_{1-x}Sr_xF_{3-x}$ with x=0.05 and x=0.5 based on them. The DC-conductivity of pure SrF_2 is estimated above 500K only, where the activation energy is 770meV. The 5% solid solution has the most conductivity between all possible combinations of solid solutions LaF_3+SrF_2 [9], and in our case it has high conductivity with low activation energy ~420meV. According to [10] the 50% solid solution must have two different mixed phases LaF_3 and SrF_2 separately, however it would be seen on the hodograph of impedance as a combination of two semicircles (two different processes of conductivity), but it is not observed in our case and the hodograph are described the equivalent circuit is shown in the insert of figure 1.

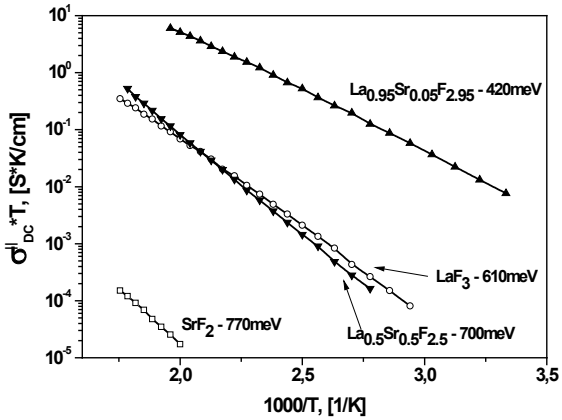

Figure 4. The temperature behavior of the planar conductivity of films SrF2 and LaF3, and the solid solutions La1-xSrxF3-x (with x = 0.05 and 0.5) grown on MgO with the thicknesses 200nm.

Thus all investigated planar DC-conductivities for heterostructures are into the interval of conductivities of pure LaF_3 and solid solution $La_{0.95}Sr_{0.05}F_{2.95}$, based on it the offer that between the interfaces exist the nanolayers enriched F^- ions can be assumed.

IV. CONCLUSION

It is possible to investigate the specific electro-physical parameters of electrochemistry cells of thin films with different thicknesses down to a few nanometers by method of impedance spectroscopy with using Nyquist plots.

It is possible to get materials with desired electrophysical properties by creating heterostructures with different period of layers. There is a peak of conductivity at N = 10 among all grown heterostructures, which corresponds to the thickness 20nm per each layer. Activation energies of heterostructures have the lowest conductivity at N from 6 to 10 and it is equal ~430meV which is comparable to activation energy of 5% solid solution. Deviation Debay spectra is probable the result of strong mechanical stresses in the superlatticies.

REFERENCES

[1] Jeffrey W. Fergus // Sensors Actuators B Chemical, V.42, pp.119-130 (1997)
[2] Guo-Long Tan, Xi-Jun Wu, Li-Ren Wang, Yu-Quan Chen // Sensors Actuators B Chemical, V.34, pp.417-421 (1996)
[3] M. Anji Reddy, M. Fichtner // Journal of Material Chemistry, V.21, #43, pp. 17009-17548 (2011)
[4] Xingbo Na, Wencheng Niu, Huawei Li, Jianxiang Xie // Sensors Actuators B Chemical, V.87, pp.222-225 (2002)
[5] Sata N., Eberman K., Eberl K. & Maier J. // Nature. V. 408. p.946 (2000)
[6] Sorokin N.I., Fominykh M.V., Krivandina E.A., Zhmurova Z.I., Sobolev B.P. // Kristallografiya. 1996. T. 41. #4. S. 310.
[7] A.K. Ivanov-Schitz, I.V.Murin. // Ionic of solid state. V.1. SPbSU 2000. 617 pages.
[8] Yan-Zhen Wei and S. Sridhar // J. Chem. Phys. 99(4). (1993)
[9] Sorokin N.I., Sobolev B.P. // Solid State Physics. 2008.v.50. №.3. p. 402.
[10] Ivanov-Schitz A.K., Sorokin N.I., Sobolev B.P., Fedorov P.P // Int. Symp. on Systems with Fast Ionic Transport. Bratislava, 1985. p.99

POLARIZATION TRANSFORMATION OF SPECTRAL CHARACTERISTICS OF THE OUTGOING AND ECHO RADIO FREQUENCY IDENTIFICATION SIGNALS

Anna Vershinina

Saint-Petersburg State University of Aerospace Instrumentation,
Saint-Petersburg, Russia

E-mail: avershinina1203@gmail.com

Abstracts

Polarization transformations of signals of radio-frequency identification systems at their distribution and receiving antenna are investigated. Polarization spectra of vector signals are entered. The method of research is based on representation of polarization characteristics of a signal in the form of Jones vector. Properties of the medium for transmission and the receiving antenna, transformative a polarization state, are described is frequency dependent Jones matrix. Thus the base Jones's matrix is presented in the form of a matrix series.

I. INTRODUCTION

Methods of radio frequency identification (RFID) find the increasing application in various fields of activity. It puts forward a number of tasks which demand the urgent solution. For example, research of polarization distortions at propagation of electromagnetic signals of RFID and correction of these distortions in receiving device.

Research of polarization distortions in the medium for transmission of electromagnetic waves demands equipment creation for measurement of these distortions and, probably, their automatic adaptive correction.

In this work it is supposed that research of polarization transformations of electromagnetic waves should be based on introduction of vector stochastic model of an electromagnetic signal and polarization spectra of these signals.

Here the polarization spectrum is considered as most a general characteristic of a vector electromagnetic signal. From a polarization spectrum by the corresponding transformations it is possible to receive all other characteristics and parameters of this signal, including the most important in the real consideration information on correction of polarization distortions in a receiving device.

Within researches carried out in this work further development of methods and ideas of polarizing measurements, with reference to the solution of problems of RFID devices is offered.

II. MATHEMATICAL MODEL OF POLARIZATION SPECTRA

In this work electromagnetic fields with the plane wave front, which will extend in linear medium and interact with linear devices are considered. The device is the system which is carrying out polarization transformations. However unlike traditional considerations where continuous radiations are considered [1, 2], polarization characteristics and transformations of pulse radio signals here are considered.

The vector of intensity of electric field can be presented in the form

$$\mathbf{E}(\mathbf{r},t) = \mathbf{i}E_x(\mathbf{r},t) + \mathbf{j}E_y(\mathbf{r},t) + \mathbf{k}E_z(\mathbf{r},t), \quad (1)$$

where **i**, **j**, **k** - basis vectors, connected with axes x, y, z; E_x, E_y, E_z, - projections of the vector to axes x, y, z.

Any scalar a component $E(t)$ in expansion (1) is representable in the form of double the Fourier integral:

$$E(t) = \frac{1}{2\pi} vp \int_{-\infty}^{\infty} d\omega \int_{-\infty}^{\infty} E(t') \exp[i\omega(t-t')]dt', \quad (2)$$

where *vp* means a principal value of integral at integration on a variable ω; ω - temporary angular frequency.

From double the Fourier integral (2) formulas of Fourier transformation follow:

$$S(\omega) = \int_{-\infty}^{\infty} E(t)\exp(i\omega t)dt, \qquad (3)$$

$$E(t) = \frac{1}{2\pi}\int_{-\infty}^{\infty} S(\omega)\exp(i\omega t)d\omega. \qquad (4)$$

Spectral components $S(\omega)$ of a signal $E(t)$ extend in the linear environment independently from each other. The behavior of a scalar wave is given by superposition of harmonious waves of infinitesimal amplitude. The equation (4) allows to present such scalar wave extending along an axis z, in shape:

$$E(z,t) = \frac{1}{2\pi}\int_{-\infty}^{\infty} S(\omega)\exp[i(\omega t - kz)]d\omega, \qquad (5)$$

where $k = \omega/c$ - the wave number, c - speed of light.

The ratio (5) is suitable for the description vertically or horizontally polarized electromagnetic wave, as special case. The general case of polarization state of an electromagnetic field demands introduction of vector model of a dynamic signal [1].

The vector model of a signal [1] assumes what it is possible to present both horizontal and vertical components of a plane electromagnetic field in the equation (5). Then the vector signal will register in a kind:

$$\begin{aligned}\mathbf{E}(t,z) &= \mathbf{i}\frac{1}{2\pi}\int_{-\infty}^{\infty} S_x(\omega)\exp[i(\omega t - kz)]d\omega + \\ &+ \mathbf{j}\frac{1}{2\pi}\int_{-\infty}^{\infty} S_y(\omega)\exp[i(\omega t - kz)]d\omega = \\ &= \frac{1}{2\pi}\int_{-\infty}^{\infty}\left\{\left[\mathbf{i}S_x(\omega) + \mathbf{j}S_y(\omega)\right]\exp[i(\omega t - kz)]\right\}d\omega.\end{aligned} \qquad (6)$$

Just as the scalar ratio (5) is superposition of infinitesimal scalar oscillations, expression (6) represents superposition of infinitesimal vector oscillations. The equation (6) acts as generalization of spectral representation of a scalar wave (5). In this equation it is supposed that each pair infinitesimal spectral wave component with angular frequency ω'

$$\begin{aligned}&S_x(\omega')\exp[i(\omega' t - k' z)]d\omega', \\ &S_y(\omega')\exp[i(\omega' t - k' z)]d\omega'\end{aligned} \qquad (7)$$

has the individual condition of polarization. In aggregate these components make a vector signal (6) with this or that polarization state: from complete polarization to its total absence. The infinite continual set of sets (7) makes a polarizing range of a signal in the form of a wave.

Pair of waves (7) can be written down in the form of column vector

$$\begin{bmatrix}|S_x(\omega')|\cdot\exp i[\varphi_x(\omega')] \\ |S_y(\omega')|\cdot\exp i[\varphi_y(\omega')]\end{bmatrix}\cdot\exp[i(\omega' t - k' z)]d\omega, \qquad (8)$$

which is quite similar to a column vector describing a plane monochromatic electromagnetic field, extending along the axis z [1].

$$\mathbf{J} = \begin{bmatrix}\dot{E}_x \\ \dot{E}_y\end{bmatrix} = \begin{bmatrix}H\exp i\varphi_x \\ V\exp i\varphi_y\end{bmatrix}\cdot\exp[i(\omega t - kz)]. \qquad (9)$$

In equation (9) variable quantity in time $\dot{E}_x$ and $\dot{E}_y$ describe complex oscillations horizontal and vertical a component of an electromagnetic field, amount H and V - amplitudes of these oscillations, and amounts φ_x and φ_y - their initial phases. The column vector in the right part of eq. (9) is called as the Jones vector of monochromatic plane wave.

As a result of interaction of incident wave with polarizing system on an exit of system appears one or several modified plane waves [3]. In this work the system which consists of a transmitting antenna, a medium for transmission of an electromagnetic wave and a receiving antenna is considered. Thus, the electromagnetic wave is affected by two polarizing systems: a medium for transmission and a receiving antenna. Polarization properties of each of these systems are described by corresponding Jones matrixes.

$$\mathbf{I}_M = \begin{bmatrix}M_{11}M_{12} \\ M_{21}M_{22}\end{bmatrix}. \qquad (10)$$

Jones matrix $\mathbf{I}_M$ in eq. (10) characterizes properties of a medium for transmission for a flat monochromatic wave of a certain frequency. The transmitted signal is superposition of infinitesimal monochromatic oscillations with different frequencies which are included into its structure. Therefore, it is possible to enter Jones matrix $\mathbf{I}_M(\omega)$ which describes polarizing properties of a medium for transmission depending on frequency.

$$\mathbf{I}_M(\omega)=\begin{bmatrix} M_{11}(\omega) & M_{12}(\omega) \\ M_{21}(\omega) & M_{22}(\omega) \end{bmatrix}. \qquad (11)$$

The summation convention of matrixes allows to present Jones matrix (11) in the form of a Jones matrix series. For this purpose it is necessary to spread out elements of the matrix $\mathbf{I}_M(\omega)$ in the Taylor series near ω_0- central frequency of the spectrum:

$$M_{ij}(\omega)=M_{ij}(\omega_0)+\frac{1}{1!}\frac{dM_{ij}}{d\omega}\bigg|_{\omega=\omega_0}\times \\ \times(\omega-\omega_0)+\frac{1}{2!}\frac{d^2M_{ij}}{d\omega^2}\bigg|_{\omega=\omega_0}\cdot(\omega-\omega_0)^2+\ldots \qquad (12)$$

As a result the sum of the matrixes which elements are members of series (12). According to the differentiation rule of matrixes, the operator of differentiation it is possible to take out for a matrix sign, then taking into account it we have:

$$\mathbf{I}_{\grave{I}}(\omega)=\begin{bmatrix} \grave{I}_{11}(\omega_0) & \grave{I}_{12}(\omega_0) \\ \grave{I}_{21}(\omega_0) & \grave{I}_{22}(\omega_0) \end{bmatrix}+ \\ +\sum_{n=1}^{\infty}\frac{1}{n!}\cdot(\omega-\omega_0)^n\frac{d^n}{d\omega^n}\bigg|_{\omega=\omega_0}\cdot\begin{bmatrix} \grave{I}_{11}(\omega) & \grave{I}_{12}(\omega) \\ \grave{I}_{21}(\omega) & \grave{I}_{22}(\omega) \end{bmatrix}. \qquad (13)$$

where all summands after the first show frequency dependence of polarization properties of a medium for transmission.

All terms except the first term show frequency dependence of polarizing properties of the medium for transmission.

Polarizing properties of a receiving antenna are expressed by a matrix

$$\mathbf{I}_A=\begin{bmatrix} A_{11}A_{12} \\ A_{21}A_{22} \end{bmatrix}, \qquad (14)$$

Joint action of a medium for transmission and the receiving antenna on infinitesimal monochromatic oscillation which is a part of a transmitted signal are given by Jones matrix in the form of product of these matrixes [2]:

$$\mathbf{I}_0=\mathbf{I}_A\times\mathbf{I}_M, \qquad (15)$$

$$\mathbf{I}_0=\mathbf{I}_A\times\mathbf{I}_M=\begin{bmatrix} A_{11}A_{12} \\ A_{21}A_{22} \end{bmatrix}\times\begin{bmatrix} M_{11}M_{12} \\ M_{21}M_{22} \end{bmatrix}= \\ =\begin{bmatrix} \hat{A}_{11} & \hat{A}_{12} \\ \hat{A}_{21} & \hat{A}_{22} \end{bmatrix}. \qquad (16)$$

Further consideration assumes that the transmitting antenna radiates an electromagnetic wave to which there corresponds Jones vector

$$\mathbf{J}_1=\begin{bmatrix} H_1\exp i\varphi_{x1} \\ V_1\exp i\varphi_{y1} \end{bmatrix}. \qquad (17)$$

Equations (10), (14), (15) allow to write down result of polarization transformations of an electromagnetic wave in form

$$\mathbf{J}_2=\begin{bmatrix} H_2\exp i\varphi_{x2} \\ V_2\exp i\varphi_{y2} \end{bmatrix}=\begin{bmatrix} A_{11}A_{12} \\ A_{21}A_{22} \end{bmatrix}\times\begin{bmatrix} M_{11}M_{12} \\ M_{21}M_{22} \end{bmatrix}\times \\ \times\begin{bmatrix} H_1\exp i\varphi_{x1} \\ V_1\exp i\varphi_{y1} \end{bmatrix}=\begin{bmatrix} \hat{A}_{11}\hat{A}_{12} \\ \hat{A}_{21}\hat{A}_{22} \end{bmatrix}\cdot\begin{bmatrix} H_1\exp i\varphi_{x1} \\ V_1\exp i\varphi_{y1} \end{bmatrix}. \qquad (18)$$

The vector column of $\mathbf{J}_2$ defines polarization characteristics of a field after influence of the polarization distortions brought by a medium for transmission and the receiving antenna in a general view.

Further consideration assumes that transmitting antenna is a polarizer (half-wave dipole or flagpole antenna). Therefore to the incident electromagnetic wave on polarization system is put in correspondence Jones's vector of vertically polarized electromagnetic wave which is radiated by the transmitting antenna

$$\mathbf{J}_1=\begin{bmatrix} 0 \\ S_y(\omega) \end{bmatrix}. \qquad (19)$$

Influence of medium for transmission on polarization characteristics of an electromagnetic wave are defined equation (10).

Also it is supposed that the receiving antenna is an ideal polarizer which is directed along a vertical axis. Polarization properties of such antenna are described by following Jones matrix:

$$\mathbf{I}_A=\begin{bmatrix} 00 \\ 01 \end{bmatrix} \qquad (20)$$

The polarization state of electromagnetic wave transmitted through the polarizing system written by Jones vector

$$\mathbf{J}_2=\begin{bmatrix} 0 & 0 \\ M_{21}(\omega) & M_{22}(\omega) \end{bmatrix}\times\begin{bmatrix} 0 \\ S_y(\omega) \end{bmatrix}= \\ =\begin{bmatrix} 0 \\ M_{22}(\omega)S_y(\omega) \end{bmatrix}. \qquad (21)$$

The eq. (21) defines a scalar signal in frequency domain, its complex spectrum

$$S_0(\omega)=M_{22}(\omega)S_y(\omega)=K_0(\omega)S_y(\omega). \qquad (22)$$

The complex-valued function $M_{22}(\omega)$ in eq. (22) plays a role of transfer constant $K_0(\omega)$ some two-port network. It considers a result of the polarization distortions brought by the medium for transmission in which the electromagnetic wave of RFID system extends. These distortions can be compensated by introduction in a receiving device of the correcting two-port network with transfer constant

$$K_K(\omega) = \frac{1}{M_{22}(\omega)} = \frac{1}{K_0(\omega)}, \quad K_0(\omega) \neq 0. \qquad (23)$$

Equation (23) may be called the polarization transfer function with the above conditions respect to the transmitting and receiving antenna.

III. CONCLUSION

Researches of polarization transformations of signals leaned on vector model of a signal, polarization spectrum and the Jones matrix defining polarization properties of the medium for transmission of the electromagnetic wave.

Generally elements of the matrix are complex functions of frequency. The matrix is presented in the form of expansion in series on Jones's matrixes. By means of a number of matrixes it is possible to describe polarizing distortions.

On condition of transmission and receiving of vertically polarized electromagnetic radiation distortions of the processed signal spectrum and transfer constant of the correcting two-port network were defined.

Researches are executed within the limits of the State contract № 14.527.12.0019; the prize code number 2011-2.7-527-025; the demand code number2011-2.7.-527-025-002.

REFERENCES

[1] О'Нейл, Е.Л. Введение в статистическую оптику: Пер. с англ. / Е.Л. О'Нейл. - Москва: Изд-во Мир,.1966. – 254 с

[2] Аззам, Р. Эллипсометрия и поляризованный свет: Пер. с англ. / Р. Аззам, Н. Башара. М.: Мир 1981. – 584 с.

[3] Козлов, А.И. Поляризация радиоволн. Поляризационная структура радиолокационных сигналов / А.И. Козлов, А.И. Логвин, В.А. Сарычев.М.: Радиотехника, 2005. – 704 с.

A RESEARCH OPPORTUNITY: THE AMERICAN JOURNEY TO THE EMV SECURITY STANDARD AS A CASE STUDY IN TECHNOLOGY ADOPTION

Hubert C. Williams
Doctoral Student attending Indiana State University

Abstract

In 2012 Visa, MasterCard and Discover announced deadlines for the American adoption of (Europay, MasterCard and Visa) security standard. These regulations are compelling merchants to make significant infrastructure investments to meet the EMV security standard during a time when the effectiveness of EMV is in question and disruptive innovation in mobile payments technologies may be rendering current EMV and point-of-sale infrastructures obsolete. The implications for fuel retailers are especially difficult and expensive because of EMV's impact to established pay-at-the-pump infrastructure.

A range of publications in journals and information from internet web sites provide corroboration and details some of the issues surrounding EMV implementation. This paper describes the reasons for the regulations and frames the issues faced by American retailers as the deadlines approach. The paper may also serve as a useful source of current information on how American retailers cope with the adoption of the EMV security standard in light of questions of its obsolescence and the effect of disruptive innovations in mobile payment technologies. It may also contribute to the recognition of research opportunities in areas such as Technology Acceptance and Innovation Diffusion.

Keywords: Credit Card Fraud, Disruptive Technology, Mobile Payment, EMV, Technology Adoption

Introduction

The EMV (Europay, MasterCard and Visa) is a security standard effort begun in 1993 and made available in 1996 to address an increase in counterfeit card fraud in Europe. EMV, which is sometimes referred to as "Chip and PIN," provides a global security standard for the interoperability of smart cards otherwise known as integrated circuit cards or "chip cards" and point-of-sale infrastructure. The EMV interoperability standard is managed by EMVco (http://www.emvco.com) which was formed in 1999 by EuroPay, MasterCard and Visa, and is based on ISO/IEC 7816 for contact cards and ISO/IEC 14443 for contactless cards using Radio-frequency Identification (RFID) and Near Field Communications (NFC). EMV transaction processing provides several security advantages over legacy magnetic stripe card transaction processing by ensuring card authentication that protects against counterfeit cards and skimmers (devices that can read encoded information surreptitiously on a credit or debit card's magnetic strip), and verifies the legitimacy of the cardholder to protect against use of stolen cards.

While most of the world has adopted the EMV standard for credit card payment security, the United States has not yet done so. However, between August 2011 and June 2012, Payment Card Network companies American Express, Discover, MasterCard and Visa each announced their plans to move to an EMV-based payments infrastructure in the United States. The migration to EMV by American financial institutions has already begun with the issuance of dual-interface (which operate in either EMV or in non-EMV modes) EMV smart cards for debit and credit payments by Discover and American Express in 2012. (Smartcard Alliance, 2013)

Payment card network providers will encourage the transition to the EMV standard by shifting fraud liability away from issuers to parties involved (or victimized) in non-EMV fraudulent transactions beginning in 2015 (2017 for fuel retailers). So, once the liability shift goes into effect, banks and other financial institutions may no longer absorb fraud related chargebacks to non-EMV compliant parties. As an example, if the card issuer is EMV compliant and the merchant is non-EMV compliant, the merchant may be responsible for chargebacks. However, if the issuer is non-EMV compliant and the merchant is EMV compliant, the card issuer may be held liable for fraud related chargebacks against the merchant.

While the effect of this shift in liability is to shift fraud costs to parties that are not EMV compliant, there are significant costs to issuers and merchants with regards to infrastructure to become compliant to the standard. Issuers must provide chip-embedded cards which are more expensive than the current magnetic stripe cards most commonly used in the United States

and do so without necessarily recognizing a financial return on the investment in the infrastructure required to create those cards. For merchants, point-of-sale (POS) terminals must have the ability to accept chip-embedded cards resulting in another investment in infrastructure. This cost is especially high for the approximately 124,000 convenience store operators in the United States who take payment cards at fuel pumps of which 56% are owned by single store operators. (NACS, 2013) Convenience retailers commonly have anywhere from 4 to 64 gas pumps per store and the cost of converting a pump card reader to EMV can vary from a few hundred to thousands of dollars per pump island (generally consisting of 2 pumps) making the EMV requirement especially costly to this group of retailers. Visa, MasterCard and most of the other payment network providers have given the fuel retailers 2 more years (2017) to comply as a result.

Fraud and EMV Security Aspects

The United States currently accounts for 47 percent of global credit and debit card fraud though it generates only 27 percent of the total volume of purchases and cash, according to Global Card Fraud, from a recent issue of The Nilson Report. (The Nilson Report, 2011) Therefore it would seem there are sound business advantages in American compliance with EMV. However, in the United States the percentage of fraud to revenue is about the same as a percentage of revenue as that experienced globally. According to a report from the Aite Group LLC, a Boston-based consulting firm, fraudulent transactions represent approximately .004% U.S. payment card spending. (Boyer, 2010) This seems to match the global trend in 2009 which according to the Nilson Report was .0046%. (The Nilson Report,2011) The difference is that in the United States the liability for fraud primarily resides with the card payment card network providers not the merchants or card holders (as a result of the liability shift associated with EMV), which may explain some of the motivation for pushing EMV compliance in the United States.

A significant security advantage of the EMV standard is the reduction in card fraud resulting from counterfeit, lost and stolen cards. The embedded electronic chip protects against the physical use of counterfeit cards while the entry of a numeric PIN verifies the authenticity of the user. Recently however, several papers have raised questions about the security benefits of EMV. Researchers at the University of Cambridge published a paper at the 2010 IEEE Symposium on Security and Privacy demonstrating how to perform a man-in-the-middle attack on a Chip and Pin transaction "…which allows criminals to use a genuine card to make a payment without knowing the card's PIN, and to remain undetected…". (Murdoch, et al., 2010) In this demonstration, from the payment card network perspective, it appears that a valid PIN was used. The result of which, once the liability shift is in place, may be that the cardholder bears the responsibility for the fraud because there is no evidence that the transaction was not valid. Murdoch and his fellow researchers indicate that this may help explain the results of a 2009 survey in the U.K. which indicated that 20% of fraud victims indicated they were held responsible for the fraud committed on their "Chip and PIN" cards.

EMV security does not address all payment card fraud opportunities. For example, CNP (Card-Not-Present) transactions such as online purchases, phone and mail orders transactions are not readily addressed by EMV. VISA and MasterCard offer alternative methods for securing these types of transactions such as "Verified by VISA" and "Secure Code" (MasterCard). EMV Card skimmers present another problem as these devices which are placed physically in Point of Sale or Pay at the Pump card accepters can "harvest" PIN numbers as well as intercept card data in an EMV environment (as demonstrated by Murdoch et al.). Moreover, the EMV security standard revision no longer requires the "PIN" number entry which has the effect of no longer protecting users against stolen cards as an alternative dual-interface "Chip and Signature" method is being employed whereby the card is only accepted without the use of PIN where a human attendant is assisting the transaction. While this is more secure than pure the current magnetic stripe standard, it does have weaknesses compared to pure Chip and PIN since a stolen payment card may be used if the criminal is at hand and presents a signature.

Mobil Payment Implications

Adoption of dual-interface chip technology by Visa and MasterCard may act to encourage activity to prepare U.S. payment infrastructure for Near Field Communication (NFC) mobile payments by creating the necessary network to accept and process chip transactions. According to the Smart Card Alliance, "EMVCo has been active in defining the architecture, specifications, requirements and type approval processes for supporting EMV mobile contactless payments." (Smartcard Alliance, 2013) However, exactly what form these payment technologies will ultimately take and their rate of adoption for brick and mortar retail site transactions are unknown at this point. The evolution of mobile payments, how they

interact with points-of-sale or perhaps even replace the point-of-sale may significantly change the infrastructure requirements for processing payments and the way consumers interact with retailers. "The challenge of understanding the driving forces in the market for electronic payments is that there are an accelerating range of solutions that address shortcomings in legacy payment processes…Smart phones seek to associate the payment transaction with other customer related processes such as loyalty points programs, but are by definition focused on a particular segment of Smart phone using consumers. While such developments espouse key technology adoption factors such as consumer convenience and ease of use, they also tend to obscure visibility of the comparative value of choosing a particular payment instrument over an alternative." (Carton et al., 2011) In 1993 when the EMV effort began, Smartphones and the mobile payment technology were not necessarily on the technology roadmap for retailers. As stated above EMVco is addressing the gap but there is uncertainty as to what the gap is. "Mobile payments are predicted to have a bright future as m-commerce becomes more popular. However, this promising application has not been as successful as anticipated. This can be partially explained by the infancy of the market and a lack of standards. Moreover, technological and business issues create a market uncertainty that mobile network operators and financial institutions have difficulties managing. Thus, the evolution of the mobile payment market is subject to many speculative scenarios." (Ondrus, 2005)

Conclusion and Opportunities for Research

The "Technology Acceptance Model (TAM)" was proposed by Davis in 1989. He proposed that perceived ease of use and perceived usefulness affect the acceptance and use of information systems technology. Rogers in 1995 proposed the Innovation Diffusion Technology (IDT) theory which he described as adoption of an innovation based on a 5 step process related to Knowledge, Persuasion, Decision, Implementation and Confirmation. Other theories of innovation adoption exist as well but the adoption of EMV by American retailers given the complexities of emerging mobile payment technologies, implementation expense and concerns about infrastructure obsolescence may ultimately be one of forced adoption. While the financial institutions and payment card network providers have accepted or even helped develop EMV technology, retailers may not be compelled by the standard processes of technology acceptance as it is not clear that the advantages of EMV for the retailer are significant enough to push them to the EMV standard without being compelled to do so by the major payment card providers. "Once organizations adopt an innovation, they may force various individuals to use it. While researchers have frequently studied perspectives of suppliers and their customers, they have sometimes neglected the important roles of those who must use the innovation when it is provided to them." (Ram & Jung, 1991) The American Journey to the EMV security standard may prove to be an interesting case study in technology adoption.

Reference

Ram, S. & Jung, H. (1991). "Forced adoption of innovation in organizations: Consequences and implications." *Journal of Product Innovation Management*, 8 (2), 117-26.

Ondrus, J., Pigneur, Y. (2005) "A Disruption Analysis in the Mobile Payment Market," *System Sciences, 2005. HICSS '05. Proceedings of the 38th Annual Hawaii International Conference on* , vol., no., pp.84c,84c, 03-06 Jan. 2005

The Nilson Report, "U.S. Leads the World in Credit Card Fraud, states The Nilson Report
Global Credit Card Fraud Losses Increased 10.2% over 2009". Issue 980. November, 2011. Retrieved from http://www.nilsonreport.com/pdf/news/112111.pdf

Smart Card Alliance, "Card Payments Roadmap in the United States: How Will EMV Impact the Future Payments Infrastructure?" January, 2013. Retrieved from http://www.smartcardalliance.org/
NACS, "Who Sells Motor Fuels in the United States?" February, 2010. Retrieved from http://www.nacsonline.com/NACS/Resources/campaigns/2010GasPriceKit/Pages/WhoSellsMotorFuels.aspx

Carton, F., Hedman, J., Damsgaard, J., Tan, K-T., & McCarthy, J. B. (2011). Towards a Framework for the Evaluation of Mobile Payments Integration. In Castelnovo, W., & Ferrar, E. (Eds.), *Proceedings of the 5th European Conference on Information Management and Evaluation*. (pp. 84-91). Reading: Academic Publishing Limited

Davis, F. D. (1989), "Perceived usefulness, perceived ease of use, and user acceptance of information technology", *MIS Quarterly* 13(3): 319–340

Rogers, E. M. (1995). *Diffusion of innovations* (4th ed.). New York: Free Press.

TREE EXTENSION FOR HMMINGBIRD COMPILER: SUPPORT FOR RECURSIONS ON TREES

Alexander Wood, Balazs Koszegi, Dmitrii Bychkov

Oxford Summer School in Computational Biology 2012,
University of Oxford , Oxford, UK.

I. INTRODUCTION

Trees are widely used structures in computational biology and bioinformatics. The most well-known usage of trees is phylogenetic trees. Analyzing evolutionary data is an active research area of computational biology nowadays. The usage of tree structures is indispensable in these researches. The most common problems are searching for similarities in phylogenetic trees or simplifying tree structures or applying recursion formulas on them.

The phylogenetic data analysis becomes increasingly infeasible as the set of genomes grows, so to be able to manage tens, hundreds, or even thousands of genomes models and methods were developed for segmenting larger trees into smaller parts. The computational time of different biological problems will be always an issue. Bioinformatics is a domain which requires high-performance implementations in order to tame the complexity of typical analysis problems. It is important to make best use of the computing resources available, such as the processing units found in graphics cards (GPUs). The off-the-shelf GPUs have hundreds of cores running in parallel. These can make computations on GPU very efficient. The run time speed-ups are on the order of 10-30 times a comparable CPU solution.

The goal of the project is to be able to compute recursive biological tasks on GPU (like weighted parsimony, tree segmentations). In order to achieve the goal we make an extension for the already existing recursive language which compiles for GPUs. To avoid low level implementation on GPUs, a Domain Specific Language (DSL) is defined for describing trees, related data and recursion equations on them. The complier generates a code by using this language that runs on NVidia GPU. This allows for non-computer scientist to work on GPUs without knowledge of parallelization or scheduling.

II. DSL: TREE RECURSIONS

In order to support any recursive operations over trees, we should first define a tree itself. A source code example below shows a simple binary tree definition:

```
%%%%%%%%%%%%%%%%%%%%%%%%%%%%%%%%
    define tree myTree {
       root a;
       node b, c, d;
       leaf e, f, g, h;

       a -> b -> e;
            b -> f;
       a -> c -> d -> g;
            c -> h;
       dataorder e, f, h, g;
    }
%%%%%%%%%%%%%%%%%%%%%%%%%%%%%%%%
```

However, explicit node declaration such as *root*, *leaf* or *internal node* appears unnecessary and may remain only for consistency. That means that tree can be defined only by its edges. One more optional declaration is determined by *dataorder* keyword. Nodes that are specified under this declaration correspond to nucleotide/amino acid sequences in the data file in the order how they appear in declaration. This tree definition is easy to understand in comparison for example Newick format. Here are several dot expressions for querying the type of node: *isleaf*, *isroot*, *hasparent* and *haschildren* can be used determine whether a node is a leaf, is the root, has a parent or has children.

Other dot expressions exist to ask about related nodes. Some of these return a single node of interest. *Parent* returns the parent of this node. *Left* and *right* load the first and second child of this node and only work on binary trees. The rest are iterators that can be used in *max*, *min* and *sum* expressions. *Children* is the set of the children of a node. *Subtree* is a set of all nodes under this node. *Subtreeleaves* is the set of all leaves under this node.

At the next step we want to utilize the tree in some operations. The language provides means for accessing tree elements using dot notation. The code below illustrates a simple example of tree usage and compute three depth.

```
%%%%%%%%%%%%%%%%%%%%%%%%%%%%%%%%
int d(tree t, treenode[t] n) =
    if n.isleaf
         then 1
    else max(child in n.children :
d(child)) + 1

result = d(phylogenyExample)
%%%%%%%%%%%%%%%%%%%%%%%%%%%%%%%%
```

Here we work with constant, predefined tree structure. Thereto, it is impossible that a tree being modified during runtime so far.

Functions in the language may be evaluated in two ways - using a function call, or by mapping a function to the series of values. In the latter case we utilize multiple processors on the GPU and allow parallelization. That can be done using function *map*. In the example below we apply function *w* to a sequence of parameters uploaded from the data file:

```
%%%%%%%%%%%%%%%%%%%%%%%%%%%%%%%%
Datafile =
load(treeseq[foo, DNA],"file.txt")

result = map(w, myTree (*) datafile)
%%%%%%%%%%%%%%%%%%%%%%%%%%%%%%%%
```

In this example, sequences in data file are associated with leaves of *myTree* (in the order specified under *dataorder* definition) so that a single tree instance evaluates a set of characters in a single position. It results in N tree instances evaluating on N processors concurrently. The parallelization can be also achieved over recursion itself as it exhibits a pattern of regular dependencies (e.g. over dynamic programming table).

One more issue to be considered in terms of DSL syntax is a matrix definition. Many bioinformatics algorithms require model of evolution or a substitution matrix for sequence characters or some other data in matrix format. Therefore, the language has a matrix type which can be defined as follows:

```
%%%%%%%%%%%%%%%%%%%%%%%%%%%%%%%%
define matrix scoreMatrix[DNA] {
  A G C T
A 0 2 3 3
G 2 0 3 3
C 3 3 0 2
T 3 3 2 0
}
%%%%%%%%%%%%%%%%%%%%%%%%%%%%%%%%
```

,where DNA is an inbuilt alphabet which consists of corresponding nucleotide characters.

III. EXAMPLE: WEIGHTED PARSIMONY

In this section we outline one well-known recursive algorithm on trees that have been implemented in the language.

One of the most direct examples of application of Darwin's speciation principle is weighted parsimony or likelihood computation on a tree. In this situation we have a character from a finite type Σ that has been observed at all the leaves in the tree, e.g. the nucleotides or amino acids observed in the column of an alignment of DNA or protein sequences. Furthermore, we have a score for one character changing into another character, d: Σ × Σ → R. The aim is to find assignments of characters at all the internal nodes, such that the sum of the scores of changes observed on each branch is minimized. If L(u) (R(u)) denotes the left (right) child of a node u, then the most parsimonious score when assigning character σ in Σ to node u is:

$$w(u,\sigma) = \begin{cases} 0 & \text{if observed character is } \sigma \\ \infty & \text{if observed character different from } \sigma \end{cases}$$

if u is a leaf node and:

$$w(u,\sigma) = \min_{\tau\in\Sigma}\{w(\mathrm{R}(u),\tau) + d(\sigma,\tau)\} + \min_{\tau\in\Sigma}\{w(\mathrm{L}(u),\tau) + d(\sigma,\tau)\}$$

The same recursion can be applied in stochastic settings, where we would multiply probabilities from child nodes and take either the maximum or the sum to obtain a maximum likelihood or a total data probability.

The following code shows the weighted parsimony example in the tree recursion language:

```
%%%%%%%%%%%%%%%%%%%%%%%%%%%%%%%%
score w(tree t, treenode[t] n,
treeseq[t] seq,
matrix[DNA] change_score,
char[DNA] ch) =

  if n.isleaf then
    if seq[n] == ch then 0
    else infinity
  else
    sum(child in n.children :
          min(nextch in DNA :
                w(child, nextch) +
change_score[ch, nextch]))
%%%%%%%%%%%%%%%%%%%%%%%%%%%%%%%%
```

In this example, the recursion progresses on the nodes in the phylogeny, with a single phylogeny being fixed (see Figure 1 below).

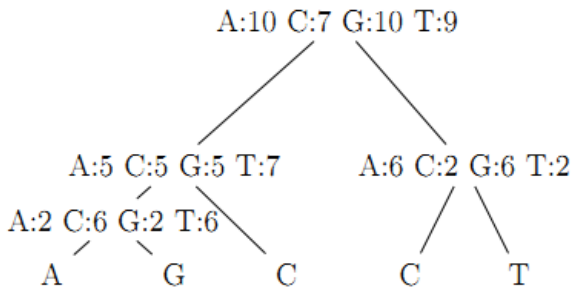

Figure 1 - Weighted parsimony: example phylogeny

IV. RESULTS

The aim of the extension is to support recursions over trees and thus enhance the speed of calculations when dealing with massive data sets. In order to estimate performance of new HMMingbird functionality we run tests that compare execution time on both CPU and GPU.

The CPU implementation was written in java. It was tested on CPU-PC (Intel Core2 Duo) and skynet server. The GPU implementation was tested on GPU-PC (MAC) and skynet GPU-server. The following figures shows the computational time of weighted parsimony method. The Y axis is the time in millisecond. The X axis is the amount of tree sequences in each leaf.

The result shows the CPU computational time increasing linearly with the size of data but the GPU is close to constant. The reason is the GPU implementation spend the most of the time on setup the system, but after that the parsing and the calculation is really fast. The GPU-PC is not able to work with a huge amount of data because it has limited memory.

Figure 3 shows exact results. The x axis is not scaled. It shows that the CPU works faster with small data because to setup the compiler it takes more time. If the data is more than 500000 the GPU works better and faster. Around 500000 the CPU implementation and the GPU implementation have approximately the same computational time. The GPU is more than 11 times faster than the CPU-PC if the length of the data is 10^7.

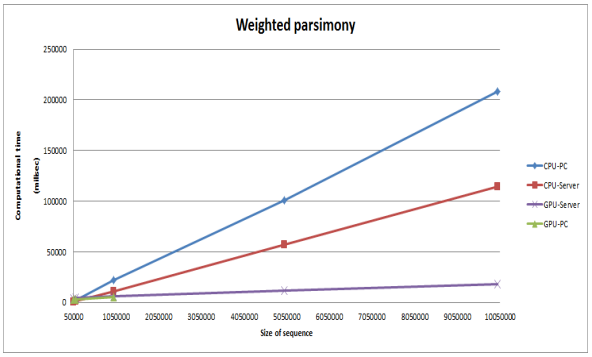

Figure 2 - Weighted parsimony: computational speed vs data size on linear scale

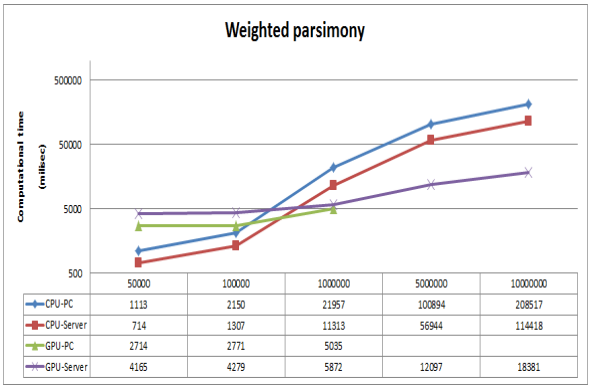

	50000	100000	1000000	5000000	10000000
CPU-PC	1113	2150	21957	100894	208517
CPU-Server	714	1307	11313	56944	114418
GPU-PC	2714	2771	5035		
GPU-Server	4165	4279	5872	12097	18381

Figure 3 - Weighted parsimony: exact measurements

V. CONCLUSION

The HMMingbird tree extension was design to allow for recursions on trees. The DSL is designed to match as closely as possible the mathematical description algorithms. This makes the usage of the language easy and simple for non-computer scientist too.

The algorithm supports different type of parallelization. One of these is the parallelization over date sequences. The other one is over the recursion. The compiler uses a dynamic table to optimize the computational time of the program.

The GPU implementation provides an efficient solution for recursion on trees. The GPU implementation up to 10 times faster than CPU.

REFERENCES:

[1] L. Cartey, R. Lyngsoe and O.de. Moor Synthesizing Graphics Card Programs from DSLs Proceedings of the 33rd ACM SIGPLAN conference on Programming Language Design and Implementation, 121-132, 2012.

[2] W. M. Fitch. Toward defining the course of evolution: Minimum change for a specific tree topology. Systematic Biology, 20(4):406-416, 1971.

POSITIVE STATE ESTIMATION WITH H_∞ PERFORMANCE FOR POSITIVE CONTINUOUS-TIME TAKAGI SUGENO SYSTEMS

Ines ZAIDI

Department of Systems Engineering and Automatic, University of Valladolid, Spain.

ines.zaidi@autom.uva.es

Abstract **—** This paper presents a positive observer design methodology for Takagi Sugeno systems with unmeasurable premise variables. For that, a positive Takagi-Sugeno observer is developed in order to estimate the system states and to guarantee the nonnegativity of the estimates at each time. Conditions are established in order to guarantee the convergence of the state error. These conditions are given in Linear Matrix Inequalities (LMIs) formulation which makes possible to obtain the gains of the fuzzy observer. Finally, simulation results show the effectiveness of the proposed positive observer.

I. Introduction

State estimation and observation of nonlinear systems is an important problem in modern control [1], [2], [3]. There is an additional problem usually found in dynamical systems [4], [5] and [6]: the no-negativity of the states. The study of systems with no-negative states is important in practice because many chemical, physical and biological processes involve quantities that have nonnegative sign: concentrations of substances, level of liquids, etc. (see for example: [7], [8] and [9]). These so-called positive systems have been extensively studied in the literature: See for example [10], [11], [12] and [13].

This paper deals with the positive observation problem, which consists of constructing observers that ensure the no-negativity of the estimates of the states. These observers are very important in practice and possess physical meaning (negative estimated values might be illogical if we think of negative concentrations, negative volumes, etc.)[14], [15] and [16]. Unfortunately, the classical Luenberger observers might lead to negative estimates. For this reason, Luenberger observers are not adequate to estimate states that are inherently nonnegative. Instead, positive observers must be used. Many papers on positive observers have been published. We may note [17], [18], [19] and [20].

This paper concentrates on a classy of nonlinear positive that can be represented by Takagi Sugeno models: Takagi-Sugeno (TS) modeling has been successfully applied to the design of nonlinear systems [21], [22], [23] and [24]. This representation is an interesting way to approach a large type of nonlinear systems: by a qualitative knowledge of the system, local dynamics in different state space regions are represented by linear models and then interpolated using the system nonlinearities [25].

The main contribution of this paper is to synthesize positive fuzzy observers for a TS model, with weighting functions that could depend on unmeasured premise variables (for example, the system state).The observer gains are then obtained using linear matrix inequalities (LMI) [26],[27],[28] which can be solved efficiently using convex optimization techniques.

The paper is organized as follows: Section II gives some notations used in the paper, presents the Takagi Sugeno model structure and the problem studied. Section III presents how to design a positive observer to obtain the convergence conditions of the state estimation error. The main results are given under LMI formulation. In Section IV, the proposal is applied to a numerical example. Finally, Section V gives some conclusions.

II. Notations and problem statement

In this paper, the following notations are used:

$$\sum_{i=1}^{r}\sum_{j=1}^{r}\sum_{k=1}^{r} h_i h_j h_k \quad <=> \quad \sum_{i,j,k=1}^{r} h_i h_j h_k$$

I is the identity matrix with appropriate dimensions.

Definition 1 [12, 14]:

A square real matrix M is called a Metzler matrix if all its off-diagonal elements are nonnegative:

$$m_{ij} \geq 0, i \neq j.$$

We consider the following class of Takagi-Sugeno continuous-time models C :

$$C:\begin{cases} \dot{x}(t) = \sum_{i=1}^{r} h_i\big(x(t)\big)\big(A_i x(t) + B_i\, u(t)\big) \\ y(t) = C\, x(t) \\ x(0) = x_0 \end{cases} \quad (1)$$

where:

$x(t) \in \mathbb{R}^n$ is the state vector

$h_i(x(t))$ are fuzzy weighting functions that satisfy:

$0 \leq h_i\big(x(t)\big) \leq 1$,

$\sum_{i=1}^{r} h_i\big(x(t)\big) = 1$ (2)

$u(t)$ is the control input vector

$y(t) \in \mathbb{R}^m$ is the output vector

$A_i = [a_{jk}] \in \mathbb{R}^{n\times n}$, $B_i = [b_{jk}] \in \mathbb{R}^{n\times l}$ and

$C_i = [c_{jk}] \in \mathbb{R}^{m\times n}$ are given system matrices.

Observe that, for simplicity, we have assumed that the output matrix C is common for all subsystems ($C_i = C$, for $i \in \{1,2,\dots,r\}$).
We suppose also that $D_i = 0$, for $i \in \{1,2,\dots,r\}$.
However, the results can be extended to the non-common output matrices, as in [29].
Next, we present some results that will be used later to simplify the formulation of the Takagi-Sugeno model in order to obtain better results:

Lemma 1:

Let:

$\{X_i\}$ be a set of matrices of given dimensions.

$h_i(x(t))$ be fuzzy weighting functions that satisfy the following properties:

$0 \le h_i\big(x(t)\big) \le 1$,

$$\sum_{i=1}^{r} h_i\big(x(t)\big) = 1 \qquad (2)$$

Then, we may write:

$$\sum_{i=1}^{r}\big(h_i(x) - h_i(\hat{x})\big)X_i = \sum_{i,j=1}^{r} h_i(x)h_j(\hat{x})(X_i - X_j) \quad (3)$$

Proof:

$$\sum_{i,j=1}^{r} h_i(x)h_j(\hat{x})\big(X_i - X_j\big)$$
$$= \sum_{i,j=1}^{r} h_i(x)h_j(\hat{x})X_i - \sum_{i,j=1}^{r} h_j(x)h_i(\hat{x})X_j$$
$$= \sum_{i,j=1}^{r} h_i(x)(1 - h_j(\hat{x}))\, X_i - \sum_{i,j=1}^{r} h_j(\hat{x})\,(1 - h_i(x))\, X_j$$
$$= \sum_{i=1}^{r} h_i(x)\, X_i - \sum_{j=1}^{r} h_j(\hat{x})\, X_j - \sum_{i=1}^{r} h_i(x)h_i(\hat{x})X_i + \sum_{j=1}^{r} h_j(\hat{x})h_j(x)X_j = \sum_{i,j=1}^{r} h_i(x)h_j(\hat{x})\big(X_i - X_j\big)$$

Lemma 2:

Let:

$\{X_i\}$ be a set of matrices of given dimensions.

$h_i(x(t))$ be fuzzy weighting functions that satisfy the following properties:

$0 \le h_i\big(x(t)\big) \le 1$,

$$\sum_{i=1}^{r} h_i\big(x(t)\big) = 1 \qquad (2)$$

Then, we may write:

$$\sum_{i,j=1}^{r} h_i(x)h_j(x) = \sum_{i,j=1}^{r} h_i(x)h_j(\hat{x}) \qquad (4)$$

Proof:

$$\sum_{i,j=1}^{r} h_i(x)h_j(x) = h_1(x)h_1(x) + h_1(x)h_2(x) + \cdots + h_r(x)h_{r-1}(x) + h_r(x)h_r(x)$$
$$= \big(h_1(x) + \cdots + h_r(x)\big)\big(h_1(x) + \cdots + h_r(x)\big)$$
$$= \big(h_1(x) + \cdots + h_r(x)\big)\big(h_1(\hat{x}) + \cdots + h_r(\hat{x})\big)$$
$$= \sum_{i=1}^{r} h_i(x) \sum_{j=1}^{r} h_j(\hat{x}).$$

Taking into account that the state is estimated, the multiple model with unmeasurable variables (2) can be reduced [30] to :

$$C:\begin{cases} \dot{x}(t) = \sum_{i=1}^{r} h_i\big(\hat{x}(t)\big)\,(A_i\hat{x}(t) + B_i\,u(t)) + w(t) \\ y(t) = Cx(t) \\ x(0) = x_0 \end{cases} \qquad (5)$$

where :

$$w(t) = \sum_{i=1}^{r} (\, h_i\big(x(t)\big) - h_i\big(\hat{x}(t)\big))\,(A_i x(t) + B_i u(t)) \quad (6)$$

Using Lemma 1, we have :

$$\sum_{i=1}^{r}\big(h_i(x) - h_i(\hat{x})\big)X_i = \sum_{i,j=1}^{r} h_i(x)h_j(\hat{x})\Delta X_{ij} \qquad (7)$$

where $X_i \in \{A_i\,, B_i, C_i\}$ and ΔX_{ij} is defined by:

$$\Delta X_{ij} = X_i - X_j \qquad (8)$$

Then, System (1) can be transformed into the following system:

$$C:\begin{cases} \dot{x}(t) = \sum_{i,j=1}^{r} h_i(x)h_j(\hat{x})\Big(\big(A_j + \Delta A_{ij}\big)x + \big(B_j + \Delta B_{ij}\big)u\Big) \\ y(t) = Cx(t) \\ x(0) = x_0 \end{cases}$$

(9)

where ΔX_{ij} are known constant matrices defined in (8).
Our aim is to design a positive observer which guarantees simultaneously the state estimation and the positivity of their estimates.

III. Positive Takagi-Sugeno Observer design

This step is devoted to the construction of the positive fuzzy observer in order to estimate the inaccessible states of the Takagi-Sugeno model described in (5). The observer is structured as follows:
Suppose that the studied system has r fuzzy rules:
Observer Rule *i :*
If $(x_1(t))$ is M_{i1}) and $(x_2(t))$ is M_{i2})…and $(x_r(t))$ is

M_{ir}) then $\dot{\hat{x}}(t) = A_i\hat{x}(t) + B_i u(t) + L_i\big(y(t) - \hat{y}(t)\big)$,
$i = 1, \dots, r$ (10)
where $\hat{x}(t)$ and $\hat{y}(t)$ denote the estimations of $x(t)$ and $y(t)$, respectively, L_i are the observer gains to be determined.
The overall fuzzy observer is represented as follows:

$$\dot{\hat{x}}(t) = \sum_{i=1}^{r} h_i\left(\hat{x}(t)\right)\Big(A_i\hat{x}(t) + B_i u(t) + L_i\big(y(t) - \hat{y}(t)\big)\Big) \quad (11)$$

$$\hat{y}(t) = C\,\hat{x}(t) \quad (12)$$

Let us consider the state estimation error as:
$e(t) = x(t) - \hat{x}(t)$ (13)
Using (9), (11), (12) and using Lemma 2, the dynamics of the state estimation error is:

$$\dot{e}(t) = \sum_{i,j=1}^{r} h_i(x)h_j(\hat{x})\Big(\big(A_j - L_jC\big)e(t) + \Delta A_{ij}\,x(t) + \Delta B_{ij}\,u(t)\Big) \quad (14)$$

We define the augmented state $\tilde{x} = [e^T \;\; x^T]^T$. Using the expressions in (9) and (14), the dynamics of the augmented state are given by the following augmented system:

$$\dot{\tilde{x}}(t) = \sum_{i,j=1}^{r} h_i(x)h_j(\hat{x})(R_{ij}\,\tilde{x}(t) + S_{ij}\,u(t)) \quad (15)$$

$$z = H\,\tilde{x} \quad (16)$$

where:

$$R_{ij} = \begin{bmatrix} A_j - L_jC & \Delta A_{ij} \\ 0 & A_j + \Delta A_{ij} \end{bmatrix},\; S_{ij} = \begin{bmatrix} \Delta B_{ij} \\ B_j + \Delta B_{ij} \end{bmatrix},\; H = [I \;\; 0] \quad (17)$$

The goal then is to determine the L_j that guarantee the stability of (15) while attenuating the effect of the input $u(t)$ on $z(t)$.

Thus, the objective of this study is to determine the observer gains L_i for the augmented model (15) such that :

- The T-S observer is asymptotically stable.
- The T-S observer is positive.

Theorem 1:

The system (15) is stable and positive and the L_2 gain from $u(t)$ to $z(t)$ is bounded, if there exist symmetric matrices P_1 and P_2, matrices K_j and a no-negative scalar γ, such that the following conditions hold:

$$\begin{bmatrix} X_{1j} & W_{ij} & Y_{ij} \\ W_{ij}^T & X_{2ij} & Z_{ij} \\ Y_{ij}^T & Z_{ij}^T & -\gamma^2 I \end{bmatrix} < 0\,, \quad \forall (i,j) \in \{1, \dots, r\}^2 \quad (18)$$

where :

$$X_{1j} = A_j^T P_1 + P_1 A_j - K_j C - C^T K_j^T + I \quad (19)$$

$$X_{2ij} = (A_j + \Delta A_{ij})^T P_2 + P_2\big(A_j + \Delta A_{ij}\big) \quad (20)$$

$$W_{ij} = P_1 \Delta A_{ij} \quad (21)$$

$$Y_{ij} = P_1 \Delta B_{ij} \quad (22)$$

$$Z_{ij} = P_2\big(B_j + \Delta B_{ij}\big) \quad (23)$$

$$\begin{cases} a_i(x,y) + \Delta a_{ij}(x,y) \geq 0 & ,\forall\; 1 \leq x \neq y \leq n \\ a_i(x,y) - \sum_{w=1}^{m} l_i(x,w)c(w,y) \geq 0 & ,\forall\; 1 \leq x \neq y \leq n \\ \sum_{w=1}^{m} l_i(x,w)c(w,y) > 0 & ,\forall\; 1 \leq x,y \leq n \\ b_i(x,z) > 0 & ,\forall\; 1 \leq x \leq n \;\; ,\forall\; 1 \leq z \leq l \\ b_i(x,z) + \Delta b_{ij}(x,z) > 0 \end{cases} \quad (24)$$

The gains of the observer are derived from
$L_j = P_1^{-1}K_j$ (25)
and the attenuation level is γ,
where
a_i, Δa_{ij}, b_i, Δb_{ij}, c and l_i are, respectively, the entries of A_i, ΔA_{ij}, B_i, ΔB_{ij}, C and L_i.

Proof :

In order to make the augmented model (16) quadratically stable, let us consider the Lyapunov function :
$V(\tilde{x}(t)) = \tilde{x}(t)^T P \tilde{x}(t)\,, \quad P = P^T$ (26)
Its derivative with regard to time is given by :
$\dot{V}(\tilde{x}(t)) = \dot{\tilde{x}}(t)^T P \tilde{x}(t) + \tilde{x}(t)^T P \dot{\tilde{x}}(t)$ (27)
By substituting $\dot{\tilde{x}}(t)$ (15) in (27), we obtain :

$$\dot{V}(\tilde{x}(t)) = \sum_{i,j=1}^{r} h_i(x)h_j(\hat{x})\Big(\tilde{x}(t)^T\big({R_{ij}}^T P + P R_{ij}\big)\tilde{x}(t) + \tilde{x}(t)^T P S_{ij} u(t) + u(t)^T {S_{ij}}^T P \tilde{x}(t)\Big) \quad (28)$$

Our goal is to attenuate the effect of the input $u(t)$ on $z(t)$. So, in order to guarantee the stability of (15) and the boundedness of the transfer from $u(t)$ to $z(t)$:

$$\frac{\|z(t)\|_2}{\|u(t)\|_2} < \gamma\,, \quad \|u(t)\|_2 \neq 0, \quad \gamma > 0 \quad (29)$$

We consider the following criterion :
$\dot{V}(\tilde{x}(t)) + z(t)^T z(t) - \gamma^2 u(t)^T u(t) < 0$ (30)
Substituting (28) and (16) in (30), we obtain :

$$\sum_{i,j=1}^{r} h_i(x)h_j(\hat{x})\Big(\tilde{x}(t)^T\big({R_{ij}}^T P + P R_{ij}\big)\tilde{x}(t) + \tilde{x}(t)^T P S_{ij} u(t) + u(t)^T {S_{ij}}^T P \tilde{x}(t)\Big)$$
$$+\tilde{x}(t)^T H^T H\,\tilde{x}(t) - \gamma^2 u(t)^T u(t) < 0 \quad (31)$$

Taking into account the convex sum property of the weighting functions, we are allowed to write :

$$\sum_{i,j=1}^{r} h_i(x)h_j(\hat{x})\,\big(\tilde{x}(t)^T\big({R_{ij}}^T P + P R_{ij}\big)\tilde{x}(t) + \tilde{x}(t)^T P S_{ij} u(t) + u(t)^T {S_{ij}}^T P \tilde{x}(t) + \tilde{x}(t)^T H^T H\,\tilde{x}(t) - \gamma^2 u(t)^T u(t)\big) < 0 \quad (32)$$

which can be reformulated in the following way :

$$\sum_{i,j=1}^{r} h_i(x)h_j(\hat{x})\,\tilde{s}(t)^T T_{ij}\tilde{s}(t) < 0 \quad (33)$$

where :

$$T_{ij} = \begin{bmatrix} {R_{ij}}^T P + P R_{ij} + H^T H & P S_{ij} \\ {S_{ij}}^T P & -\gamma^2 I \end{bmatrix}, \tilde{s}(t) = \begin{bmatrix} \tilde{x}(t) \\ u(t) \end{bmatrix}$$

A sufficient condition for (31) to hold is:

$$\begin{bmatrix} {R_{ij}}^T P + P R_{ij} + H^T H & P S_{ij} \\ {S_{ij}}^T P & -\gamma^2 I \end{bmatrix} < 0\,, \quad \forall (i,j) \in \{1,\dots,r\}^2$$

(34)

In order to facilitate the resolution of the observer gains, the matrix variable $(P > 0)$ is chosen to be diagonal with respect to appropriate matrix blocks :

$$P = \begin{bmatrix} P_1 & 0 \\ 0 & P_2 \end{bmatrix} \qquad (35)$$

Using the definitions of R_{ij} and S_{ij} given in (17), and the change of variables :

$$K_j = P_1 L_j \qquad (36)$$

We obtain from (36) the LMI conditions expressed in (18) .

In order to prove the positivity of the system, we resort to the following augmented system :

$$\dot{X}(t) = \sum_{i,j=1}^{r} h_i(x) h_j(\hat{x}) \left(\bar{A}_{ij} X(t) + \bar{B}_{ij} u(t) \right) \qquad (37)$$

where :

$$X(t) = \begin{bmatrix} x(t) \\ \hat{x}(t) \end{bmatrix}, \bar{A}_{ij} = \begin{bmatrix} A_j + \Delta A_{ij} & 0 \\ L_j C & A_j - L_j C \end{bmatrix}$$

and $\bar{B}_{ij} = \begin{bmatrix} B_j + \Delta B_{ij} \\ B_j \end{bmatrix}$ (38)

We have to prove that :

$$\begin{cases} \bar{A}_{ij} \text{ is Metzler} \\ \bar{B}_{ij} > 0 \end{cases}, \forall\, i,j \in \{1,\dots,r\}^2 \qquad (39)$$

which means that :

$$\begin{cases} A_j + \Delta A_{ij} \text{ is Metzler} \\ A_j - L_j C \text{ is Metzler} \\ L_j C > 0 \\ B_j > 0 \\ B_j + \Delta B_{ij} > 0 \end{cases} \qquad (40)$$

which leads to the following inequalities :

$$\begin{cases} a_{ij} + \Delta a_{ij} \geq 0 & , \forall\ 1 \leq i \neq j \leq n \\ a_{ij} - \sum_{k=1}^{m} l_{ik} c_{kj} \geq 0 & , \forall\ 1 \leq i \neq j \leq n \\ \sum_{k=1}^{m} l_{ik} c_{kj} > 0 & , \forall\ 1 \leq i,j \leq n \\ b_{ij} > 0 & , \forall\ 1 \leq i,j \leq n \\ b_{ij} + \Delta b_{ij} > 0 & , \forall\ 1 \leq i,j \leq n \end{cases} \qquad (41)$$

IV. Simulation Results

We consider the system in (1) defined by:

$$A_1 = \begin{bmatrix} 5 & 6 & 5.5 \\ 2 & 4.5 & 4 \\ 3.5 & 5 & 4 \end{bmatrix}, A_2 = \begin{bmatrix} 2.5 & 2 & 3 \\ 2 & 1 & 1.5 \\ 4 & 2.5 & 3 \end{bmatrix}$$

$$B_1 = \begin{bmatrix} 1 \\ 0.5 \\ 0.25 \end{bmatrix}, B_2 = \begin{bmatrix} 2 \\ 1.5 \\ 0.5 \end{bmatrix}$$

$$C = \begin{bmatrix} 1 & 1 & 1 \\ 1 & 1 & 1 \end{bmatrix}$$

The weighting functions are defined by:

$$h_1(x) = \frac{1 - \tanh(x_1)}{2}, h_2(x) = \frac{1 + \tanh(x_1)}{2}$$

By using the Theorem, we obtain the following matrices of the controller and observer gains:

$$K_1 = [-1.212 \quad 0.515 \quad 1.104]$$
$$K_2 = [0.225 \quad -0.251 \quad 1.024]$$

$$L_1 = \begin{bmatrix} -1.854 & 5.642 \\ 7.325 & -4.802 \\ -2.421 & 5.711 \end{bmatrix}, L_2 = \begin{bmatrix} -2.125 & 3.501 \\ 5.182 & -4.205 \\ -3.451 & 5.527 \end{bmatrix}$$

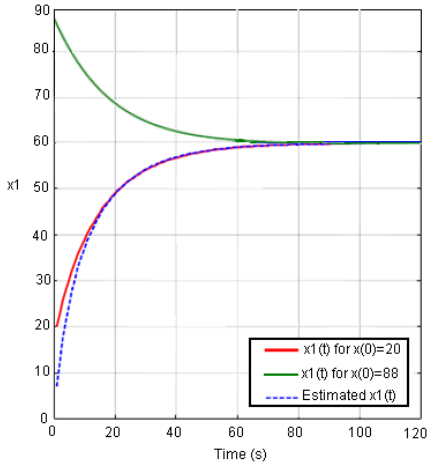

Fig 1: The Evolution of the state $x_1(t)$ and its estimated

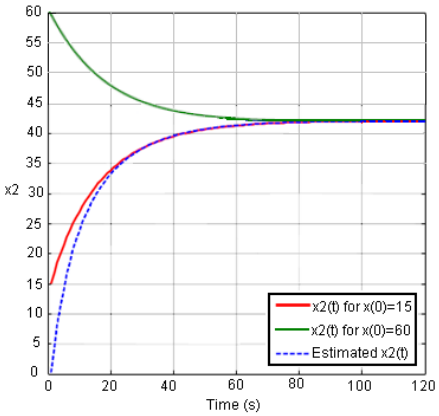

Fig 2: The Evolution of the state $x_2(t)$ and its estimated

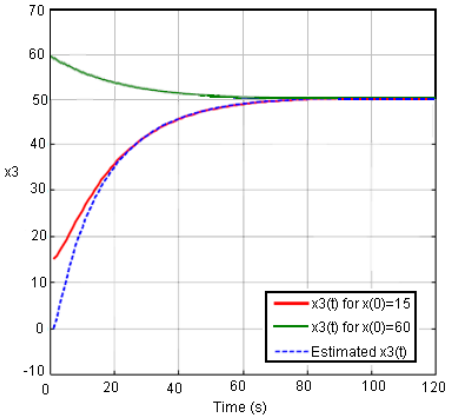

Fig 3: The Evolution of the state $x_3(t)$ and its estimated

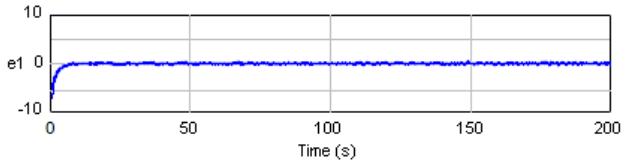

Fig 4: The Evolution of the error estimation of $x_1(t)$ *for* $x_1(0) = 20$.

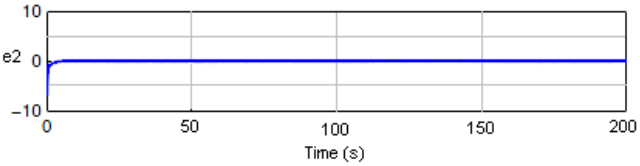

Fig 5: The Evolution of the error estimation of $x_2(t)$ *for* $x_2(0) = 15$

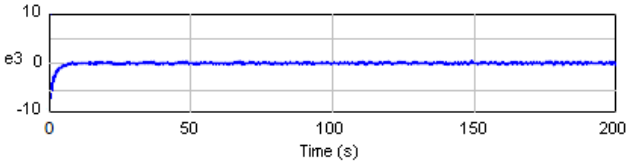

Fig 6: The Evolution of the error estimation of $x_3(t)$ *for* $x_3(0) = 15$.

We can see that the simulated states and their estimations are in the positive part of the plan. The positivity of the states and their estimations proves the effectiveness of the studied approach.

By examining the trajectories of the estimation errors in figures 4, 5 and 6, we can see that they converge rapidly to zero. So that, the positive observer guarantees a good performance. The results obtained show the efficiency of the proposed method.

V. Conclusion

This paper proposes new methods of designing a positive observer for nonlinear systems described by Takagi-Sugeno systems with unmeasurable premise variables. This observer is devoted to the estimation of the state of the given system and to guarantee its positivity at each time. The proposed approach is based on some transformations using the sommation properties of the weighting functions. The convergence of the estimation errors are obtained using the Lyapunov method and L_2 techniques. The conditions which guarantee the convergence of the estimation errors and the non negativity of the states at each time are issued from the LMIs (Linear Matrix Inequalities) formulation. In the future works, we will concentrate on the diagnosis and faults detection of this type of systems.

Acknowledgment

This work has been funded by Research supported by AECID (A/030410/10) and MiCInn (DPI2010-21589-c05.

References

[1] M. Norgaard, N. K. Poulsen and O. Ravn, "New developments in state estimation for nonlinear systems", *Automatica,* vol. 36, no. 11, pp. 1627–1638, November 2000.

[2] F. Schweppe, "Recursive state estimation: Unknown but bounded errors and system inputs", *IEEE Transactions on Automatic Control* , vol. 13, no. 1, pp. 22-28, February 1968.

[3] D. Simon, "Optimal state estimation: Kalman, Hinf and nonlinear approaches", Cleveland State University.

[4] J. A. Jacquez, "Compartmental analysis in biology and medicine", University of Michigan, 1985.

[5] J. A. Jacquez, P. Greif, "Numerical parameter identifiability and estimability: Integrating identifiability, estimability, and optimal sampling design", *Mathematical Biosciences*, Vol. 77, no. 1–2, pp. 201–227, December 1985.

[6] M. Masami and H. Caswell, "Estimating Population Projection Matrices From Multi-Stage Mark–Recapture Data", *ESA Ecology*, Vol. 83, no. 12, pp. 3257–3265, December 2002.

[7] F. Hynne, S. Dano, P.G. Sorensen, "Full-scale model of glycolysis in Saccharomyces cerevisiae", *Biophysical Chemistry*, Vol. 94, pp. 121–163, September 2001.

[8] T. Luzyanina, D. Roose, T. Schenkel, M. Sester, S. Ehl, A. Meyerhans and G. Bocharov, "Numerical modelling of label-structured cell population growth using CFSE distribution data", *Theoretical Biology and Medical Modelling*, vol. 26, no. 4, pp. 1742-4682, July 2007.

[9] R. D. Penn, M. C. Lee, A. A. Linninger, K. Miesel, S.N. Lu and L. Stylos, "Pressure gradients in the brain in an experimental model of hydrocephalus", *Journal of Neurosurgery*, Vol. 116, no. 5, pp. 1069-1075, May 2012.

[10] D. Luenberger, "Introduction to dynamic systems: theory, models, and applications", 1979.

[11] A. Berman, M. Neumann and R. J. Stern, "Nonnegative matrices in dynamic systems", 1989.

[12] L. Farina and S. Rinaldi, "Positive linear systems : theory & applications", 2000.

[13] T. Kaczorek, "Full-order perfect observers for continuous-time linear systems", Vol. 49, no. 4, pp. 549-558, 2001.

[14] M. A. Rami and F. Tadeo, "Positive observation problem for linear discrete positive systems", *Proc. 45th IEEE Conf. Decision Contr.*, pp. 4729–4733, 2006.

[15] M. A. Rami, U. Helmke, and F. Tadeo, "Positive observation problem for time-delays linear positive systems", *in Proc. 15th Mediter. Conf. Control Autom.*, Athens, Greece, 2007.

[16] M. A. Rami, F.Tadeo and U. Helmke, "Positive observers for linear positive systems, and their implications ", Vol. 84, no. 4, pp. 716-725, June 2011.

[17] M. Gilson and P. VandenHof, "On the relation between a bias-eliminated least-squares (BELS) and an IV estimator in closed-loop identification", *Automatica*, Vol. 37, no.10, pp. 1593-1600, October 2001.

[18] H. M. Hardin and J. H. van Schuppen, "Observers for linear positive systems", *Linear Algebra and its*

Applications, Vol. 425, no. 2-3, pp. 571-607, September 2007.

[19] J. Back and A. Astolfi, "Design Of Positive Linear Observers For Positive Linear Systems Via Coordinate Transformations And Positive Realizations", *Siam J. Control Optim*. Vol. 47, no. 1, pp. 345–373, 2008.

[20] Z. Shu, J. Lam, H. Gao, B. Du and L. Wu, "Positive Observers and Dynamic Output-Feedback Controllers for Interval Positive Linear Systems", *IEEE Transactions on Circuits and Systems*, Vol. 55, no. 10, pp. 3209-3222 , November 2008.

[21] B. S. Chen, C. H. Lee and Y. C. Chang, "H_∞ Tracking Design of Uncertain Non Linear SISO Systems : Adaptive fuzzy approach," *IEEE Trans. Fuzzy Syst*., vol. 4, no. 1, pp. 32-43, February 1996.

[22] H. Ghorbel, M. Ghamgui, M. Souissi and M. Chaabane, "Modelling and robust control for Three Tanks System using fuzzy approach," *International Conference on Electrical Systems and Automatic Control, JTEA*, Hammamet-Tunisia, 26-28 March 2010.

[23] T. Takagi and M. Sugeno, "Fuzzy identification of systems and its applications to modeling and control," *IEEE Trans. Syst., Man, Cybern.*, vol. 15, pp. 116-132, Jan. 1985.

[24] H. O. Wang, K. Tanaka and M. F. Griffin, "An approach to fuzzy control of nonlinear systems : Stability and design issues," *IEEE Trans. Fuzzy Syst*., vol. 4, pp. 14-23, Feb. 1996.

[25] B. S. Chen, C. S. Tseng and H. J. Uang, "Robustness design of nonlinear dynamic systems via fuzzy linear control," *IEEE Trans. Fuzzy Syst*., vol. 7, pp. 571-585, Oct. 1999.

[26] A. Benzaouia, A. Hmamed and A. Hajjaji, "Stabilization of controlled positive discrete-time T-S fuzzy systems by state feedback control", *International Journal of Adaptive Control and Signal Processing*, Vol. 24, no.12, pp. 1091-1106, December 2010.

[27] A. Benzaouia and A. Hajjaji, "Delay-Dependent Stabilization Conditions of Controlled Positive T-S Fuzzy Systems With TimeVarying Delay", *International Journal of Innovative Computing, Information and Control ICIC International*, Vol. 7, no. 4, pp. 1533-1547, April 2011.

[28] A. Benzaouia, R. Oubah, A. Hajjaji and F. Tadeo, "Stability and stabilization of positive Takagi-Sugeno fuzzy continuous systems with delay", *50th IEEE Conference on Decision and Control and European Control Conference*, pp. 8279 - 8284 , December 2011.

[29] M. Nachidi, A. Benzaouia, F. Tadeo, and M. A. Rami, "LMI-Based Approach for Output-Feedback Stabilization for Discrete-Time Takagi–Sugeno Systems", *IEEE Transactions on Fuzzy Systems*, Vol. 16, no. 5, pp. 1188- 1196, October 2008.

[30] H. Ghorbel, M. Souissi, M. Chaabane and A. Hajjaji, "Observer design for fault diagnosis for the Takagi-Sugeno model with unmeasurable premise variables", *20th Mediterranean Conference on Control & Automation (MED)*, pp. 303 - 308 , July 2012.

METHODS AND APPROACHES TO OPERATIONS ON ENCRYPTED DATA

Roman Zharinov

Saint-Petersburg State University of Aerospace Instrumentation,
Saint-Petersburg, Russia
tel: +7-906-250-58-73, e-mail: roman@vu.spb.ru

Abstract

Cloud computing is new era, attracting peoples for different services providing in cost effective manner. Privacy management is one of the critical issues in cloud when these services accessed through untrusted service provider or third party. There is risk with sending personal information to such parties. In this paper shows a comparison of safety aspects of popular cloud storage services. Also considered the methods and approaches to operations on encrypted data.

Introduction

The ever-increasing amount of valuable digital data both at home and in business needs to be protected, since its irrevocable loss is unacceptable.

However, individuals and especially businesses hesitate to entrust their data to cloud storage services since they fear that they will lose control over it. Recent successful attacks on cloud storage providers have exacerbated these concerns. The providers are trying to alleviate the situation and have taken measures to keep their customers' data secure.

The data is often of great value and its irrecoverable loss or damage could be a total disaster for its owner. For parents, videos of their children growing up may be very important, PhD students may rely on digital material, e.g., a collection of Internet references, to be used for a dissertation. For a company, the loss of data could ruin the basis for business. Additionally, companies are legally obliged to preserve tax records for a certain period (6 or 10 years), and to leave them available to the fiscal authorities.

Companies may entrust containing sensitive business data and valuable intellectual property which may be of great interest for industrial espionage. The unauthorized disclosure of customer information, business secrets or research data poses a serious threat to a company's business. In addition, compliance requirements with both internal security guidelines and legal regulations have to be met. The cloud storage provider may be subject to different legal regulations than the user.

Cloud storage services

Cloud storage services promise to be a solution for this problem. In recent years, their popularity has increased dramatically. They offer user-friendly, easily accessible and cost-saving ways to store and automatically back up arbitrary data, as well as data sharing between users and synchronization of multiple devices.

There are a lot of cloud storage services. One of the most popular: Dropbox, Mozy, TeamDrive, CloudMe, CrashPlan, Ubuntu One. Main goal of this part is answering a question if these services match the indented security requirements.

Each service includes a piece of client software and a server-side software. There are four general features, which support almost popular cloud services:

- The copy operation – cloud storage is a “mirror” of local disk or part of it. And if something happens, data can easily recover from cloud storage.
- The backup operation – allow to preserve all modifying of a file, ie creating revision of the file.
- The synchronization – user can synchronize all files at his all devices, such as laptop, mobile phone, tablet pc, etc.
- The file sharing operation – user can share his files with somebody else, e.g. with project participants.

Which services support one or more operations are listed at Table 1.

Table 1. Supported features of cloud storage services

Cloud storage service	Copy	Back up	Synchronization	File sharing
Dropbox	yes	no	yes	yes
Mozy	no	yes	no	no
TeamDrive	yes	yes	yes	yes
CloudMe	yes	no	no	yes
CrashPlan	no	yes	no	no
Ubuntu One	yes	no	yes	yes

Now, let's talk about security requirements. The basic requirements for storage are [1]:

- Authorization - using to access control to own resources.
- Transport layer security - creating secure connection between user device and server
- Encryption scheme - allow to store confidential information and deny access others people to user's resources
- Security files sharing - user can share some file or group of file with somebody else, optionally including non-subscribers of that service.
- Dedublication - to avoid privacy problems when using deduplication.

So, so the authorization process and registration as part of it was a problem for CloudMe and Dropbox because they missed to verify the email address of a new customer. Hence, an incrimination attack is possible, that means a person A can register with the email address of another person B. Now, A can upload illegal material using the account of the victim B. After that A can notify authorities, e.g. the police, about the illegal content.

Transport layer security was a problem for CrashPlan and TeamDrive because they deny the usage of SSL/TLS protocols. Instead they use unpublished, self-made protocols. CloudMe service does not take any measure to protect the security of files during transmission.

Encryption scheme missing at CloudMe, Dropbox and Ubuntu One services because they do't use client-side encryption, thus the adversary (provider or hacker) is able to read the data. Mozy doesn't encrypt filenames.

Security sharing of data was a problem for CloudMe, Dropbox and TeamDrive. Problems occur if files are shared with non-subscribers on the principle of a long, unpredictable URL. CloudMe does not obfuscate this URL adequately.

Deduplication was a problem for Mozy storage service, because in some cases it is possible to ask the cloud storage provider whether a file is already stored or not.

Public security algorithms for cloud storage

Nowadays there are several main methods and technologies to assuage privacy concerns is to store all data in the cloud encrypted, and perform computations on encrypted data. To this end, we need an encryption schemes that allows meaningful computation on encrypted data such as a homomorphic encryption scheme, order-preserving encryption (OPE) and techniques for searches on encrypted data. How that schemes and methods are work?

A. Homomorphic encryption schemes

Homomorphic encryption schemes that allow simple computations on encrypted data have been known for a long time. For example, the encryption systems of Goldwasser and Micali [2], El Gamal [3] and Paillier [4] support either adding or multiplying encrypted ciphertexts, but not both operations at the same time. Boneh, Goh and Nissim [5] were the first to construct a scheme capable of performing both operations at the same time – their scheme handles an arbitrary number of additions and just one multiplication. More recently, in a breakthrough work, Gentry [6] constructed a fully homomorphic encryption scheme (FHE) capable of evaluating an arbitrary number of additions and multiplications (and thus, compute any function) on encrypted data. FHE is efficient and simple, produces short ciphertexts, and its security is based on the "ring learning with errors" (Ring LWE) problem [7].

Also there is exist a "somewhat homomorphic encryption" (SHE) scheme, namely, one which allows a fixed number of ciphertexts' multiplications. These SHE schemes are building blocks for the FHE schemes of, e.g., [6], and provide much better efficiency guarantees than their fully homomorphic counter parts.

A Homomorphic encryption is additive, if:

Enc ($x \oplus y$) = Enc(x) $\otimes$ Enc(y), i.g.

$$Enc(\sum_{i=1} m_i) = \prod_{i=1} Enc(m_i)$$

A Homomorphic encryption is multiplicative, if:

Enc ($x \otimes y$) = Enc(x) $\otimes$ Enc(y), i.g. $Enc(\prod_{i=1} m_i) = \prod_{i=1} Enc(m_i)$

B. Order-preserving encryption

To allow efficient range queries on encrypted data, it is sufficient to have an order-preserving hash function family H (not necessarily invertible). A perfect hash function for a set S is a hash function that maps distinct elements in S to a set of integers, with no collisions. A perfect hash function has many of the same applications as other hash functions, but with the advantage that no collision resolution has to be implemented. The minimal size of the description of a perfect hash function depends on the range of its function values: The smaller the range, the more space

is required. Any perfect hash functions suitable for use with a hash table require at least a number of bits that is proportional to the size of S.

A minimal perfect hash function F is order preserving if keys are given in some order a1, a2, ..., an and for any keys aj and ak, j < k implies F(aj) < F(ak) [8].Order-preserving minimal perfect hash functions require necessarily Ω(n log n) bits to be represented [9].

A perfect hash function with values in a limited range can be used for efficient lookup operations, by placing keys from S (or other associated values) in a table indexed by the output of the function. Using a perfect hash function is best in situations where there is a frequently queried large set, S, which is seldom updated. Efficient solutions to performing updates are known as dynamic perfect hashing, but these methods are relatively complicated to implement

The overall OPE scheme would then have secret key (Kenc, Kh) where Kenc is a key for a normal (randomized) encryption scheme.

Order-preserving symmetric encryption (OPE) is a deterministic encryption scheme whose encryption function preserves numerical ordering of the plaintexts. OPE has a long history in the form of one-part codes, which are lists of plaintexts and the corresponding ciphertexts, both arranged in alphabetical or numerical order so only a single copy is required for efficient encryption and decryption [10].

A symmetric encryption scheme SE = (K; Enc, Dec) with associated plaintext-space D and ciphertext-space R consists of three algorithms [10]:

- The randomized key generation algorithm K returns a secret key K .
- The (possibly randomized) encryption algorithm E nc takes the secret key K , descriptions of plaintext and ciphertext-spaces D; R and a plaintext m to return a ciphertext c.
- The deterministic decryption algorithm Dec takes the ciphertext-spaces D; R, and a ciphertext c to return symbol ‘end’ indicating that the ciphertext was invalid.

It based on next techniques:

- Pseudorandom functions (PRFs) - A family of functions is a map F : Keys x D → $\{0, 1\}^1$, where D is plaintext-space and for each key K from Keys the map F (K; *) : D → $\{0; 1\}^1$ is a function.
- Hypergeometric (HG) probability distributions – using for help in preserving plaintext order. Let [M] is domain from plaintext-space and [N] is range from ciphertext-space. Then given S, a set of M distinct integers from [N] we can construct an order-preserving function (OPF) from [M] to [N] by mapping each i from [M] to the i^{th} smallest element in S. To justify the following equality, defined for M, N from N and any x, x + 1 from [M], y from [N]:

$$\Pr[f(x) \le y < f(x+1): f \leftarrow OPF_{[M],[N]}] = \frac{\binom{y}{x}\cdot\binom{N-y}{M-x}}{\binom{N}{M}}$$

The idea of OPE is that, to encrypt plaintext x, the encryption algorithm performs a binary search down to x. That is, it first assigns Enc(K; M/2), then Enc(K; M/4) if m < M/2 and Enc(K; 3M/4) otherwise, and so on, until Enc(K; x) is assigned. Crucially, each ciphertext assignment is made according to the output of the HG sampling algorithm run on appropriate parameters and coins from an associated portion of the random tape indexed by the plaintext (the decryption algorithm can be defined similarly).

C. *Techniques for searches on encrypted data*

There are three practical solutions: practical techniques for searches on encrypted data (SSKE) [11], searchable public key encryption (SPKE) [12] and Secure Indexes for Searching Efficiently on Encrypted Compressed Data [13] .

SSKE focused on non-index solution, ie sequential scan entire file with some text information. There are three main operations: key generation (KG), Encrypt/Decrypt and generate trapdoor.

For encrypt it using a deterministic cipher. The ciphertext is divided into 2 parts left and right respectively.

For storing information we need to divide input text W on a few blocks W_i with fixed length n. Then each block W_i encrypted with determine crypto algorithm and resulting ciphertext block is divided into 2 parts left L_i and right one R_i: $X_i = E_{k''}(W_i) = \langle L_i, R_i \rangle$. Using pseudo-random generator we must generate random bits S_i based on the location of W_i. Finally we calculate $C_i = \langle L_i, R_i \rangle \oplus \langle S_i, F_{k_i}(S_i) \rangle$. See fig. 1 for more details.

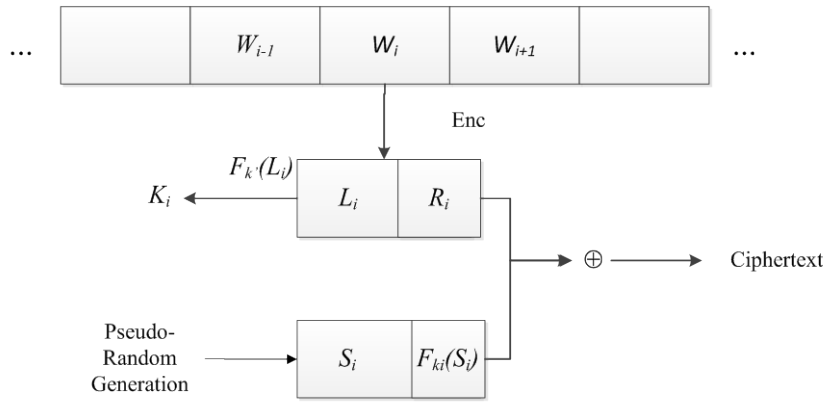

Figure 1. Arhitecture of SSKE

For searching on encrypted data, ie determine whether there is the word W_j in the ciphertext, we should transfer to the server encrypted word. For search information we denote:

k' – cipher key,

k'' – key for hash-function f,

W_j – the text we are searching for,

$X_j = E_{k'}(W_j) = \langle L_j, R_j \rangle$ – encrypted block,

$K_j = f_{k'}(L_j)$ – key for hash-function F.

Values X_j and k_j are transfer to the server. With it we can calculate a trapdoor $T_p = C_p \oplus X_j = \langle S_p, S'_p \rangle$. If $S'_p = F_{k_j}(S_p)$, then on client side server transfer $\langle p, C_p \rangle$.

Security of SSKE based on Pseudo-Random Generation and Pseudo-Random Function. The disadvantages are linear in document size and difficult to modify algorithm to handle variable length words.

Conclusion

In this article provided an overview of existing cloud services. For them are presented main shortcomings in the security. There are a lot of concepts of security which enables providing results of calculations on encrypted data without knowing the raw data on which the calculation was carried out, with respect of the data confidentiality. Also were considers modern methods and approaches to operations on encrypted data. Our future work will attempt to create algorithm to find the first occurrence of a string.

References

[1] E. M. Waidner, On the Security of Cloud Storage Services, Germany: SIT Technical Reports, 2012.

[2] S. M. Shafi Goldwasser, Probabilistic encryption and how to play mental poker keeping secret all partial information, STOC, 1982.

[3] T. El-Gamal, "A public key cryptosystem and a signature scheme based on discrete logarithms.," 1984.

[4] P. Paillier, «Public-key cryptosystems based on composite degree residuosity classes,» *EUROCRYPT,* 1999.

[5] E.-J. G. a. K. N. Dan Boneh, «Evaluating 2-DNF formulas on ciphertexts,» *Theory of Cryptography,* 2005.

[6] C. Gentry, «Fully homomorphic encryption using ideal lattices,» *STOC,* 2009.

[7] C. P. a. O. Vadim Lyubashevsky, «On ideal lattices and learning with errors over rings,» *Gilbert.*

[8] E. A. Fox, Q. F. Chen, A. M. Daoud и L. S. Heath, «Order preserving minimal perfect hash functions and information retrieval,» *Proceedings of the 13th annual international ACM SIGIR conference on Research and development in information retrieval,* 1990.

[9] N. C. Y. L. a. A. O. Alexandra Boldyreva, «Order-Preserving Symmetric Encryption».

[10] S. D. W. A. P. Dawn Xiaodong, «Practical Techniques for Searches on Encrypted Data».

[11] G. D. C. R. O. a. G. P. D. Boneh, «Public key encryption with keyword search,» *In proceedings of Eurocrypt 2004,* 2004.

[12] E.-J. Goh, «Secure indexes,» *Cryptology ePrint Archive,* 2004.

CONTENTS

The scientific edition

XIV International Forum
"MODERN INFORMATION SOCIETY FORMATION –
PROBLEMS, PERSPECTIVES,
INNOVATION APPROACHES"

2–6 June, 2013

Proceedings of the Forum

Computer imposition

Papers are published in author's edition

Approved for publishing on 12.04.2013
Page format 60x84 1/8.
Number of copies 150. Order 181.

Department of operative polygraphy
SUAI
190000, St. Petersburg, st. B. Morskaya, 67